3.8 Design of Category I Structures

The NuScale Power Plant design includes two Seismic Category I structures, the Reactor Building and the Control Building, and one Seismic Category II structure--the Radioactive Waste Building. A drawing of the site is provided in Figure 1.2-1.The arrangement of these buildings is shown in Figure 1.2-4. Additional Information about the site and primary structures is in Section 1.2.

3.8.1 Concrete Containment

The NuScale Power Plant design does not use a concrete containment. The containment and the reactor vessel are integrated to form the NuScale Power Module.

3.8.2 Steel Containment

3.8.2.1 Description of Containment

3.8.2.1.1 General

The containment vessel (CNV) is an integral portion of the NuScale Power Module (NPM). The CNV houses, supports, and protects the reactor pressure vessel (RPV), reactor coolant system (RCS), and associated structures, systems, and components. The NPM is located in the Reactor Building (RXB) and the majority of the NPM (and thus the CNV) is partially immersed in the reactor pool to facilitate decay heat removal during postulated design basis events.

The primary functions of the CNV are to:

- provide an essentially leak-tight barrier to contain fission product releases for the reactor coolant pressure boundary during design basis events
- contain the mass and energy release from a postulated loss-of-coolant accident (LOCA) and secondary-system pipe ruptures
- support operation of the emergency core cooling system (ECCS) by containment of reactor coolant and heat transfer through the CNV wall
- contain and support the RPV, RCS, and associated structures, systems, and components

The materials in contact with the reactor pool water are corrosion-resistant alloy or stainless-steel cladded, low-alloy steel and do not exhibit unacceptable degradation in service. This includes external surfaces of the CNV and threaded holes, which are submerged in the reactor pool. During refueling, the internal surfaces of the CNV are exposed to reactor pool water, and during design basis events, are exposed to RCS water. Thus, the internal surfaces of the low-alloy steel materials are also cladded with stainless steel. The materials of construction are included in Table 6.1-1 and Table 6.1-2.

The design of the CNV complies with the provisions of:

- General Design Criterion (GDC) 1 - The CNV is subject to the design, manufacturing, and operating quality assurance requirements in the NuScale Quality Assurance Program Description.
- GDC 2 - Seismic design to withstand the effects of a safe shutdown earthquake (SSE) regarding the CNV is met by using the guidance provided in Regulatory Guide (RG) 1.29, "Seismic Design Classification for Nuclear Power Plants," Revision 5.
- GDC 4 -The CNV is designed to accommodate the effects of and be compatible with environmental conditions associated with normal operation, maintenance, testing, and postulated accidents, including LOCAs.
- GDC 16 - The CNV is designed to provide a leak-tight barrier and to contain the CNV design pressure during design basis events.

- GDC 50 - The CNV is designed to ensure the component, access openings, penetrations, and containment heat removal systems have the capability to accommodate, without exceeding the design leakage rate and with sufficient margin, the calculated pressure and temperature conditions resulting from a LOCA.
- GDC 53 - The CNV is designed with provisions to permit inspection and testing for periodic verification that the CNV remains within the limits defined by the design basis.

3.8.2.1.2 Containment Configuration Description

The NuScale Power Plant CNV consists of an upright cylinder with torispherical top and bottom heads. The CNV has an upper and lower section connected with an approximate 218-inch diameter bolted flange. The flange connection permits the CNV to be separated to provide access to the RPV for refueling. Figure 3.8.2-1 provides a view of the CNV. The design characteristics, including elevations, of the CNV are shown in Table 3.8.2-1.

The lower CNV shell and bottom head are made of SA-965 FXM-19 stainless steel with a wall thickness of 3.00 inches. The lower shell has an approximate outside diameter of 135 inches. The bottom head is torispherical with an approximate outside knuckle radius of 25 inches and an approximate outside crown radius of 119 inches. The bottom head is attached to the lower CNV shell with a full-penetration weld. The shell connected to the bottom head transitions to a larger shell outside diameter of approximately 177 inches in the flange region. The shell regions are joined with full-penetration circumferential welds. The lower CNV shell in the flange region and the transition region of the lower CNV is also SA-965 FXM-19 and has a wall thickness of 3.25 inches. There are no penetrations located in the lower CNV shell or bottom head.

The upper CNV shell and top head are fabricated from SA-508 Grade 3, Class 2 low-alloy steel. The upper shell and top head are stainless steel cladded with 0.125 inches on the inside surfaces and 0.250 inches on the outside surfaces. The upper CNV shell base metal wall thickness is 3.00 inches and has an approximate outside diameter of 177 inches. The CNV has a torishperical top head with a base metal wall thickness of 5.00 inches, an approximate outside knuckle radius of 31 inches, and an approximate outside crown radius of 142 inches. The top head is attached to the upper CNV shell with a full-penetration weld.

Section views of the CNV are shown in Figure 6.2-1 and Figure 6.2-2a. Plane elevation views are shown in Figure 6.2-3a. The boundaries between the CNV and the RPV are shown in Figure 3.8.2-8 and Figure 3.8.2-9. The CNV design and operating characteristics are shown on Table 3.8.2-1. Materials used in construction of the CNV are shown in Table 6.1-1 and Table 6.1-2.

The CNV is housed in the reactor pool within the RXB, which is a Seismic Category I structure primarily embedded in soil. The discussion of the RXB is provided in Section 3.8.4 and Section 3.8.5. The CNV is partially immersed in the reactor pool to approximately the bottom of the CNV top head. The reactor pool provides a

passive heat sink for containment heat removal under LOCA conditions. The CNV rests on the reactor pool floor at elevation 25'-0". Within the reactor pool, the upper CNV is supported laterally by three support lugs. Figure 3.8.2-1 shows the support locations and elevations, and Figure 3.8.2-3 shows a plan view of the CNV lug in the reactor pool. The CNV is designed to withstand the environment of the reactor pool as well as the high pressure and temperature of a design basis accident.

Calculated peak CNV pressures and temperatures (discussed in Section 6.2.1) are less than the CNV internal design pressure of 1,000 psia and design temperature of 550 degrees F.

3.8.2.1.3 Containment Vessel Support

The CNV rests on a support skirt flange that has an approximate outside diameter of 141 inches and an approximate inside diameter of 120 inches. The support skirt sits on the bottom elevation of the reactor pool (building elevation of 25'-0") in the RXB around a passive skirt support. The support skirt has holes equally spaced around the skirt to allow steam to escape and prevent steam building up and blanketing the underside of the head. The passive skirt support provides lateral restraint for the bottom of the CNV. Figure 3.8.2-2 shows the CNV support skirt and passive skirt support at the bottom of the reactor pool.

The upper CNV is supported laterally on three sides by support lugs. Figure 3.8.2-1 shows the location and elevation of the lugs. The CNV support lugs contact restraints in the reactor bay walls. The lug restraints are part of the RXB (see Section 3.7.2.1.2.2). Figure 3.8.2-3 shows a plan view of the CNV orientation with the restraints on the reactor bay walls. The loads from the CNV are transferred through the supports to the bay walls by bearing. Each NPM is housed in an individual bay during operation.

3.8.2.1.4 Access and Manways

A flanged connection is provided between the upper and lower sections of the CNV. The flanged connection allows the CNV to be disassembled and provides access to the RPV during refueling operations and maintenance. Figure 3.8.2-1 provides the location and elevation of the flange connection. The flanged connection has a double O-ring seal with provisions for leak detection in the annular span between the dual O-rings.

Containment vessel manways and access openings on the CNV upper section provide access to components located inside the CNV not readily accessible via the main flange. Access to the steam plenums for steam generator inspection is provided through four 38-inch diameter openings. The openings are equally spaced around the CNV across from the main steam plenum access located in the RPV. Two 44-inch diameter access openings are provided for pressurizer heater access. The pressurizer access openings are located across from the pressurizer heaters access located in the RPV. Manway access to the CNV is provided through a 38-inch diameter opening. The manway provides access to the control rod drive mechanisms (CRDMs) located on the top of the RPV. Figure 3.8.2-1 shows each access opening location and elevation. Each access openings has a convex cover

plate bolted (stud/nuts) to the opening on the outside of the CNV. Each cover plate is made of SA-240 Type 304/304L stainless steel, is bolted with SB-637 UNS N07718 studs and nuts, and has a double O-ring seal with provisions for leak detection in the annular span between the dual O-rings. Figure 3.8.2-6 shows a typical access cover plate and O-ring seal.

The center of the CNV top head has a 67-inch diameter opening in the center of the top head to provide access to the CRDMs located on the top of the RPV. The CRDM access cover is a convex cover bolted (stud/nuts) to the top head and is sealed with double O-rings with an annular space for leak detection. The cover is made of SA-182 Grade F304/F304L stainless steel, and the studs and nuts are SA-564 Grade 630, S17400 (17-4 PH) Condition H1100. The top head also has an 18-inch diameter manway access to the CRDM platform. The manway opening has a bolted flat cover plate with double O-ring seals with provisions for leak detection in the annular span between the dual O-rings. Figure 3.8.2-5 shows the CRDM access and manway access.

Section 3.13 provides design requirements for Alloy 718 threaded fasteners for the mitigation of SCC.

3.8.2.1.5 Piping Penetrations

Penetrations on the CNV top head and upper shell are provided for process piping, ECCS trip and reset valves, electrical power, and instrumentation. No penetrations are located in the lower CNV. Fluid system penetrations are through integral or full-penetration welded nozzles on the CNV top head and upper shell. Safe ends are welded to the internal or external ends of the nozzles. The safe ends and the penetration nozzle-to-safe end welds are part of the CNV. Figure 3.8.2-7 shows a typical penetration configuration through the CNV shell. The CNV boundary is at the end of the safe ends furthest from the CNV shell. The pipe-to-safe end welds are part of the attached piping. This applies to the following nozzles and safe ends which are shown on Figure 3.8.2-4:

- Two nominal pipe size (NPS) 5 Sch. 120 feedwater nozzles (top head, azimuth 16 degrees and 344 degrees)
- Two NPS 12 Sch. 120 main steam nozzles (top head, azimuth 136 degrees and 225 degrees)
- Three NPS 2 Sch. 160 (inside), NPS 4 Sch. 160 (outside) chemical and volume control system nozzles (top head, azimuth 63 degrees, 180 degrees, and 248 degrees)
- One NPS 4 Sch. 160 containment evacuation system nozzle (top head, azimuth 290 degrees)
- One NPS 2 Sch. 160 containment flooding and drain system nozzle (top head, azimuth 0 degrees)
- Two NPS 2 Sch. 160 (inside), NPS 4 Sch. 160 (outside) reactor component cooling water system nozzles (top head, azimuth 0 degrees and 245 degrees)

- One NPS 2 Sch. 160 (inside), NPS 4 Sch. 160 (outside) RPV high point degasification nozzle (top head, azimuth 290 degrees)
- Two NPS 2 Sch. 160 decay heat removal system nozzles (upper CNV, elevation 56'-5" azimuth 120 degrees and 240 degrees) (these penetrations are not shown in Figure 3.8.2-4 but each has a similar configuration as the top head penetrations)

Reinforcement of the shell due to the penetration opening is provided by the nozzle and any additional thickness in the shell greater than the minimum wall thickness of the shell as calculated in accordance with American Society of Mechanical Engineers (ASME) Code, Section III, Paragraph NB-3324. The penetration designs are evaluated for external loads imposed by the attached valves and piping systems.

The penetrations have containment isolation valves (CIVs) attached to the outside safe end and designed to allow passage of fluids and gases through the CNV boundary while preserving the integrity of the boundary and preventing or limiting the release of fission products under postulated accident conditions. The primary system CIVs are welded directly to the nozzle safe ends of the CNV penetration nozzles on the CNV top head. Secondary system CIVs are welded close to the nozzle safe ends to accommodate the decay heat removal system taps on the main steam lines and other space constraints. The CIVs are discussed in Section 6.2.4.

3.8.2.1.6 Containment Electrical Penetration Assemblies

The CNV has multiple electrical penetrations on the top head. The electrical penetration assembly boundaries are at the face of the CNV flange surface for the penetration opening. The bolting (studs/nuts) is part of the electrical penetration. This applies to the following electrical penetration assemblies shown in Figure 3.8.2-5:

- Two NPS 3 Class 900 instrument and control (top head, azimuth 63 degrees and 180 degrees)
- Two NPS 12 Class 900 pressurizer power (top head, azimuth 41 degrees and 319 degrees)
- Four NPS 8 Class 900 instrument and control (top head, azimuth 111 degrees, 162.5 degrees, 197.5 degrees and 268 degrees)
- One NPS 18 Class 900 CRDM power (CRDM access cover, azimuth 45 degrees)
- Two NPS 10 Class 900 CRDM control (CRDM access cover, azimuth 180 degrees and 270 degrees)

Reinforcement of the shell due to the EPA openings is provided by the nozzle and any additional thickness in the shell greater than the minimum wall thickness of the shell as calculated in accordance with ASME Code, Section III, Paragraph NB-3324. There are no external loads imposed by the electrical penetration assemblies on their corresponding CNV flange.

Electrical penetration assembly design, construction, testing, qualification, and installation are in accordance with IEEE Standard 317-1983 as endorsed by Regulatory Guide 1.63. Production and installation testing meet IEEE Standard 317-1983 criteria. This ensures that electrical penetration assembly mechanical integrity is maintained during normal and accident events, which may also include the electrical faulting of a conductor within that electrical penetration assembly. The electrical design and environmental qualification requirements for electrical penetration assemblies are addressed in Section 8.3 and Section 3.11, respectively.

3.8.2.1.7 Emergency Core Cooling System Trip/Reset Valve Penetrations

The ECCS valve trip/reset assembly penetrations and safe ends are welded to the external side of the CNV upper shell. Two reactor recirculation trip/reset valves, NPS 3 Sch. 160 penetrations are located at an elevation of 58'-11.9", azimuth 7 degrees and 353 degrees. Three reactor vent trip/reset valves, NPS 3 Sch. 160 penetrations are located at an elevation of 89'-6.85" and azimuth 68 degrees, 188 degrees and 308 degrees, and one reactor vent trip valve, NPS 3 Sch. 160 penetration is located at an elevation of 89'-6.85" and azimuth 200 degrees. The safe ends and the penetration nozzle-to-safe end welds are part of the CNV. The valve assembly is welded to the penetration nozzle safe end. The CNV boundary is at the valve assembly-to-safe end welds and the welds are part of the CNV.

3.8.2.1.8 Attachments

The CNV provides lateral and vertical support to the RPV at four locations. Each RPV support rests on the RPV support ledge and is connected with a SB-637 UNS N07718 six-inch diameter, 8 threads per inch (6-8 UN 2A) stud, nut, and washer. The connection is a slotted hole to allow for radial growth of the RPV and the stud prevents lateral motion in the support. The CNV boundary includes the RPV support ledge and attachment weld up to the support surface. The attachment stud and nut are part of the CNV.

Lateral support of the RPV is provided at the CNV inside surface at the bottom of the CNV by an integral guide support. The guide support allows free vertical motion of the RPV, but prevents lateral motion. The CNV boundary is located at the face of the guide support.

Lateral support of the CRDMs is provided by the CNV at the inside diameter of the CRDM access opening in the CNV top head. The CRDM support frame consists of four pieces equally spaced around the opening at azimuth 45 degrees, 135 degrees, 225 degrees, and 315 degrees. Each piece of the frame is welded to the CNV shell and the CRDM access nozzle with full-penetration welds. For the purposes of the CNV, the CRDM support frame is a nonstructural attachment in accordance with ASME Code, Section III, Subarticle NE-1130 because it is not pressure retaining and does not contribute to support of the CNV. The boundary is at the surface of the CNV shell and the weld between the CRDM support frame and the CNV shell is considered part of the attachment.

Various other items are attached to the interior and exterior of the CNV (e.g., decay heat removal system passive condensers, piping supports, access platforms and ladders, and instrument enclosures). For the purposes of the CNV, these items are nonstructural attachments in accordance with ASME Code, Section III, Subsubarticle NE-1130 because they are not pressure retaining and do not contribute to support of the CNV. The boundary is at the surface of the CNV shell and the weld between the attachment and the CNV is considered part of the attachment.

3.8.2.2 Applicable Codes, Standards, and Specifications

3.8.2.2.1 Codes, Standards, and Specifications

1) The following codes, standards and specifications and other independent standards are used in the design, fabrication, testing, and inspections of the CNV:ASME Boiler and Pressure Vessel Code, Section III, "Rules for Construction of Nuclear Facility Components," 2013 Edition with no Addenda (Latest edition for NCA-3800 and NCA-4000 only in accordance with NCA-1140(g))

    a) Subsection NCA, "General Requirements for Division 1 and Division 2"

    b) Subsection NB, "Class 1 Components"

    c) Subsection NE, "Class MC Components"

    d) Subsection NF, "Supports"

    e) Division 1 Nonmandatory Appendix C, "Certificate Holder's Design Report"

    f) Division 1 Nonmandatory Appendix D, "Preheat Procedures"

    g) Division 1 Nonmandatory Appendix G, "Fracture Toughness Criteria for Protection Against Failure"

2) ASME Boiler and Pressure Vessel Code, Section II, "Materials," 2013 Edition

3) ASME Boiler and Pressure Vessel Code, Section V, "Nondestructive Examination," 2013 Edition with no Addenda

4) ASME Boiler and Pressure Vessel Code, Section IX, "Welding and Brazing Qualifications," (Latest Edition and Addenda may be used)

5) ASME Boiler and Pressure Vessel Code, Section XI, "Rules for Inservice Inspection of Nuclear Power Plant Components," 2013 Edition

6) ASME NQA-1-2008/1a-2009, "Quality Assurance Requirements for Nuclear Facility Applications"

7) ASME B16.25-1997, "Buttwelding Ends"

8) ASME Code Case N-759-2, "Alternative Rules for Determining Allowable External Pressure and Compressive Stresses for Cylinders, Cones, Spheres, and Formed Heads, Class 1, 2, and 3, Section III, Division 1"

9) American Society of Mechanical Engineers, ASME NOG-1, "Rules for Construction of Overhead and Gantry Cranes (Top Running Bridge, Multiple Girder)," 2004.

10) ASME Y14.5-2009, "Dimensioning and Tolerancing"

11) Institute of Electrical and Electronics Engineers (IEEE), IEEE Std 323-1974, "IEEE Standard for Qualifying Class 1E Equipment for Nuclear Power Generating Stations"

12) IEEE Std 344-2004, "IEEE Recommended Practice for Seismic Qualification of Class 1E Equipment for Nuclear Power Generating Stations"

13) IEEE Std 384-1992, "IEEE Standard Criteria for Independence of Class 1E Equipment and Circuits"

14) Crane Manufacturers Association of America, CMAA Specification #70-2010, "Specifications for Top Running Bridge and Gantry Type Multiple Girder Electric Overhead Traveling Cranes"

15) American Society for Testing and Materials, ASTM A262 (latest revision), "Standard Practices for Detecting Susceptibility to Intergranular Attack in Austenitic Stainless Steels"

16) American Welding Society, AWS A2.4:2012, "Standard Symbols for Welding, Brazing, and Nondestructive Examination, 7th Edition"

17) Electric Power Research Institute (EPRI), TR-101108, "Boric Acid Corrosion Evaluation (BACE) Program, Phase I – Task 1 Report," December 1993

18) EPRI, NP-5985, "Boric Acid Corrosion of Carbon and Low Alloy Steel Pressure Boundary Components in PWRs," August 1988

19) EPRI, NP-5558-SL, "Boric Acid Application Guidelines for Intergranular Corrosion Inhibition (Rev. 1)," December 1990

20) EPRI 3002000505, "Pressurised Water Reactor Primary Water Chemistry Guidelines," Volume 1, Rev. 7

21) EPRI 1016555, "Pressurized Water Reactor Secondary Water Chemistry Guidelines," Volume 1, Rev. 7

3.8.2.2.2 Code Classification and Compliance

Classification and compliance of the CNV is in accordance with the ASME Boiler & Pressure Vessel Code, (ASME Code). The CNV is an ASME Code Class MC component including:

- access and inspection openings and associated flanges
- penetrations for ECCS trip/reset valves and CIVs
- openings and associated flanges for electrical penetration assemblies

The CNV support lugs use a set-in type design and therefore constitute part of the ASME Code Class MC component. As permitted by ASME Code, Section III, NCA-2134(c), the complete CNV is designed, constructed and stamped as an ASME Code Class 1 vessel in accordance with ASME Code, Section III, Subsection NB, except that overpressure protection is in accordance with ASME Code, Section III, Article NE-7000 in lieu of ASME Code, Section III, Article NB-7000.

The CNV support skirt is classified as an ASME Code Class MC support. The bolting for the RPV upper support ledge is classified as ASME Code Class 1 supports. The top auxiliary mechanical access structure mounting assemblies are in the support load path for the ASME Code Class 2 NPM top auxiliary mechanical access structure and, therefore, are classified as ASME Code Class 2 supports. However, all these items are constructed as ASME Code Class 1 supports in accordance with ASME Code, Section III, Subsection NF.

The CNV materials conform to the requirements of ASME Code, Section III, Article NB- 2000. The CNV fabrication conforms to the requirements of ASME Code, Section III, Article NB-4000 and Article NF-4000. Nondestructive examination of pressure-retaining and integrally attached materials meet the requirements of ASME Code, Section III, Article NB-5000 and Article NF-5000.

3.8.2.3 Loads and Load Combinations

Stresses and fatigue for the CNV pressure retaining components have been evaluated in accordance with ASME Code, Section III, Subsection NB. The loads for which the CNV is designed are:

DW	Deadweight of the CNV which includes the weight of the structure, any internal equipment or piping systems and enclosed water. Deadweight refers to any moments or forces due to the deadweight.
B	Buoyancy provided to the CNV by the reactor pool water.
P_{des}	CNV internal pressure for Design conditions is 1,000 psia. The external pressure for Design conditions is 60 psia.
P	Highest operating pressure load due to normal and abnormal operating conditions resulting from pressure variations either inside or outside the CNV. The lowest internal pressure of less than 0.1 psia during normal operating conditions is also considered. The external pressure during operating conditions is 60 psia.
T_{des}	The CNV temperature for Design conditions is 550 degrees F, and the CNV support temperature for Design conditions is 300 degrees F.
T	The maximum temperature of the CNV during normal operating conditions is 295 degrees F and the minimum temperature is 40 degrees F.

TH	Transient loads due to normal operating conditions and anticipated operational occurrences, infrequent and accident, resulting from thermal and pressure variations either inside or outside the CNV.
EXT	External mechanical loads from structures other than piping, such as support structures and nonstructural attachments to the CNV (e.g., access platforms/ladders, instrument enclosures, etc.).
M	Piping mechanical and thermal loads produced on the nozzle penetrations and safe ends from piping system due to pressure and thermal variations in the piping system.
R	Pressure and transient loads as a result of a steam generator tube failure are evaluated. Dynamic loads as a result of a steam generator tube failure are not significant and not evaluated.
REA	Rod ejection accident (REA) pressure and transient loads are evaluated as a result of a rod being ejected form the core. No loss of the RCS pressure boundary occurs and dynamic loads as a result of a rod ejection are not significant.
LOCA	Loss-of-coolant accident dynamic loads produced by a postulated pipe break on a primary coolant pipe with a break larger than RCS make-up. There are no piping systems in the NPM that fall into this category. So no LOCA loads are evaluated. Pipe breaks and spurious valve openings that occur in the NPM are evaluated as design basis pipe breaks (DBPBs).
MSPB	Main steam pipe break (MSPB) dynamic loads due to a postulated pipe break in the main steam pipe system. Main steam piping inside of the CNV is covered by leak before break so no postulated failures inside of the CNV are considered. Main steam pipe breaks may occur outside of the CNV and are considered.
FWPB	Feedwater pipe break (FWPB) dynamic loads due to a postulated pipe break in the feedwater pipe system. Feedwater piping inside of the CNV is covered by leak before break so no postulated failures inside of the CNV are considered. Feedwater pipe breaks may occur outside of the CNV and are considered.
DBPB	Design basis pipe break other than FWPB, MSPB, or LOCA dynamic loads due to a postulated pipe break or spurious valve actuation of the reactor safety valve, reactor vent valve, or reactor recirculation valve. This includes chemical and volume control system pipe breaks in RPV high point degasification, pressurizer spray, RCS discharge and RCS injection piping inside of containment.
H	Hydrostatic test pressure of a minimum of 1.25 x P_{des} or 1,250 psi and a maximum of 1,325 psi at the lowest point of the CNV. The hydrostatic test is performed at a test temperature greater than 70 °F, but not greater than 140 degrees F.
P_{g1}	Hydrogen detonation short duration (less than 5 msec) pressure pulse of 852 psia resulting from a combustible gas that results from a fuel-clad metal-water reaction followed by an uncontrolled hydrogen burn during a post-accident condition. Evaluated per the rules defined in 10 CFR 50.44, 10 CFR 50.34 and RG 1.7, "Control of Combustible Gas Concentrations in Containment," Revision 3.
P_{g2}	Hydrogen detonation with deflagration-to-detonation transition short duration (less than 5 msec) pressure pulse of 3,834 psia resulting from a combustible gas that results from a fuel-clad metal-water reaction followed by an uncontrolled hydrogen burn during a post-accident condition. Evaluated per the rules defined in 10 CFR 50.44, 10 CFR 50.34 and RG 1.7.
SSE	Safe shutdown earthquake, the CNV is designed to withstand vertical and lateral loading due to seismic ground accelerations considering the appropriate damping values for the CNV in accordance with RG 1.61, "Damping Values for Seismic Design of Nuclear Power Plants," Revision 1. The operating basis earthquake (OBE) is defined as 1/3 of SSE. In accordance with Appendix S of 10 CFR 50, OBE seismic loads need not be explicitly analyzed in the design analysis; however, they are considered in the fatigue analysis.

Pressure Loading

Design of the CNV includes a maximum internal pressure applied to all inside surfaces. The design pressure of 1,000 psia bounds all service level pressures except for hydrostatic test conditions. Hydrostatic test conditions use a minimum pressure of 1.25 times the design pressure (1,250 psia) as specified by ASME Code, Section III, paragraph NB-6221. During normal operating conditions, pressure inside the CNV is maintained at a pressure less than the saturation pressure corresponding to the reactor pool pressure; this results in a vacuum condition. The internal pressure variation that occurs inside the CNV during abnormal conditions is defined by the transient loading.

During normal and abnormal conditions the external design pressure on the CNV is 60 psia.

Seismic Loading

The methodologies and structural models that are used to analyze the dynamic structural response, due to seismic loads acting on the NPM, are described in Appendix 3A.

Blowdown Loading

Short-term transients are those caused by the failure or actuation of Class 1 and 2 piping and valves, and include high-energy line breaks. The evaluation of short-term transients within the NPM is addressed in Appendix 3A. These events potentially result in system internal pressure waves and asymmetric cavity pressurization waves exterior to the pipe break or valve outlet, and require special treatment due to the rapidly changing thermal hydraulic conditions and the resulting dynamic mechanical loads.

Transient Loading

Design basis normal, anticipated operational occurrences, and infrequent events and accident events are categorized into ASME Service Levels (A-D) and evaluated. Section 3.9.1.1 provides the transient categorization and the number of cycles that are anticipated over the design life of the CNV.

Most of the design basis events are simulated using NRELAP5 (see Section 3.9.1.2). Results from the NRELAP5 analysis for representative nodes and control variables for various regions of the CNV are selected to provide representative time history results. Time history pressure, temperature, phase composition, velocity and mass flow rate transient results are provided for various regions inside and outside the CNV up to the outermost isolation valve. A few of the design basis events are simple in nature. Characterization of the time history results for these events can be made based on the event definition and do not require an NRELAP5 analysis in order to adequately analyze the event.

The design basis events that are simulated using NRELAP5 use the NRELAP5 base model. The NRELAP5 base model contains the NPM reactor core, hydraulic regions representing the primary and secondary fluid systems, containment and reactor pool. The NRELAP5 base model include heat structures to simulate heat transfer between the

regions, and both safety and non-safety controls to simulate plant actions and operations. See Section 1.5.1.6 for discussion of validation of the NRELAP5 software and Section 6.2.1.1.1 for further discussion of software's use in CNV analyses.

Time-history thermal analysis data are applied to CNV finite-element thermal models to determine CNV metal temperatures for the design basis events. The resulting temperature gradients in the CNV from the thermal analysis and NRELAP5 pressure transient data are then applied to a CNV structural model to determine stresses on the CNV.

External Environment Loading

The effects of missiles and external events such as a hurricane, tornado, aircraft hazards, and explosion pressure waves are not considered because the CNV is protected from these effects by the Seismic Category I RXB.

Lifting and Transportation

The lifting and handling loads analysis considers the full range of positions during transportation evolution, field installation work, transfer to and from the upender, and installation in the plant. Lifting and handling loads are also considered for the full NPM refueling evolution, including lift and transport of the NPM and its subassemblies using the RXB crane, assembly and disassembly of the CNV and the RPV, and flange fastener tensioning and de-tensioning.

Transportation loads are evaluated with the CNV in the horizontal position. Shipping restraints are installed between the CNV and the RPV at the location of the lateral support lugs at the CNV upper flange.

The lifting, handling, and transportation load contains a 15% dynamic load factor, for a total load of 115% times the DW load applied at all lifting and transportation support points.

Lifting, handling, and transportation loads are not required to meet ASME stress limits. However, the Service Level B primary limits are used as the allowable limits for the lifting, handling, and transportation loads. The platform mounting assemblies are analyzed to ensure minimum safety factors of five for material ultimate strength and three for material yield strength per Reference 3.8.2-3 and are maintained for dual-load-path loading conditions considering the dynamic load factor specified above.

Load Combinations

The ASME Code Design, service level (Level A, Level B, Level C, Level D) and Test loads and load combinations for the CNV and CNV support design are shown in Table 3.8.2-2 and for the CNV bolts are shown in Table 3.8.2-3. The load combinations meet the requirements of ASME Code, Section III, Paragraph NCA-2141(b) and consider the guidance of RG 1.57, "Design Limits and Loading Combinations for Metal Primary Reactor Containment System Components," Revision 2. The loads and load

combinations used in the analysis are a part of the method of evaluation. Alternatives to the RG 1.57 load combinations are discussed below.

Alternatives to Regulatory Guide 1.57 Load Combinations

The load combinations used for the design of the CNV follow the same load combinations specified for the RPV, which follow the guidelines provided in NUREG-0800, Standard Review Plan 3.9.3 for ASME Code Class 1, 2 and 3 components and component supports, and core support structures. These load combinations differ slightly from the suggested load combinations provided in RG 1.57 for metal primary reactor containment system components. Some of the differences are load combination of seismic loads with LOCA loads evaluated to service level C, the service level used in evaluating hydrogen detonation loads and loads resulting from a pipe break, i.e., pipe whip, jetting, etc.

The load combinations provided in RG 1.57 are intended for structures designed, fabricated, inspected, and tested to ASME Code, Section III, Subsection NE requirements. The load combinations used for the CNV are typical load combinations used for vessels designed, fabricated, inspected, and tested to ASME Code, Section III, Subsection NB requirements. Vessel load combinations and allowable limits differ slightly from containment structures because the inspection and testing requirements for vessels are more restrictive, which allows a higher design limit. Justification is provided below why this is acceptable for the CNV.

As previously discussed, during normal operation, the inside of the CNV is maintained under a vacuum and is partially submerged in the reactor pool to just below the upper head. The reactor pool is the ultimate heat sink that removes residual core decay heat during normal and accident conditions. The CNV has a design pressure and temperature of 1,000 psia and 550 degrees F, which is greater than typical pressurized water reactor (PWR) containments. The CNV has a relatively low volume compared to typical large PWR metal containments. The internal volume is 6,144 ft^3 with no internal sub-compartments. The design prevents isolated pockets of concentrated gases. The upper portion of the CNV is fabricated of low-alloy carbon steel with stainless steel cladding on the inside and outside surfaces. The bottom portion of the CNV is fabricated of stainless steel. Typical PWR metal containment structures are constructed from carbon steel plate.

As stated in previous sections, the CNV is an ASME Code, Section III Class MC component; however, the CNV is designed, fabricated, inspected, and tested as an ASME Code, Section III, Subsection NB Class 1 component. The pressure boundary forgings and weld filler materials are tested for mechanical and fracture toughness to the requirements of ASME Code, Section III, Article NB-2000. The CNV is a high-quality, shop-fabricated vessel, fabricated to the requirements of ASME Code, Section III, Article NB-4000, with all low-alloy steel welds post-weld heat treated in the shop. Many ASME Code requirements for an NB Class 1 and a Class MC vessel are similar. However, one significant difference is in preservice weld inspection. The main welds forming the pressure boundary shell are Category A, B and C full-penetration butt welds. In an NB Class 1 vessel, these welds are required to have a volumetric and either liquid penetrant or magnetic particle inspection performed per ASME Code, Section III, Subarticle NB-

5200. The corresponding welds in a Class MC vessel only require a fully radiographed inspection per Subarticle NE-5200.

After fabrication of the CNV is completed, a shop hydrostatic test of the vessel is performed to Article NB-6000 requirements. Prior to hydrostatic testing, 100 percent of the pressure boundary welds are inspected. Inspection is performed in accordance with Subarticle NB-5280 and Subarticle IWB-2200 using examination methods of ASME Code, Section V except as modified by ASME Code, Section III, Paragraph NB-5111. The hydrostatic pressure and temperature are held for a minimum of 10 minutes. The pressure is then decreased to design pressure and held for a minimum of four hours and the CNV is inspected for leaks. After the test is completed, pressure boundary welds are inspected again to the same requirements used prior to the test. The ASME Code, Section III, Article NB-6000 hydrostatic test is performed to a greater pressure than required by Article NE-6000. That is, Paragraph NE-6321 specifies a minimum test pressure of only 110 percent and Paragraph NE-6322 specifies a maximum test pressure of 116 percent. The CNV is tested to a pressure 15 percent greater than conventional steel containment structures and 25 percent greater than design pressure in accordance with NB-6221.

The CNV design pressure and temperature of 1,000 psia and 550 degrees F bounds design basis events including a LOCA. The Design condition pressure exceeds the requirements of ASME Code, Section III, Paragraph NCA-2142.1(a) and NB-3112.1(a) by bounding the most severe Level A service level pressure and the requirements of Paragraph NE-7120(b) by the design not exceeding service limits specified in the design specification.

The design does not have a typical postulated LOCA compared to traditional PWR reactor coolant systems. Reactor coolant in the NuScale design is captured by the CNV and passively recirculated through the RPV and core by the ECCS (see Section 6.3). The reactor coolant level is never below the level of the core and reactor coolant makeup is not required. The reactor coolant piping within the CNV is NPS 2. Secondary-side piping for feedwater and main steam are larger. Breaks in the feedwater and main steam pipes within the CNV are not considered because of leak-before-break design and monitoring. Breaks in these piping systems outside containment are excluded as discussed in Section 3.6.2.5. Pipe breaks for reactor coolant piping inside containment and spurious opening of a reactor safety valve or reactor vent valves are addressed in Appendix 3A. Pipe breaks and spurious valve openings inside the CNV are evaluated as DBPBs. The DBPB load is evaluated to Level C service limits and when combined with SSE loads, is evaluated to Level D service limits. Reactor Coolant System Chemical and Volume Control System (RCS CVCS) line breaks outside of the CNV are evaluated to Level D service limits. Pipe whip and jetting due to a pipe break is mitigated by the integral jet impingement shield and pipe whip restraint (ISR) as described in Section 3.6.5. Therefore, no pipe whip or jetting loads are considered.

The guidelines of RG 1.57 recommend DBPB loads to be evaluated to Level B service limits and DBPB combined with SSE loads to be evaluated to Level C service limits. Because the CNV is designed, fabricated, inspected, and tested as an NB Class 1 vessel, evaluation of these loads to more restrictive allowable limits is conservative. The increased inspection and testing for a Class 1 vessel discussed below offsets the more restrictive allowable limit guidelines provided in RG 1.57.

Regulatory Guide 1.57 provides recommended load combinations and service levels for hydrogen pressure due to 100 percent fuel clad metal-water reaction, hydrogen burn, and post-accident carbon dioxide inerting. The CNV hydrogen detonation event is evaluated to Level C service limits, which bounds pressure due to 100 percent fuel clad metal-water reaction. Hydrogen detonation with deflagration-to-detonation transition is evaluated to Level D service limits and bounds pressure due to hydrogen burn. The CNV design does not include post-accident carbon dioxide inerting; thus any load due to this event is not applicable. Control of hydrogen within the CNV is discussed in TR-0716-50424-P, "Combustible Gas Control," (Reference 3.8.2-4).

Inservice inspection (ISI) provides an essential function for containment system integrity by ensuring no new leakage paths are present. Age-based failure mechanisms are detected and mitigated through the compact and accessible design of the CNV, along with inspections and examinations performed in accordance with ASME Code, Section XI, Division 1. The CNV components and welds are fully capable of being inspected. The CNV design allows for visual inspection of the entire inner and outer surfaces and is designed to accommodate comprehensive inspections of welds, including volumetric and surface inspections. Welds are accessible and there are no areas that cannot be inspected. Periodic, comprehensive ISI ensures that any degradation mechanism is detected and addressed before CNV integrity is threatened.

ASME Code, Section XI, Subsection IWE requires, for Class MC structures, only 80 percent of the containment boundary be accessible for a single-side visual examination for structures, systems, and components subject to normal degradation and aging. This requirement is less restrictive than the examination requirements applied to the NuScale CNV design as discussed below.

Based on the high pressure and the safety function of the CNV, enhanced inspection requirements are needed for the CNV. Therefore, the CNV is inspected to ASME Code NB Class 1 requirements. See Section 3.8.2.7 for CNV inspection requirements. The CNV design allows visual inspection of the entire inner and outer surfaces; therefore, developing an undetected leak through the metal pressure boundary is unlikely.

The CIVs are located outside of the CNV. The reduced ISI requirements permitted by ASME Code, Section XI for small primary system pipe welds between the CNV and the CIVs are not applied to these welds. Welds between the CNV and the CIVs are ASME Code NB Class 1 and are inspected with a volumetric and surface exam at each test interval. The CNV design allows comprehensive inspections of welds, including volumetric and surface inspections. Pressure boundary welds are accessible and there are no areas that cannot be inspected.

The simplicity of the NPM design includes minimizing the number of containment penetrations required. As discussed in Section 3.8.1.2.4 and Section 3.8.1.2.6, the CNV has a limited number of access openings (7), manways (2), and electrical penetration assemblies (11), and each penetration uses the same seal design. The CNV flange separating the upper and lower CNV assemblies uses the same seal design as the RPV, and is similar to the access opening and manway seal designs. As discussed in Section 3.8.1.2.5, there are a limited number of containment fluid line penetrations (14). Eight fluid line penetrations are protected by primary system CIVs; four are each protected by a closed loop and a secondary system containment isolation valve; and two are

protected by a closed loop inside and outside containment. There are no air locks, flexible sleeves, or nonmetallic boundaries in the CNV design.

The containment system meets the underlying intent of 10 CFR 50, Appendix J to ensure leak tightness of the CNV and ensure new leak paths do not develop. This is achieved by the local leak rate testing and ISI performed on the CNV, and is facilitated by the CNV design incorporating the following aspects.

- The CNV is an ASME Code Class 1 pressure vessel with a relatively low volume and no internal subcompartments.
- Preservice test and inspections are similar to RPV requirements, including hydrostatic pressure tests.
- There are no penetrations in the CNV design that would only be tested in a 10 CFR 50, Appendix J, Type A integrated leak rate testing.
- There are a limited number of known leakage pathways, each with similar seal designs, that are tested in accordance with Type B or Type C requirements of 10 CFR 50, Appendix J.
- The ISI Program and planned CNV examinations meet ASME Code NB Class 1 criteria to ensure no new leakage pathways develop.
- Disassembly and reassembly procedures and controls for the CNV are similar to the RPV.

Containment vacuum pressure and leak rate into the CNV are constantly monitored during normal operation. The small containment volume and evacuated operating conditions allow for wide-ranging detection capabilities for liquid or vapor leakage. Automatic engineered safety feature actuation systems initiate on high containment pressure; therefore, containment pressure is maintained below 9.5 psia during operations.

In summary, the CNV is made of corrosion-resistant materials, has a low number of penetrations (26 Type B, 8 Type C), and no penetrations have resilient seals. All penetrations are either ASME Code, Section III NB Class 1 flanged joints capable of 10 CFR 50, Appendix J, Type B testing or NB Class 1 welded nozzles with isolation valves capable of 10 CFR 50, Appendix J, Type C testing. The use of welded nozzles and testable flange seals at the containment penetrations ensure that 10 CFR 50 Appendix J Type B and Type C testing provides an adequate assessment of overall containment leak rate.

Use of typical RPV load combinations for Class 1 vessels is more applicable to the CNV than using the load combinations specified in RG 1.57 because of the increased quality of the fabrication, inspection, and testing required by ASME Code, Section III, Subsection NB for a Class 1 vessel. The intent of RG 1.57 is satisfied by evaluating LOCAs, hydrogen burn, and seismic loads. Evaluations of these loads are to allowable limits, which provide a design that performs its intended function during design basis events.

3.8.2.4 Design and Analysis Procedures

The CNV design and analysis conform to the requirements of ASME Code, Section III, Subarticle NB-3200 and the CNV support design and analysis conform to the requirements of Subarticle NF-3200. The CNV fabrication conforms to the requirements of Article NB-4000 and Article NF-4000. Nondestructive examination of pressure retaining and integrally attached materials meet the requirements of Article NB-5000 and Article NF-5000.

Detailed analyses of ASME Code primary stresses for the CNV use a combination of standard text book hand calculations for simple structures, such as nozzles, and the ANSYS (Reference 3.8.4-3) general purpose finite element program for more complex geometry, such as the CNV top head. Other ASME Code evaluations are performed using ANSYS. Buckling of the torispherical lower head is evaluated using ASME Code Case N-759-2 (See Section 3.8.2.2.1). Alternatively, limit analyses to determine lower bound limit buckling loads may be employed in lieu of Code Case N-759-2.

The CNV ANSYS models used for structural analysis use three-dimensional solid elements for the analysis. Mesh discretization is chosen to ensure adequate representation of the controlling stresses in key design regions.

Stress analyses are performed using the load combination defined in Section 3.8.2.3. The allowable limits are in accordance with ASME Code, Section III, Subarticle NB-3200 and NF-3200. Allowable limits are based on the mean metal temperature for the applicable service level or a conservative higher temperature, i.e., design temperature.

Computer code verification, validation, configuration control, and error reporting and resolution are performed according to the quality assurance requirements of Chapter 17.

3.8.2.4.1 Containment Vessel Stress Analysis

The CNV is evaluated for deadweight, buoyancy, internal pressure, blowdown loads, seismic, thermal, and pressure transient loads.

Minimum wall thickness for nozzles on the CNV shell, nozzle reinforcement, and limits of reinforcement along the CNV wall and normal to the CNV wall are in accordance with ASME Code, Section III, Subarticle NB-3300. If rules of NB-3300 are not satisfied, then Subarticle NB-3200 design by analysis is applied as permitted by Paragraph NB-3331(c).

Integrity of the pressure-retaining function of the CNV is provided by compliance with the ASME Code. The evaluation of the stress levels and fatigue usage for the CNV pressure boundary is calculated for the specified loading conditions discussed in Section 3.8.2.3 and demonstrates that the values are less than the allowable limits.

The CNV shell, top head, and bottom head are evaluated for buckling during normal operating conditions. During normal operating conditions, a vacuum exists inside the CNV which causes an external pressure on the outside surface of the

CNV. Also, during a Level D seismic event, the CNV sees a vertical compressive load which is also checked for buckling. Buckling checks are made using ASME Code Case N-759-2. Alternatively, limit analyses to determine lower bound limit buckling loads may be employed in lieu of Code Case N-759-2.

Additionally, buckling is checked on the inside knuckle region of the top head and bottom head. Internal pressure causes compression in the knuckle which is checked using hand calculation based on equation 4.3-19 from ASME Code, Section VIII, Division 2.

Piping and electrical penetrations are evaluated using the loads and load combinations discussed in Section 3.8.2.3. The effects of the penetration loads on the CNV top head shell are also evaluated.

Stress and fatigue results are evaluated in accordance with ASME Code, Section III, Subarticle NB-3200 limits. The fatigue analysis of the CNV process fluid penetrations considers the effects of the PWR environment in accordance with RG 1.207, "Guidelines for Evaluating Fatigue Analyses Incorporating the Life Reduction of Metal Components Due to the Effects of the Light-Water Reactor Environment for New Reactors," Revision 0, and NUREG/CR-6909. The ASME Code design report summarizes the results of the CNV analyses and evaluations.

3.8.2.4.2 Containment Vessel Lateral Support Lugs

The CNV is supported in the RXB reactor pool by lateral support lugs located on the CNV upper shell. The CNV lateral support lugs are attachments to the CNV, as defined by ASME Code, Section III, Paragraph NB-1132.1(a), and use the rules of ASME Code, Section III. The lateral support lugs are constrained by the NPM lug restraints located on the NPM bay walls. The loads and load combination discussed in Section 3.8.2.3 are used to evaluate the CNV support lug. Stress and fatigue results are evaluated in accordance with Subarticle NB-3200 limits.

3.8.2.4.3 Containment Vessel Lower Support

The bottom of the CNV is supported vertically and laterally by the CNV support skirt. The CNV support skirt is an ASME Code Class MC support that is constructed as an ASME Code, Section III Class 1 support in accordance with the requirements of Article NF-4000. The support skirt is located below the CNV bottom head and includes two parts that are welded together: the support bearing flange and the support skirt ring. Lateral restraint is provided by contact with a metal ring called the passive skirt support, which is attached to the reactor pool floor. Vertical support is provided by bearing on the reactor pool floor. The loads and load combination discussed in Section 3.8.2.3 are used to evaluate the CNV support skirt. Stress and fatigue results are evaluated in accordance with ASME Code, Section III, Subarticle NF-3200 limits.

3.8.2.4.4 Containment Vessel Reactor Pressure Vessel Supports

Internal to the CNV, the RPV is supported by the CNV using RPV upper support ledges that are located in the CNV upper section. The RPV supports are connected

to the CNV reactor pressure vessel upper support ledges located on the inner wall of the CNV by studs at each connection. The loads and load combination discussed in Section 3.8.2.3 are used to evaluate the CNV reactor pressure vessel upper support ledge. Stress and fatigue results are evaluated in accordance with ASME Code, Section III, Subarticle NF-3200 limits.

3.8.2.4.5 Containment Vessel Ultimate Capacity

A series of non-linear (plastic) 3-dimensional finite element analysis were performed to determine the ultimate pressure capacity of the CNV; the analyses conform to the guidance provided in Appendix A of NUREG/CR-6906 (Reference 3.8.2-2). The failure criteria that determine the ultimate pressure capacity of the CNV are based on guidance provided in RG 1.216, "Containment Structural Integrity Evaluation for Internal Pressure Loadings Above Design-Basis Pressure," Revision 0. Technical report TR-0917-56119, CNV Ultimate Pressure Integrity (Reference 3.8.2-7), addresses the details of the predicted containment internal pressure capacity above design pressure. The CNV is assumed to fail when one of the following criteria is met:

A. A maximum global membrane strain away from discontinuities of 1.5 percent is reached.

B. Loss of bolt preload occurs at any bolted CNV opening.

C. Buckling occurs in the knuckle of the upper or lower CNV head due to internal pressure.

D. A flange gap greater than 0.03 inches is reached at the outer O-ring of any bolted CNV opening.

A series of ANSYS finite element models using three-dimensional solid elements were developed to represent the various aspects of the CNV to evaluate the failure criteria above. The closure flange and all bolted covers greater than NPS 18" were modeled including the studs and nuts. Studs preload is applied prior to applying the pressure load. Key assumptions used in the analysis are provided in Table 3.8.2-4.

The stud preload is applied at ambient temperature. The CNV design temperature of 550 degrees Fahrenheit is then used for the thermal conditions in the ultimate pressure capacity analysis. The thermal condition as a result of a design basis pipe break or spurious valve actuation will result in an elevated temperature below the design temperature for a short period. The ultimate heat sink cooling of the reactor pool will keep fasteners and outside surface wall temperature at the reactor pool temperature. Joint tightness is maintained using the design temperature and will remain as tight or tighter during the design basis events as a result of differences in thermal expansion between the flange and stud.

The plastic modulus of the materials are determined at the design temperature and shown to be below the materials true stress - true strain curve based on ASME Code minimum properties at design temperature. The average material temperature is

expected to be below design temperature. So additional strain hardening will be present in the material during the design basis event.

Initial yielding of the CNV steel shell (not including cladding), away from discontinuities, occurs in the CNV core region in the bottom section midway between the refueling flange and transition shell region at a pressure of approximately 1,400 psi. The maximum total hoop strain of 1.5 percent for criteria A is reached in the same CNV shell location, away from discontinuities, at a pressure of approximately 1,750 psi.

Sufficient bolt preload is applied so that a tight joint is maintained for all joints for a pressure of 2,200 psi or higher. So criteria B is satisfied and bolt preload will not be overcome below the ultimate pressure shown below.

A linear (eigenvalue) buckling analysis using full-static structural models was performed to demonstrate the torispherical CNV top and bottom head would not fail by buckling from a hoop compression zone in the knuckle region due to an internal pressure. Load multipliers (eigenvalues) calculated for the first 10 buckling modes (and corresponding buckling pressures) were negative, demonstrating that the top and bottom heads do not fail due to buckling when subjected to internal loads. Conservative hand calculations were also used to evaluate buckling in the knuckle to confirm the eigenvalue buckling analyses. The hand calculation showed buckling would not occur until a significant pressure of 4,556 psi or higher. This evaluation satisfies criteria C above.

The pressure needed to open a gap of 0.03 inches at the outer O-ring seal for criteria D above is evaluated for the pressurizer access cover, steam generator inspection access cover, CRDM access cover, CRDM power cover, top head manway cover, and refueling closure flange. The pressurizer access cover is determined to be the most limiting location and a flange gap of 0.03 inches is reached at the outer O-ring of the pressurizer access flange at an approximate pressure of 1,240 psi.

As discussed above, criterion D is limiting resulting in the ultimate pressure capacity of the CNV at 1,240 psi. This pressure is assumed to be the initiation of the CNV failure. The seal of the outer O-ring at the joint will be lost as a result of closure head expanding outward and prying open the joint. The stud preload is maintained and a tight joint would still exist with compression of the flanges past the O-ring seal. Only minor leakage can occur through the compressed flanges. As pressure continues to increase the prying action will continue until the first fastener fails as a result of the prying. Once the initial fastener fails the remaining fasteners will immediately pick up the load that was carried by the failed fastener. The adjoining fastener to the failed fastener will then become overstressed and quickly fail, followed by the next fastener until the fasteners un-zip and the cover is lost.

3.8.2.4.6 Containment Vessel Radiation Exposure Effects

The materials of construction of the lower CNV do not lend themselves to fracture toughness concerns resulting from radiation degradation effects. Further discussion is provided in Section 6.2.7.

3.8.2.4.7 Containment Vessel Cyclic Fatigue

The CNV is evaluated for fatigue based on the ASME Code, Section III, Paragraph NB-3222. Applicable cyclic, dynamic, pressure, and thermal transient loads and load combinations discussed in Section 3.8.2.3, are considered in the fatigue evaluation. For CNV process fluid penetrations classified as ASME Code Class 1, the fatigue analysis considers the effects of the PWR environment in accordance with the requirements of RG 1.207 and NUREG/CR-6909.

In accordance with 10 CFR 50, Appendix S, OBE seismic loads need not be explicitly analyzed in the design analysis; however, they are considered in the fatigue analysis. The OBE load is defined as one-third of the SSE loads.

During the life of the plant, at least one SSE and five OBEs with 10 maximum stress cycles per event are assumed. The fatigue analysis may consider one of the following.

- Two SSE events with 10 maximum stress cycles each for a total of 20 full cycles. This is considered equivalent to the cyclic load basis of one SSE and 4 OBEs.
- The number of fractional vibratory cycles equivalent to that of 20 full SSE vibratory cycles may be used (but with an amplitude not less than the OBE) when derived in accordance with IEEE Std. 344-2004 (see Section 3.8.2.2.1), Annex D. When this method is used and if the amplitude of the vibration is taken as the OBE, then ($3^{2.5}$ x 20)= 312 fractional amplitude SSE cycles are considered.

3.8.2.5 Structural Acceptance Criteria

The CNV structural integrity acceptance criteria limits are developed in accordance with ASME Code, Section III, Subarticle NB-3200 and Subarticle NF-3200 for plate-type and shell-type supports for the CNV support. The ASME Code limits for the defined load combinations is shown in Table 3.8.2-2 and Table 3.8.2-3. The CNV is also fabricated, installed and tested according to ASME Code, Section III, Subsection NB and Subsection NF.

In addition, the CNV is designed to meet the maximum leakage rate as discussed in Section 6.2. The items that form the CNV pressure boundary and support are stamped in accordance with the applicable section of the ASME Code used for their design or fabrication.

3.8.2.6 Materials, Quality Control, and Special Construction Techniques

The CNV materials conform to the requirements of Article NB-2000. The CNV fabrication conforms to the requirements of Article NB-4000 and Article NF-4000. The quality control program involving materials, welding procedures, and nondestructive examination of welds conforms with Subsection NB-2000, NB-4000 and NB-5000 of the ASME Code. The CNV uses no special construction techniques. The materials of construction are shown in Table 6.1-1 and Table 6.1-2.

3.8.2.7 Testing and Inservice Inspection Requirements

Nondestructive examination of the CNV pressure-retaining and integrally attached materials meet the requirements of ASME Code, Section III, Article NB-5000 and NF-5000 using examination methods of ASME Code Section V except as modified by NB and NF.

A non-destructive examination plan will be prepared and implemented for the examinations to be performed to satisfy the fabrication and preservice examination requirements of ASME Code, Section III, Article NB-5000 and Article NF-5000, as applicable, and Section XI.

All surfaces to be clad are magnetic particle or liquid penetrant examined in accordance with ASME Code, Section III, Paragraph NB-2545 or NB-2546 prior to cladding.

For those CNV pressure boundary items defined as ASME Code, Section III, Class 1, preservice examinations are in accordance with ASME Code, Section III, Subsubarticle NB-5280 and ASME Section XI, Subarticle IWB-2200 using examination methods of ASME Code, Section V except as modified by NB-5111. These preservice examinations include 100 percent of the pressure boundary welds. Final preservice examinations are performed after hydrostatic testing but prior to code stamping.

In-service inspection of the CNV is performed as described in Section 6.2.1.6.

Each Type B penetration is local leak-rate tested in accordance with 10 CFR 50, Appendix J prior to performance of the hydrostatic test. For electrical penetration assemblies, this only includes the flange seals. The sheath modules are tested as part of another specification.

The test pressure is the containment peak accident pressure. The leak rate is established by containment leakage rate program.

Pneumatic testing at a pressure not to exceed 25 percent of design pressure may be applied prior to a hydrostatic test, as a means of locating leaks, in accordance with ASME Code, Section III, Paragraph NB-6112.1(b).

Hydrostatic testing of the CNV is done in accordance with the requirements of NB-6000. The CNV is pressurized using water to a minimum pressure of 1,250 psig and a maximum pressure of 1,325 psig, the pressure being measured at the bottom of the CNV. The test is performed with the CNV at a minimum temperature of 70 degrees F and a maximum temperature of 140 degrees F. Following a minimum time of 10 minutes at the hydrostatic test pressure, pressure is reduced to design pressure and held for at least four hours before examining for leaks.

If the CNV is hydrostatically tested with the RPV installed, both primary and secondary sides of the RPV are vented to the CNV to preclude a differential pressure external to the RPV greater than considered for design of the RPV.

The hydrostatic test procedure includes measures for sampling the test fluid (water) which contacts the CNV during hydrostatic testing.

Drain water is tested following hydrostatic testing for compliance with the purity requirements. The hydrostatic test procedure includes corrective actions to be taken (e.g. circulating flushes or fill and drains) in the event the exit fluid exceeds purity requirements.

Immediately following hydrostatic testing, the CNV is drained and dried by circulating air until the exit air dew-point temperature is less than 50 degrees F. The circulating air is oil free and does not to contain combustion products from the heating source. The temperature of the dry heated air is controlled to preclude damage to the SGs due to excessive differential temperature.

The shop hydrostatic tests of the CNV are witnessed by an authorized nuclear inspector and a NuScale inspector.

No leakage indications at the examination pressure are acceptable.

3.8.2.8 References

3.8.2-1 NUREG/CR-6909, "Effect of LWR Coolant Environments on the Fatigue Life of Reactor Materials," Draft Report for Comment

3.8.2-2 NUREG/CR 6906, "Containment Integrity Research at Sandia National Laboratories - An Overview," July 2006

3.8.2-3 ANSI N14.6-1993 "for Radioactive Materials - Special Lifting Devices for Shipping Containers Weighing 10000 Pounds (4500 kg) or More"

3.8.2-4 NuScale Technical Report TR-0716-50424-P, Rev 0, “Combustible Gas Control”

3.8.2-5 ANSYS Computer Program, Release 15.0, October 2013. ANSYS Incorporated, Canonsburg, Pennsylvania

3.8.2-6 IEEE Std. 317-1983, Standard for Electric Penetration Assemblies in Containment Structures for Nuclear Power Generation Stations

3.8.2-7 NuScale Technical Report TR-0917-56119, Rev 0, "CNV Ultimate Pressure Integrity"

Table 3.8.2-1: Design and Operating Parameters

Parameter	Value
Upper vessel diameter (uncladded) (approximate)	177 in.
Lower vessel diameter (approximate)	135 in.
Height from support base to crown of CNV top head cover (top auxiliary mechanical access structure not included) (approximate)	76 ft
Bottom of CNV building elevation (reactor pool floor)	25 ft
Top of CNV elevation (approximate)	101 ft
Design internal pressure	1,000 psia
Design temperature	CNV: 550 °F Support Skirt: 300 °F
External design pressure	60 psia(2)
Normal operating internal pressure (nominal)	See Note 1
Normal operating external pressure (nominal)	60 psia(2)
Normal operating temperature (nominal)	295 °F
Materials	See Table 6.1-1 and Table 6.1-2.

Notes:

1) Pressure inside the CNV is maintained less than the saturation pressure corresponding to the reactor pool pressure; this results in a vacuum condition less than 0.1 psia.

2) Includes reactor pool water static head pressure for a depth of 100 feet.

Table 3.8.2-2: Load Combinations for Containment Vessel and Support ASME Code Stress Analysis

Plant Event	Service Level[2]	Load Combination[3],[9]	Allowable Limits[4]
Design	Design	DW + P_{des} + B + EXT + M	NB-3221 NF-3221.1
CNV hydrostatic test	Test	DW + H + B + EXT + M	NB-3226 NF-3221.3
Normal operations	A	DW + P + B + EXT + M + TH	NB-3222 NF-3221.2
Transients[1]	B	DW + P + B + EXT + M + TH	NB-3223 NF-3221.2
Transients + OBE[1]	B	DW + P + B + EXT + M + TH ± OBE	NB-3223 NF-3221.2
Design basis pipe breaks	C	DW + P + B + EXT + M + DBPB[5]	NB-3224 NF-3221.2
Hydrogen detonation	C	DW + P_{g1} +B	NB-3224 NF-3221.2
Steam generator tube failure[7]	C	P + DW + B + EXT + M +R	NB-3224 NF-3221.2
Rod ejection accident	D	P + DW + B + EXT + M + REA	NB-3224 NF-3221.2[8]
MSPB and FWPB	D	DW + P + B + EXT + M + MSPB/FWPB[5]	F-1331 NF-3221.2
SSE + DBPB/MSPB/FWPB	D	DW + P + B + EXT + M ± SRSS(SSE + DBPB/MSPB/FWPB)[5]	F-1331 NF-3221.2
Hydrogen detonation with DDT[6]	D	DW + P_{g2} + B	F-1331 NF-3221.2

Notes:

1) Fatigue analysis of applicable items is evaluated in accordance with ASME Code, Section III, considering the effects of the PWR environment in accordance with RG 1.207 and NUREG/CR-6909. The OBE loading is only applicable to the fatigue analyses.
2) For supports, service limits meet RG 1.124, Rev 3 and RG 1.130, Rev 3, as applicable.
3) Applicable loads are consistent with those recommended by NUREG-0800, Standard Review Plan (SRP) 3.9.3.
4) Allowable limits are as defined in the applicable subsection of ASME Code, Section III for the specified level.
5) Dynamic loads are combined considering the time phasing of the events in accordance with RG 1.92, Rev 3 and NUREG-0484, Rev 1.
6) DDT- deflagration-to-detonation.
7) Dynamic load due to steam generator tube failure is considered. Pressure and thermal transient response applies.
8) In accordance with NUREG-0800, SRP 15.4.8, Acceptance Criterion 2.
9) Acronyms are defined in Section 3.8.2.3.

Table 3.8.2-3: Load Combinations for Containment Vessel Bolt ASME Code Stress Analysis

Plant Event	Service Level [2]	Load Combination[3][9]	Allowable Limits[4]
Design	Design	DW + P_{des} + B + EXT + M	NB-3231
CNV hydrostatic test	Test	DW + H + B + EXT + M	NB-3232
Normal operations	A	DW + P + B + EXT + M + TH	NB-3232
Transients[1]	B	DW + P + B + EXT + M + TH	NB-3233
Transients + OBE[1]	B	DW + P + B + EXT + M + TH ± OBE	NB-3233
Design basis pipe breaks	C	DW + P + B + EXT + M + DBPB[5]	NB-3234
Hydrogen detonation	C	DW + P_{g1} +B	NB-3234
SG tube failure[7]	C	DW + P + EXT + M + R	NB-3234
Rod ejection accident	D	DW + P + B + EXT + M + REA	NB-3234[8]
MSPB and FWPB	D	DW + P + B + EXT + M + MSPB/FWPB[5]	F-1335
SSE + DBPB/MSPB/FWPB	D	DW + P + B + EXT + M ± SRSS(SSE + DBPB/MSPB/FWPB)[5]	F-1335
Hydrogen detonation with DDT[6]	D	DW + P_{g2} + B	F-1335

Notes:

1) Fatigue analysis of applicable items is evaluated in accordance with ASME Code, Section III. OBE loading is only applicable to the fatigue analyses.
2) For supports, service limits meet RG 1.124, Rev 3, and RG 1.130, Rev 3, as applicable.
3) Applicable loads are consistent with those defined in ASME Code, Section III.
4) Allowable limits are as defined in the applicable subsection of ASME Code, Section III, for the specified level.
5) Dynamic loads are combined considering the time phasing of the events in accordance with RG 1.89, Rev 1, and NUREG-0484, Rev 1.
6) DDT - deflagration-to-detonation.
7) Dynamic load to steam generator tube failure. Pressure and thermal transient response applies.
8) In accordance with NUREG-0800, SRP 15.4.8, Acceptance Criterion 2.
9) Acronyms are defined in Section 3.8.2.3.

Table 3.8.2-4: Key Assumptions for CNV Ultimate Pressure Analysis

Assumption	Basis
O-rings used to seal the CNV bolted openings are assumed to be of the self-energizing O-ring type or similar. Therefore, for flanged openings on the CNV, zero compression pressure is required to produce a seal.	Bolted openings on the CNV are designed for two self-energizing O-rings. By definition, the self-energizing O-rings and gaskets do not require compression pressure to produce a seal.
The maximum allowable gap between flanges (or flange cover - top of flange) at the center of the outer O-ring is assumed to be 0.03 inch.	The maximum allowable gap is based on a review of O-ring groove depth tolerances for several O-ring manufacturers.
The stud preload is assumed to be applied at cold conditions via direct tension. Thermal stress relaxation effects are not considered in this calculation.	The studs are tensioned while in the refueling bay filled with reactor pool water. This establishes the cold conditions for tensioning. The stud preloads are based on two-thirds of yield strength, which produces the maximum preload for the stud. This preload is large enough to prevent loss of preload at thermal conditions seen by the stud and still maintain margin.
The static coefficient of friction is 0.2 for wet steel.	The coefficient of friction of wet steel is conservatively assumed to be equal to that of greased steel. A lower coefficient of friction results in conservative flange gap values.
CNV components on the outer surface, electrical penetrations, Control Rod Drive Mechanism (CRDM) support frame, and piping penetrations such as feedwater lines, steam lines, valves, etc., do not affect the ultimate pressure capacity of the CNV and can be excluded from finite element analysis models.	The steam and feedwater lines do not form part of the CNV pressure boundary. Per the guidance in Appendix A of NUREG/CR-6906 (Reference 3.8.2-2), small CNV penetrations can be reasonably ignored in terms of their effect on the overall containment response. The proximity of these penetrations to CNV bolted openings is judged not to negatively impact the ultimate pressure capacity of the CNV. Because the force on a bolted flange cover is proportional to the square of the diameter on which the pressure acts, it is reasonable to assume that the larger diameter bolted openings will fail before smaller diameter bolted openings.
Mechanical properties of all CNV welds are at least equal to the properties of the parent material and failure of the CNV will not occur at the welds or in the heat affected zone of the parent material.	Per normal practice, welds will be post weld heat treated to minimize residual stresses at or near the welds.
The dead weight of the NuScale Power Module (NPM) access platform, including instrumentation does not negatively affect the ultimate pressure capacity of the CNV and is excluded from the model.	The weight of the NPM access platform is transferred to the CNV via four platform mount supports on the CNV top head, mainly resulting in shear loads on four areas on the outside surface of the CNV top head. These loads are small relative to the hoop stress induced in the CNV at the design pressure.
Buckling will not occur if the first ten load multipliers (eigenvalues) based on the first ten buckling mode shapes for a linear (eigenvalue) buckling analysis are negative. Positive load multipliers correspond to internal pressure in this analysis.	The first buckling mode shape always yields the lowest load multiplier. Therefore, additional buckling mode shapes generate higher load multipliers. If the first ten mode shapes yield load multipliers that are all negative, it is highly unlikely that additional mode shapes will yield positive load multipliers.

Figure 3.8.2-1: Containment Vessel Components and Building Elevations

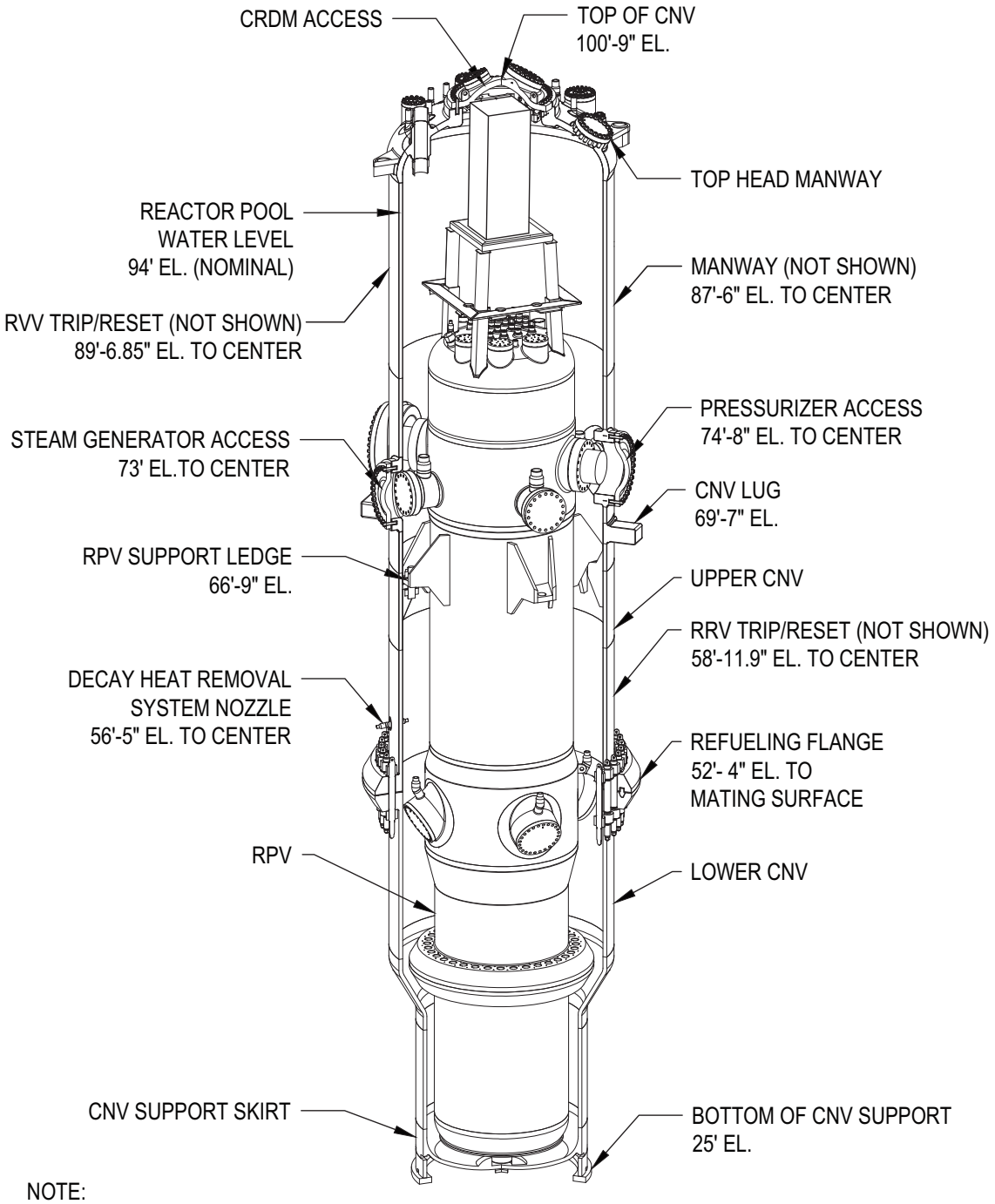

NOTE:
1. ALL DIMENSIONS ARE APPROXIMATE.

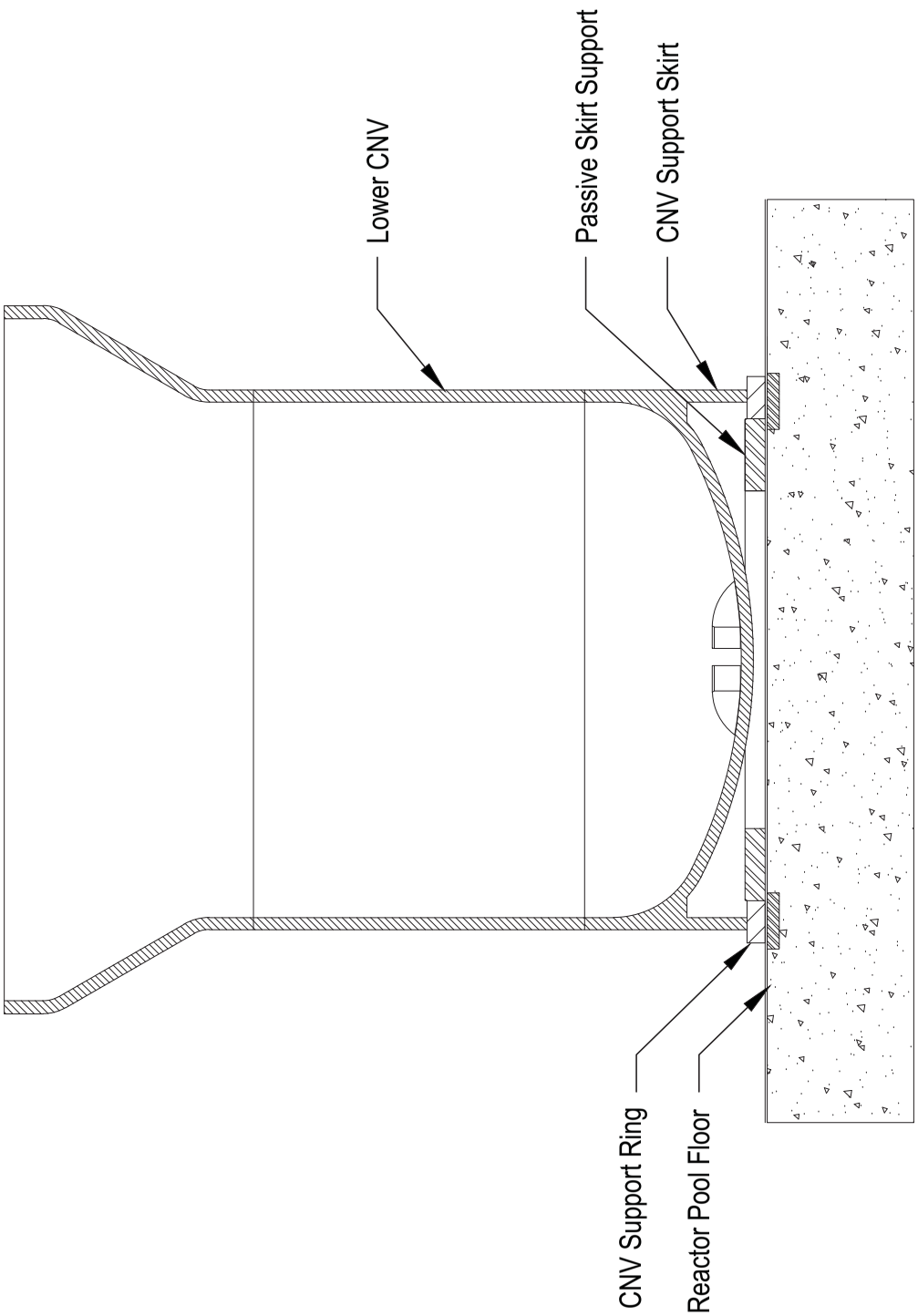

Figure 3.8.2-2: Passive Support Skirt

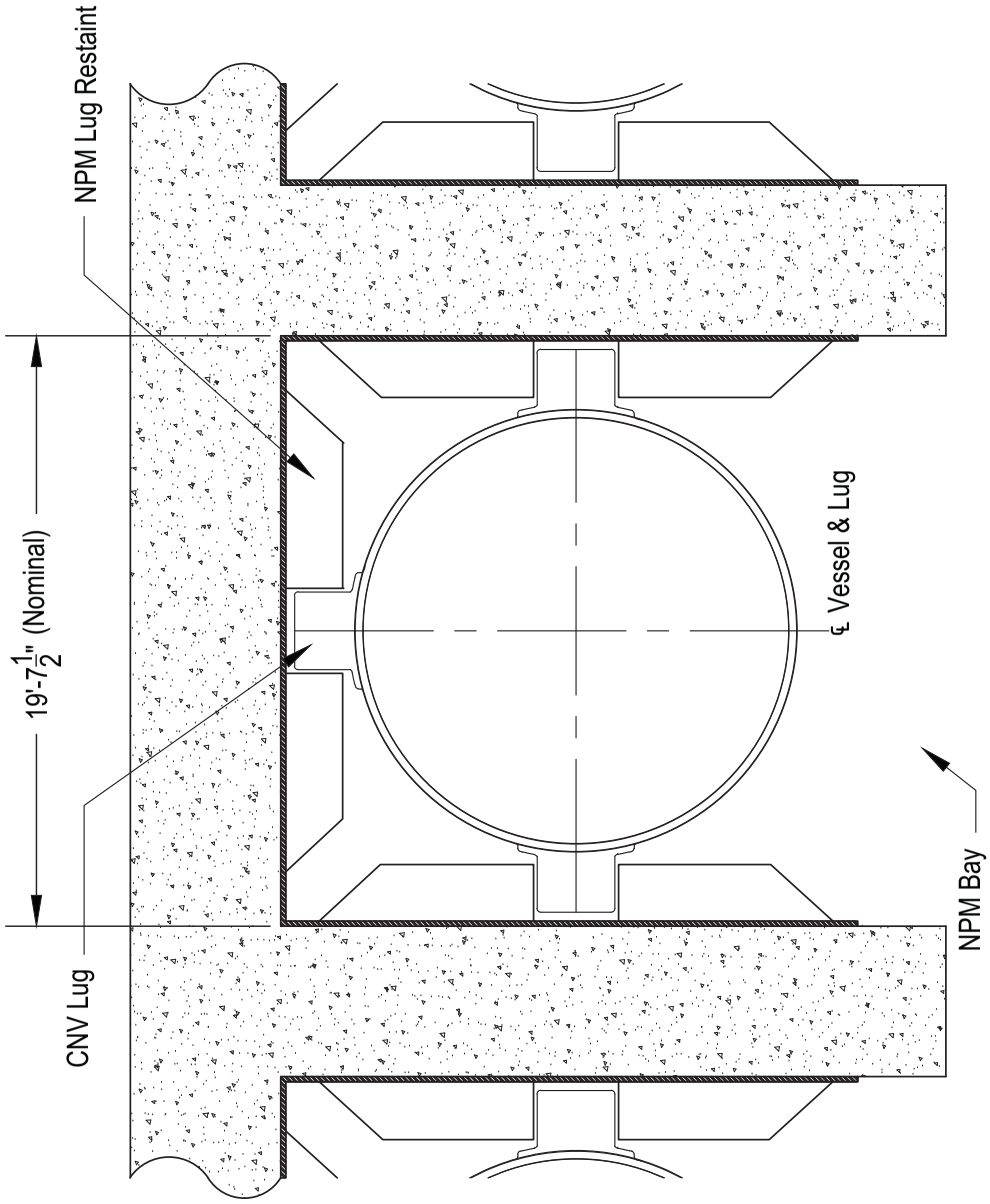

Figure 3.8.2-3: Containment Vessel Lateral Lug Located within the NuScale Power Module Lug Restraints

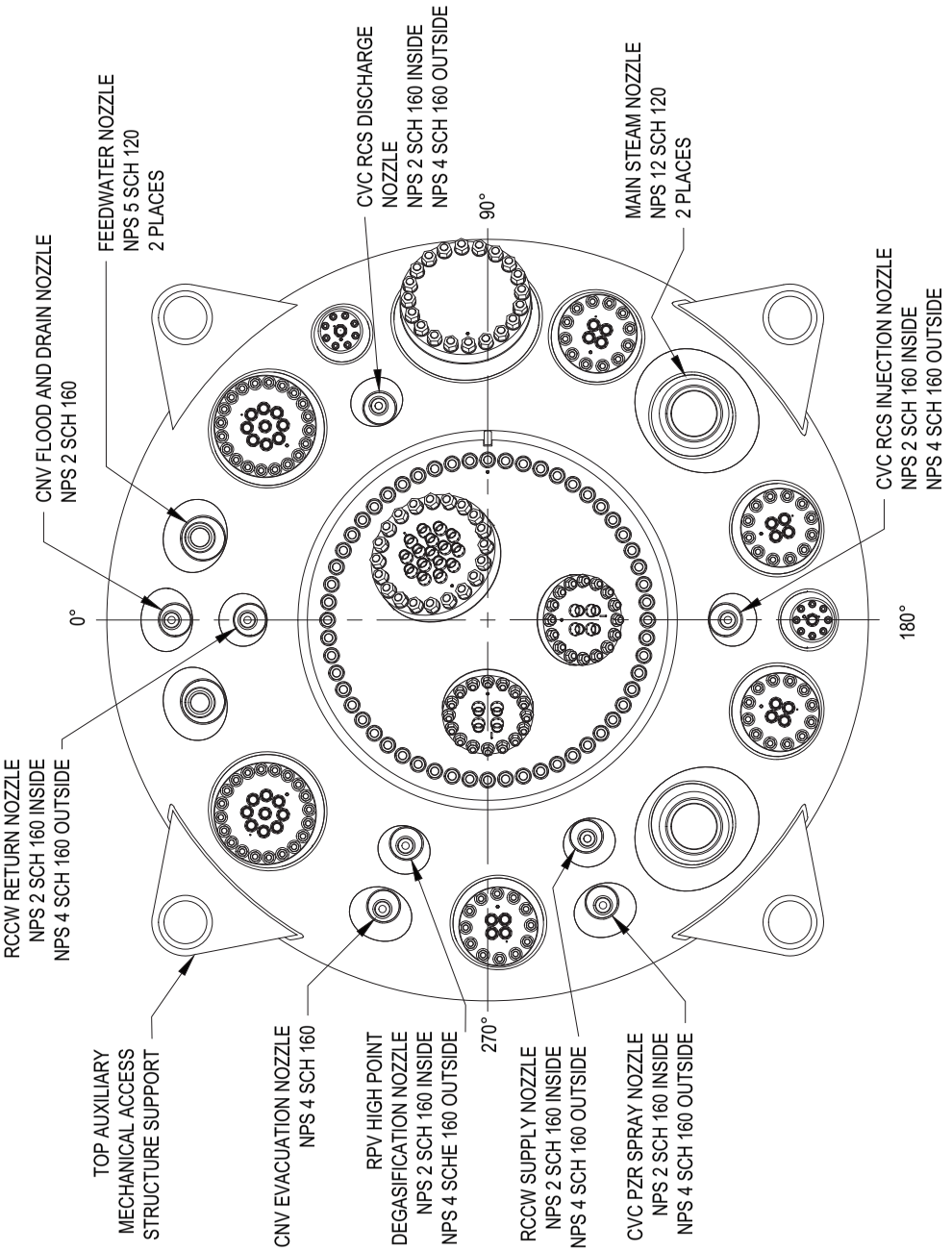

Figure 3.8.2-4: Containment Vessel Top Head Mechanical Penetrations

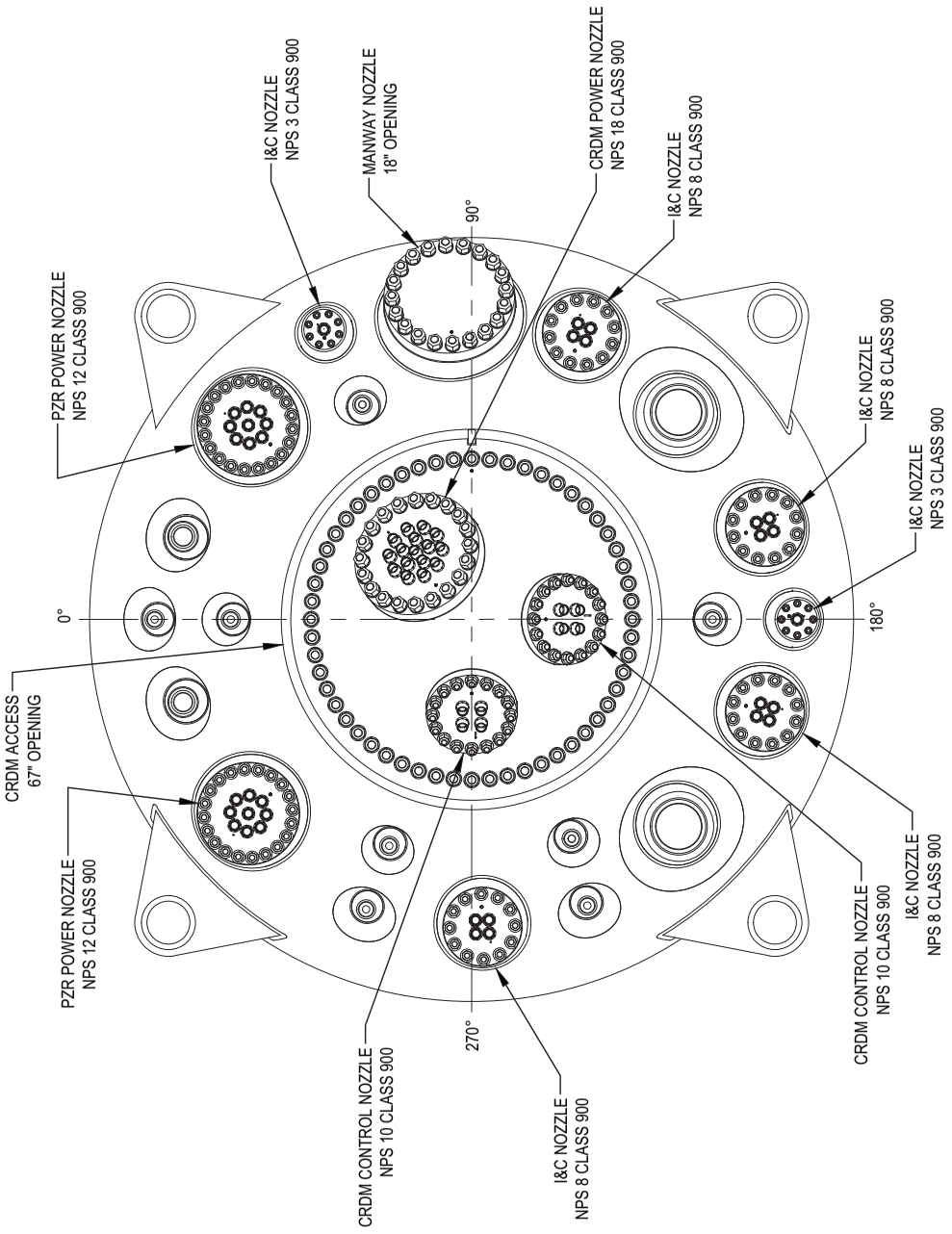

Figure 3.8.2-5: Containment Vessel Top Head Instrumentation and Controls, Electrical, and Access Penetrations

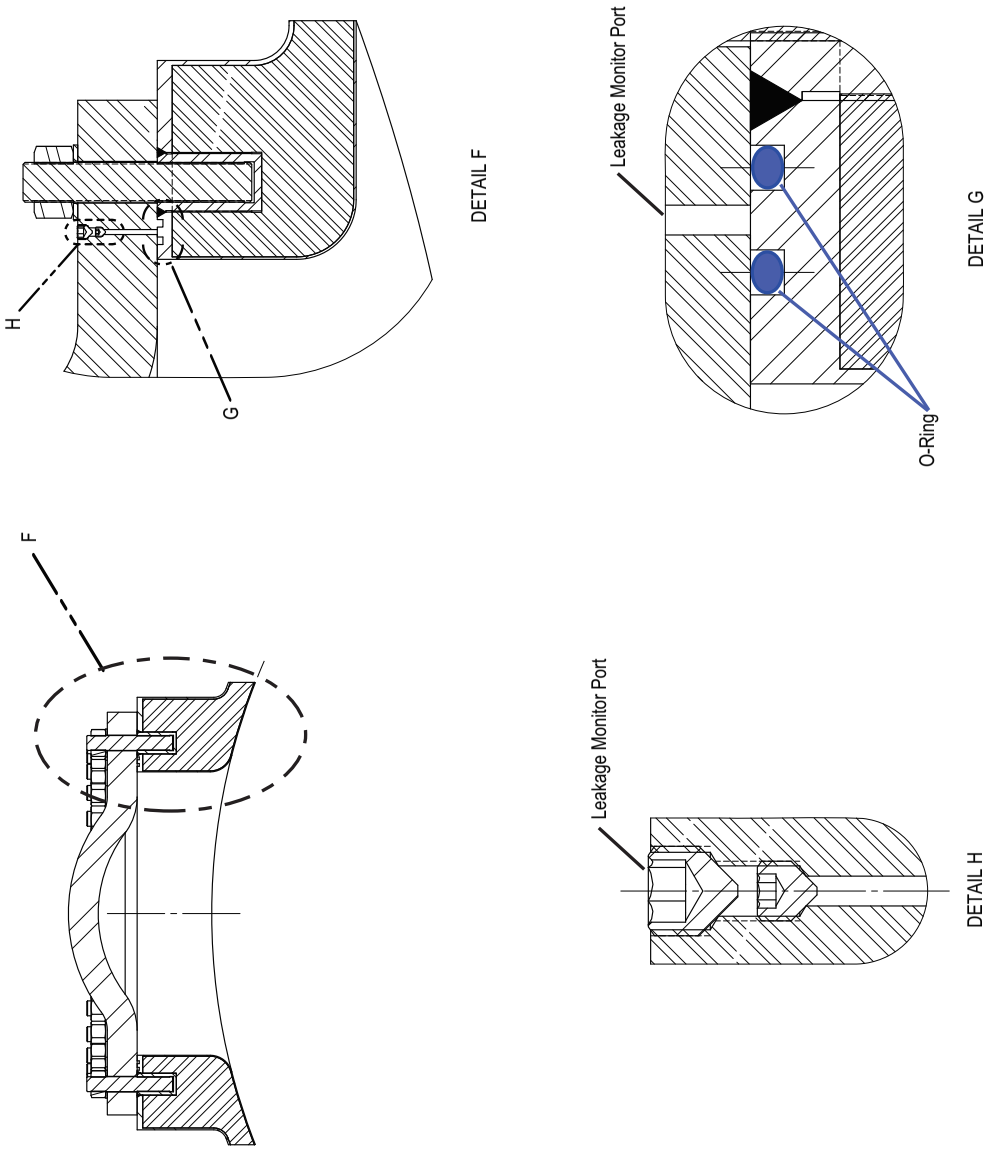

Figure 3.8.2-6: Typical Access Cover and O-Ring Seals

Figure 3.8.2-7: Typical Non Secondary Side Containment Vessel Penetration Configuration

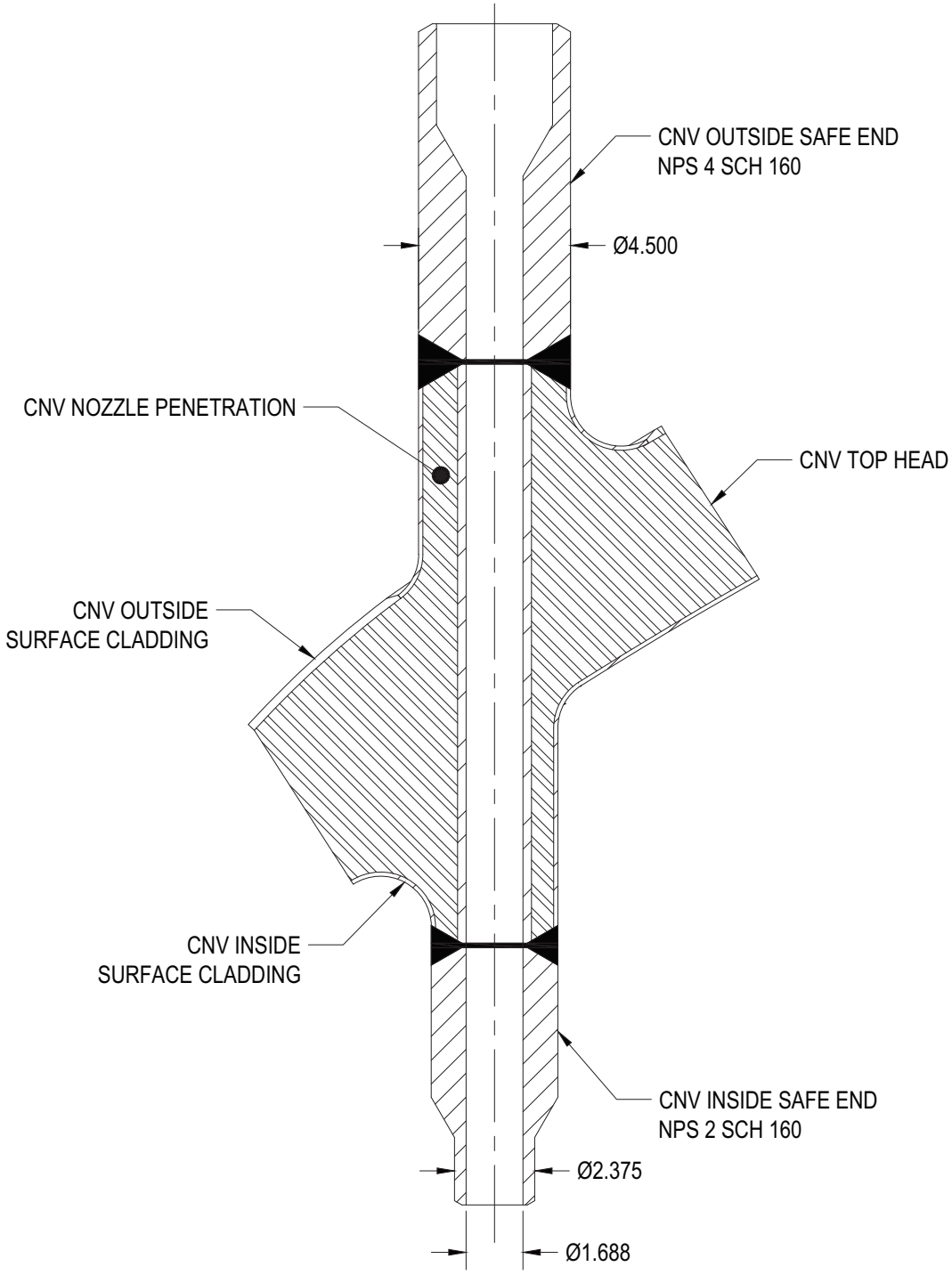

Figure 3.8.2-8: Containment Vessel Reactor Pressure Vessel Support Boundary

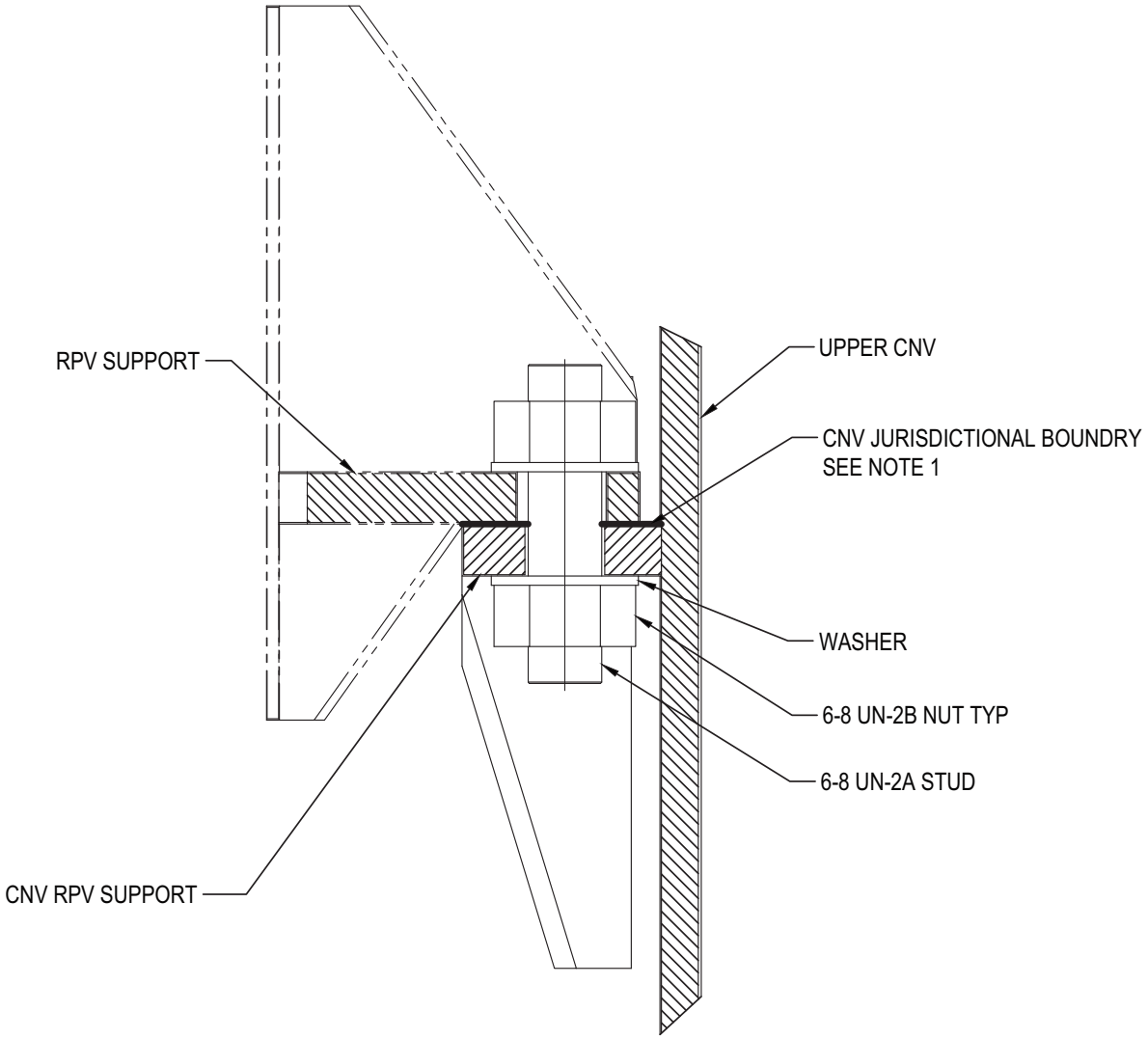

NOTE:
1. STUD, NUT, AND WASHER BELONG TO THE CNV.

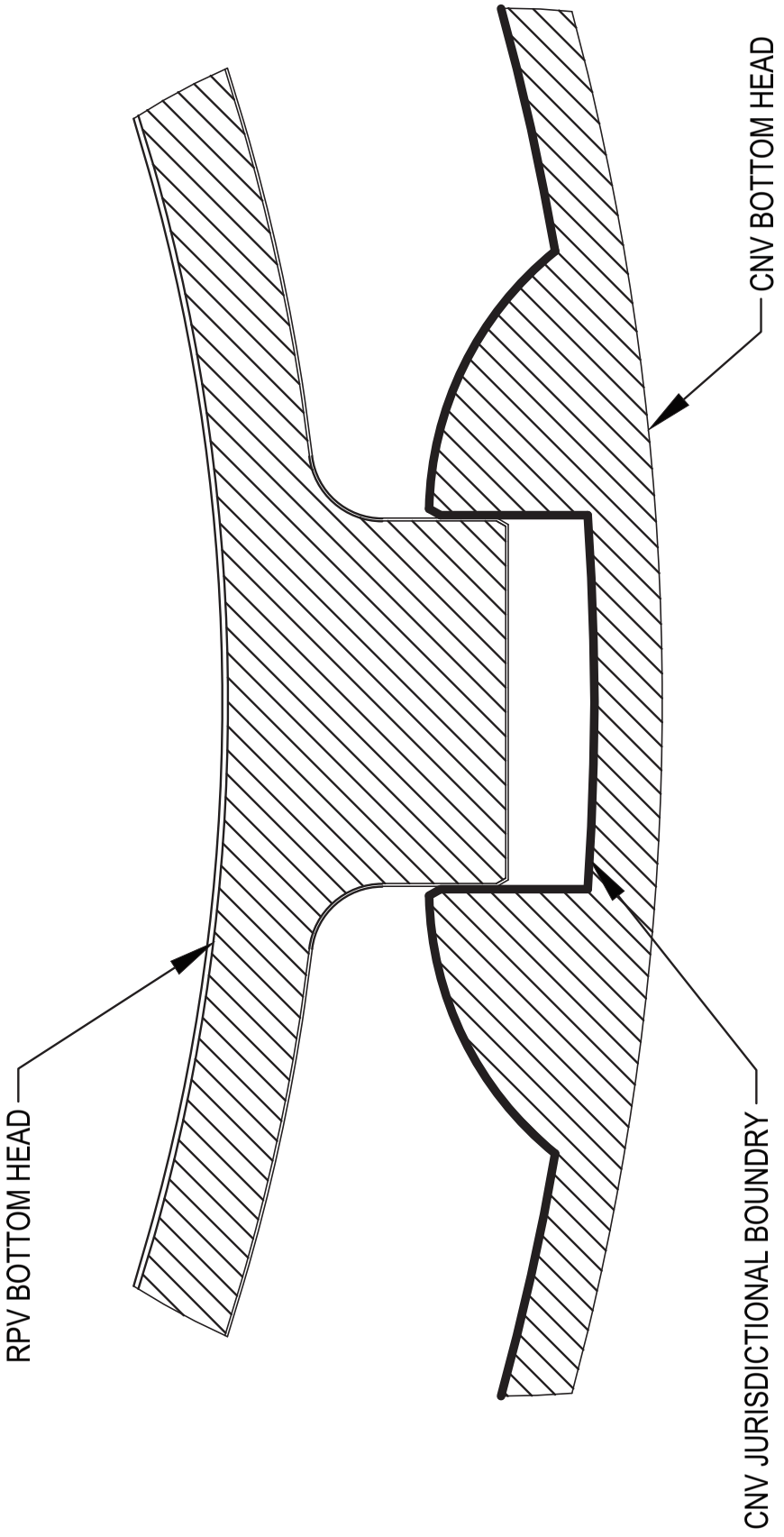

Figure 3.8.2-9: Containment Vessel Bottom Head Boundary

3.8.3 Concrete and Steel Internal Structures of Steel or Concrete Containments

The NuScale Power Module does not use internal structures (compartments, pedestals, or walls). Connections between the containment vessel and the reactor vessel are discussed in Section 3.8.2.

3.8.4 Other Seismic Category I Structures

The Seismic Category I structures are the RXB and the CRB. These buildings are site independent and designed for the Certified Seismic Design Response Spectra (CSDRS) and the CSDRS-HF (high frequency) described in Section 3.7.1. The static analysis is performed with SAP2000 (Reference 3.8.4-1), the seismic analysis is performed using SASSI2010 (Reference 3.8.4-2), and added fluid loads are determined using ANSYS (Reference 3.8.4-3.) Validation of these computer programs is provided in Section 3.7.5. All of the loads are combined using Excel and Mathcad to determine the overall demand to capacity ratio. A summary of the analysis cases is provided in Table 3.7.2-35.

3.8.4.1 Description of the Structures

3.8.4.1.1 Reactor Building

A discussion of the RXB and the major features and components is provided in Section 1.2.2.1. Architectural drawings, including plan and section views are provided in Figure 1.2-10 through Figure 1.2-20.

The RXB is a reinforced concrete structure that is deeply embedded in soil, supported on a single basemat foundation, and is designed to withstand the effects of natural phenomena (earthquake, rain, snow, wind, tornado, hurricane) without affecting the operability of the safety-related SSCs within the building.

The RXB has an outside length (excluding pilasters) of 346.0 feet in the east-west direction and a width (excluding pilasters) of 150.5 feet in the north-south direction. There are five pilasters along both the north and south walls and three pilasters on the east and west walls. These pilasters are 5.0 feet wide and extend 5.0 feet out from the wall. In addition, there are four corner pilasters. These pilasters are 12.5 feet wide and extend 2.5 feet out from the wall. The Reactor Building is centered on a below grade basemat with dimensions of 358'-0" by 162'-6." The overall height of the building is approximately 167 feet from the top of roof to the bottom of the basemat. The RXB roof is sloped on north and south sides with a flat segment in the middle; the top of roof elevation is 181'-0".

The ground floor or baseline top of concrete (TOC) is elevation (EL.) 100'-0." The bottom of the foundation concrete is typically 14' -0." There are some portions that extend deeper, which are discussed in Section 1.2.2.1 and in Section 3.8.5. Actual site grade is approximately 6 inches below baseline TOC and sloped away from the structures. However, the terms "grade" and "site grade" refer to EL. 100'-0." The embedment of the RXB is approximately 86 feet.

The predominant feature of the RXB is the ultimate heat sink pool. This pool consists of the spent fuel pool, refueling area pool, and the reactor pool. This large pool occupies the center of the building and runs approximately 80% of the length of the building. The normal reactor pool level is maintained at 69 feet, which equates to a building elevation of 94'-0". The reactor pool has bays to house up to twelve NPMs. The structural analysis assumes all twelve NPMs are in their respective bays. A study of the dynamic effects of an earthquake that occurs when operating with less than twelve modules is provided in Section 3.7.2.9.1.

The typical thickness for the main structural interior and exterior concrete walls is 5 feet. The primary floor slabs are 3 feet thick with embedded reinforced concrete T-beams. All of the exterior and major building walls line up with each other from floor to floor. Reinforced concrete pilaster columns are encased within the exterior walls of the RXB. Several buttress elements and stiffener walls are located around the exterior and interior of the structure. The basemat foundation thickness is 10 feet; the foundation top of concrete is EL. 24'-0". The reactor pool area and spent fuel pool area is elevated so that the top of the steel (TOS) liner is at EL. 25'-0" (TOC is 24'-11.75".) The refueling pool area has a top of concrete elevation of 18'-11.75" for a TOS elevation of 19' 0".

"W" shapes are used as beams and columns for the steel platforms located at TOS elevations 35'-6 3/4", 61' - 10 3/8", and 85' - 10 3/4". Tube steel is used in the steel partition walls and in the floors located at elevations 62'-0" and 86'-0".

The RXB has five primary floors. These floors are listed below. The associated figure provides an isometric view showing the primary walls on that floor.

Floor No. 1 - TOC Elevation 24'-0" (TOC for basemat foundation), Figure 3.8.4-1

Floor No. 2 - TOC Elevation 50'-0", Figure 3.8.4-2

Floor No. 3 - TOC Elevation 75'-0", Figure 3.8.4-3

Floor No. 4 - TOC Elevation 100'-0" ground floor, Figure 3.8.4-4

Floor No. 5 - TOC Elevation 126'-0", Figure 3.8.4-5

Reactor Building Crane Rail - TOC Elevation 145' 6", Figure 3.8.4-6

Roof - TOC Elevation 181'-0" , Figure 3.8.4-7

The RXB is centrally located with respect to other key buildings. The CRB is to the east, the RWB to the west, and [[two Turbine Generator Buildings are to the north and south]]. Above grade, the RXB and the CRB are separated by a distance of approximately 34 feet between the centerline of the walls. There is a tunnel provided between the RXB and the CRB. This tunnel is part of the CRB.

The RWB is approximately 25 feet west of the RXB above grade. There are no safety-related utilities between the RXB and RWB.

3.8.4.1.2 Control Building

A general discussion of the CRB and the major features and components is provided in Section 1.2.2.2. Architectural drawings, including plan and section views are provided in Figure 1.2-21 through Figure 1.2-27.

The CRB is located approximately 34 feet east of the RXB and its primary function is to house the Main Control Room and the Technical Support Center.

The CRB is a reinforced concrete building with an upper steel structure as a roof. The reinforced concrete portion of the building is Seismic Category I. The SSC on the top floor have no safety-related or risk-significant functions. The walls and roof above this floor are provided for weather protection/climate control. This part of the structure is not required to be Seismic Category I. However, to ensure it will not fail and affect the Seismic Category I portion of the building, or the Seismic Category I RXB, the steel portion of the building is classified and analyzed as a Seismic Category II structure. The codes, standards, specifications, loads and loading combinations, design and analysis procedures, and structural acceptance criteria for the Seismic Category I portion of the CRB also apply to the Seismic Category II portion of this building to the extent required to comply with DSRS 3.7.2 - Section II - Acceptance Criteria 8 (a), (b), or (c). The vestibule at the front of the building is decoupled from the building with an expansion joint. The vestibule is not included in the CRB model.

The CRB is 81' 0″ wide (excluding pilasters) in the East-West direction and 119' 8″ wide (excluding pilasters) in the North-South direction. The dimensions between the centerlines of the outer walls are 78' 0" by 116' 8". There are two pilasters along both the east and west walls and a single pilaster on the north and south walls. These pilasters are 3.0 feet wide and extend 3.0 feet out from the wall. In addition, there are four corner pilasters. These pilasters are 7.5 feet wide and extend 1.5 feet out from the wall. The Control Building is centered on a below grade basemat with dimensions of 91' 0" by 129' 8". The building has a total height of approximately 96 feet from the top of the steel roof to the bottom of the basemat foundation. The embedded portion of the CRB is approximately 55 feet below grade. Consequently, the top of the CRB is approximately 41 feet above grade. The steel super structure exists from EL. 120'-0" to EL. 141'-2" and consists of a vertical and horizontal steel bracing system.

The typical thicknesses for the exterior and interior structural concrete walls are 3 feet and 2 feet, respectively. The primary floor slabs are 3 feet thick and other minor slabs are 2 feet thick. Embedded in the 3 foot thick slabs are reinforced concrete T-beams which are 3 feet wide and 2 feet deep. The basemat foundation thickness is 5 feet and the foundation top of concrete is at EL. 50'-0".

A tunnel exists between the CRB and the RXB. The top of the tunnel is at EL. 100'-0" and the tunnel extends down to the bottom of foundation. The tunnel is comprised of two levels; the upper tunnel floor is for personnel access to the RXB at approximately EL. 76'-6" and the lower tunnel floor at EL 50'-0" is a utilities tunnel. The tunnel has an external width of 22' 8″ and the exterior walls and top slab are 3.0 feet thick. The tunnel extends out 24.5 feet from the CRB wall. There is a 6″ expansion gap between the end of the tunnel and the corresponding connecting walls on the RXB.

The CRB has four primary floors. These floors are listed below. The associated figure provides an isometric view showing the primary walls on that floor.

Floor No. 1 - TOC Elevation 50'-0" (TOC for basemat foundation), Figure 3.8.4-8

Floor No. 2 - TOC Elevation 76'-6" (Main Control Room), Figure 3.8.4-9

Floor No. 3 - TOC Elevation 100'-0" ground floor, Figure 3.8.4-10

Floor No. 4 - TOC Elevation 120'-0" (Seismic Category I roof), Figure 3.8.4-11

Roof - High Point TOS Elevation 141'-2" (top of weather enclosure), Figure 3.8.4-12

3.8.4.1.3 Radioactive Waste Building

A general discussion of the RWB and the major features and components is provided in Section 1.2.2.3. Architectural drawings, including plan and section views are provided in Figure 1.2-28 through Figure 1.2-33. The RWB is separated from the RXB by approximately 25 feet above grade. No safety-related SSCs are located in the RWB. The RWB is Seismic Category II.

3.8.4.1.4 Other Structures

[[The Turbine Generator Buildings are conceptual design, but are separated from the RXB by a minimum distance of 70 feet]]. Other site structures shown in Figure 1.2-1 are part of the standard plant, but not part of the certified design.

3.8.4.1.5 Fuel Storage Racks

The fuel storage racks are described in Section 9.1 and Technical Report TR-0816-49833 (Reference 3.8.4-4).

3.8.4.1.6 Bioshields

The bioshields are concrete and steel covers that are placed over the NPM bays. The bioshields are discussed in Section 3.7.3.

3.8.4.1.7 Reactor Building Pools

The Reactor Building pools are the ultimate heat sink for the NPMs. The ultimate heat sink is discussed in Section 9.2.5. The pool has a liner to prevent potential pool inventory leakage. The liner is a 304L, or equivalent, stainless steel that is 0.25 in. thick in most locations and covers the pool floor and walls up to the 100 foot elevation. The liner is included as a dead weight in the analysis of the RXB. There is a pool leakage detection system embedded in the concrete beneath the pool. The pool leakage detection system is discussed in Section 9.1.3.2.5.

3.8.4.1.8 Platforms and Miscellaneous Structures

Platforms and miscellaneous structures (e.g., ladders, guard rails, stairs) are utilized in the RXB and CRB. These components are constructed of steel beams, angles, channels, tubing, and grating. Platforms and miscellaneous structures may be Seismic Category I, II, or III depending on their safety function and potential interaction with Seismic Category I SSC. These SSC are included in the seismic analysis of the structure as part of the standard floor load.

3.8.4.1.9 Buried Conduit and Duct Banks

The design does not include any buried safety related pipes or pipe ducts.

3.8.4.1.10 Buried Pipe and Pipe Ducts

The design does not include any buried safety related pipes or pipe ducts.

3.8.4.1.11 Masonry Walls

Masonry walls are not used in the Reactor Building or in the Control Building.

3.8.4.1.12 Modular Construction

The design of the Seismic Category I RXB and CRB structural walls does not include steel-concrete (SC) modular subsystems. Modular construction techniques (including sacrificial steel) that do not alter the design, normal construction techniques, or analysis may be employed.

3.8.4.1.13 Reactor Building Crane

The Reactor Building crane (RBC) is a bridge crane that rides on rails anchored to the RXB at EL 145' 6". The RBC is part of the Overhead Heavy Load Handling System and is discussed in Section 9.1.5. For analysis of the RXB, the RBC is included as a beam and spring model as described in Section 3.7.2.1.2.3.

The RBC is supported at the bridge wheels by a crane rail connected to a steel anchor plate embedded into the reactor building (RXB) at a wall offsets. Normal operating loadings from the RBC are resisted by the crane rails. During a seismic event, all lateral, transverse, and upward loadings are resisted by a seismic restraint system and all vertical downward forces are resisted by the crane rail. The crane rails and seismic restraints transfer the RBC loadings to the RXB structure. Safe shutdown earthquake loading is based on a modal analysis and subsequent response spectrum analysis for low frequency input and high frequency input configurations.

The steel rails and anchor plates meet the design criteria set by AISC N690 Specification for Safety-Related Steel Structures for Nuclear Facilities and ACI 349 Code Requirements for Nuclear Safety-Related Concrete Structures and Commentary, consistent with 10 CFR 50, Appendix A, GDC 1, 2, and 4 and DSRS Section 3.8.4.

3.8.4.1.14 Fuel Handling Machine

Design aspects of the Fuel Handling Machine (FHM) are described in Section 9.1.4.2.2.

The FHM is supported at the bridge wheels by a machined rail connected to a steel anchor plate embedded into the reactor building (RXB) walls. Normal operating loadings from the FHM are resisted by the rails. During a seismic event, all lateral,

transverse, and upward loadings are resisted by a seismic restraint system and all vertical downward forces are resisted by the rail. The rails and seismic restraints transfer the FHM loadings to the RXB structure. Safe shutdown earthquake loading is based on a modal analysis and subsequent response spectrum analysis.

The steel rails and anchor plates meet the design criteria set by AISC N690 Specification for Safety-Related Steel Structures for Nuclear Facilities and ACI 349 Code Requirements for Nuclear Safety-Related Concrete Structures and Commentary.

3.8.4.2 Applicable Codes, Standards, and Specifications

The following codes and standards are applicable for the design and construction of Seismic Category I structures and basemats. For the ASTM standards, which are applicable to construction, the code year is not specified. For these standards, the latest endorsed version at the time of construction is used.

3.8.4.2.1 Design Codes and Standards

ACI 207.1R	2005	Guide to Mass Concrete
ACI 211.1	1991	Standard Practice for Selecting Proportions for Normal, Heavyweight, and Mass Concrete
ACI 301	2010	Specification for Structural Concrete for Buildings.
ACI 304R	2000	Guide for Measuring, Mixing, Transporting and Placing Concrete
ACI 305.1	2014	Specification for Hot-Weather Concreting.
ACI 306.1	1990	Specification for Cold-Weather Concreting.
ACI 318	2005	Building Code Requirements for Structural Concrete
ACI 347R	2014	Recommended Practice for Concrete Formwork.
ACI 349/349R	2006	Code Requirements for Nuclear Safety-Related Concrete Structures and Commentary
ACI 349.1R	2007	Reinforced Concrete Design for Thermal Effects on Nuclear Power Plant Structures
ACI SP-2	2007	Manual of Concrete Inspection
ACI SP-66	2004	ACI Detailing Manual

AISC N690	2012	Specification for Safety-Related Steel Structures for Nuclear Facilities
AISC 325	2014	Steel Construction Manual
AISC 360	2010	Specification for Structural Steel Buildings
AISI S100	2012	North American Specification for the Design of Cold-Formed Steel Structural Members
ANS 6.4	2006	Nuclear Analysis and Design of Concrete Radiation Shielding for Nuclear Power Plants
ANSI/NAAMM MBG 531	2009	Metal Bar Grating Manual
ANSI/NAAMM MBG 532	2009	Heavy Duty Metal Bar Grating Manual
ASCE 3	1991	Standard for the Structural Design of Composite Slabs
ASCE 4	1998	Seismic Analysis of Safety-Related Nuclear Structures
ASCE 7	2005	Minimum Design Loads in Buildings and Other Structures (wind loads)
ASCE 7	2010	Minimum Design Loads in Buildings and Other Structures "(as applicable for all loads other than wind loading)"
ASCE 8	2002	Specification for the Design of Cold-Formed Stainless Steel Structural Members
ASCE 37	2002	Design Loads on Structures During Construction
ASCE 43	2005	Seismic Design Criteria for Structures, Systems, and Components in Nuclear Facilities
ASME BPVC Section 3	2007	Rules for Construction of Nuclear Facility Components
ASTM A36/A36M		Standard Specification for Carbon Structural Steel
ASTM A53/A53M		Standard Specification for Pipe, Steel, Black and Hot-Dipped, Zinc-Coated, Welded and Seamless

ASTM A108	Standard Specification for Steel , Carbon and Alloy, Cold Finished
ASTM A185/A185M	Standard Specification for Steel Welded Wire Reinforcement, Plain, for Concrete
ASTM A193/A193M	Standard Specification for Alloy-Steel and Stainless Steel Bolting for High Temperature or High Pressure Service and Other Special Purpose Applications
ASTM A194	Standard Specification for Carbon Steel, Alloy Steel, and Stainless Steel Nuts for Bolts for High Pressure or High Temperature Service, or Both
ASTM A240/A240M	Standard Specification for Chromium and Chromium-Nickel Stainless Steel Plate, Sheet, and Strip for Pressure Vessels and for General Applications
ASTM A307	Standard Specification for Carbon Steel Bolts, Studs, and Threaded Rod 60000 PSI Tensile Strength
ASTM A325	Standard Specification for Structural Bolts, Steel, Heat Treated, 120/105 ksi Minimum Tensile Strength
ASTM A490	Standard Specification for Structural Bolts, Alloy Steel, Heat Treated, 150 ksi Minimum Tensile Strength
ASTM A497/A497M	Standard Specification for Steel Welded Wire Reinforcement, Deformed, for Concrete
ASTM A500/A500M	Standard Specification for Cold-Formed Welded and Seamless Carbon Steel Structural Tubing in Rounds and Shapes
ASTM A501	Standard Specification for Hot-Formed Welded and Seamless Carbon Steel Structural Tubing
ASTM A572/A572M	Standard Specification for High-Strength Low-Alloy Columbium-Vanadium Structural Steel
ASTM A615/A615M	Standard Specification for Deformed and Plain Carbon-Steel Bars for Concrete Reinforcement

ASTM A653	Standard Specification for Steel Sheet, Zinc-Coated (Galvanized) or Zinc-Iron Alloy-Coated (Galvannealed) by the Hot-Dip Process
ASTM A706/A706M	Standard Specification for Deformed and Plain Low-Alloy Steel Bars for Concrete Reinforcement
ASTM A775/A775M	Standard Specification for Epoxy-Coated Steel Reinforcing Bars
ASTM A786/A786M	Standard Specification for Hot-Rolled Carbon, Low-Alloy, High-Strength Low-Alloy, and Alloy Steel Floor Plates
ASTM A992/A992	Standard Specification for Structural Steel Shapes
ASTM A1008/A1008M	Standard Specification for Steel, Sheet, Cold-Rolled, Carbon, Structural, High-Strength Low-Alloy, High-Strength Low-Alloy with Improved Formability, Solution Hardened, and Bake Hardenable"
ASTM C33/C33M	Standard Specification for Concrete Aggregates
ASTM C94/C94M	Standard Specification for Ready-Mixed Concrete
ASTM C150/150M	Standard Specification for Portland Cement
ASTM C260/C260M	Standard Specification for Air-Entraining Admixtures for Concrete
ASTM C494/C494M	Standard Specification for Chemical Admixtures for Concrete
ASTM C618	Standard Specification for Coal Fly Ash and Raw or Calcined Natural Pozzolan for Use in Concrete
ASTM C1260	Standard Test Method for Potential Alkali Reactivity of Aggregates
ASTM C1293	Standard Test Method for Determination of Length Change of Concrete Due to Alkali-Silica Reaction

ASTM F1554	Standard Specification for Anchor Bolts, Steel, 36, 55, and 105-ksi Yield Strength
ASTM D2859	Standard Test Method for Ignition Characteristics of Finished Textile Floor Covering Materials
ASTM F593	Standard Specification for Stainless Steel Bolts, Hex Cap Screws, and Studs
ASTM F594	Standard Specification for Stainless Steel Nuts
AWS D1.1/D1.1M	Structural Welding Code - Steel
AWS D1.3/D1.3M	Structural Welding Code - Sheet Steel
AWS D1.4/D1.4M	Structural Welding Code - Reinforcing Steel
AWS D1.6/D1.6M	Structural Welding Code - Stainless Steel
AWS D9.1M/9.1	Sheet Metal Welding Code

3.8.4.2.2 Regulatory Guides

The following regulatory guides (RGs) influenced or are applicable to the design and construction of the Seismic Category I RXB and CRB. Not all regulatory guides are applicable to both structures. Conformance with these regulatory guides is discussed in Section 1.9.

RG 1.13, Rev. 2	Spent Fuel Storage Facility Design Basis
RG 1.29, Rev. 5	Seismic Design Classification
RG 1.61, Rev. 1	Damping Values for Seismic Design of Nuclear Power Plants
RG 1.69, Rev. 1	Concrete Radiation Shields for Nuclear Power Plants
RG 1.76, Rev. 1	Design Basis Tornado for Nuclear Power Plants
RG 1.78, Rev. 1	Evaluating the Habitability of a Nuclear Power Plant Control Room During a Postulated Hazardous Chemical Release
RG 1.91, Rev. 2	Evaluations of Explosions Postulated to Occur at Nearby Facilities and on Transportation Routes Near Nuclear Power Plants
RG 1.92, Rev. 3	Combining Modal Responses and Spatial Components in Seismic Response Analysis
RG 1.102, Rev. 1	Flood Protection for Nuclear Power Plants

RG 1.115, Rev. 2	Protection against Low-Trajectory Turbine Missiles
RG 1.117, Rev. 1	Tornado Design Classification
RG 1.122, Rev. 1	Development of Floor Design Response Spectra for Seismic Design of Floor-Supported Equipment or Components
RG 1.142, Rev. 2	Safety-Related Concrete Structures for Nuclear Power Plants (Other than Reactor Vessels and Containments
RG 1.160, Rev. 3	Monitoring the Effectiveness of Maintenance at Nuclear Power Plants
RG 1.183, Rev. 0	Alternative Radiological Source Terms for Evaluating Design Basis Accidents at Nuclear Power Reactors
RG 1.189, Rev. 2	Fire Protection for Nuclear Power Plants
RG 1.196, Rev. 1	Control Room Habitability at Light-Water Nuclear Power Reactors
RG 1.197, Rev. 0	Demonstrating Control Room Envelope Integrity at Nuclear Power Reactors
RG 1.199, Rev. 0	Anchoring Components and Structural Supports in Concrete
RG 1.204, Rev. 0	Guidelines for Lightning Protection of Nuclear Power Plants
RG 1.217, Rev. 0	Guidance for the Assessment of Beyond-Design-Basis Aircraft Impacts
RG 1.221, Rev. 0	Design-Basis Hurricane and Hurricane Missiles for Nuclear Power Plants
RG 4.21, Rev. 0	Minimization of Contamination and Radioactive Waste Generation: Life-Cycle Planning
RG 5.68, Rev. 0	Protection Against Malevolent Use of Vehicles at Nuclear Power Plants
RG 8.8, Rev. 3	Information Relevant to Ensuring that Occupational Radiation Exposures at Nuclear Power Stations Will Be as Low as Is Reasonably Achievable
RG 8.19, Rev. 1	Occupational Radiation Dose Assessment in Light-Water Reactor Power Plants -- Design Stage Man-Rem Estimates

3.8.4.3 Loads and Load Combinations

The concrete and steel load combinations to be considered for the structural design and analysis of the RXB and CRB are based on ACI 349 (Reference 3.8.4-5) as modified by RG 1.142, and ANSI/AISC-N690 (Reference 3.8.4-6). The load combinations considered for the analysis are presented in Table 3.8.4-1 and Table 3.8.4-2.

The symbols used for the design loads in Table 3.8.4-1 and Table 3.8.4-2 are listed below and discussed in the following sections.

- D = Dead loads, including piping, equipment, and partitions
- F = Loads due to weight and pressures of fluids
- H = Loads due to weight and static pressure of soil, water in soil, or other materials
- L = Live loads due to occupancy and moveable equipment
- L_r = Roof live load
- R_o = Piping and equipment reaction loads
- R_a = Piping and equipment reaction loads due to a postulated accident
- T_o = Thermal loads due to normal operating temperatures
- T_a = Thermal loads due to accident condition temperatures
- R = Rain load
- S = Snow load
- S_e = Extreme snow load
- W = Straight line wind load
- W_t = Loads due to the design basis tornado
- W_h = Loads due to the design basis hurricane
- E_o = Seismic load due to an Operating Basis Earthquake (OBE)
- E_{ss} = Seismic load due to a Safe Shutdown Earthquake (SSE)
- C_{cr} = Loads due to the Reactor Building crane
- P_a = Pressure loads due to accident conditions
- Y_j = Jet impingement load generated by a postulated high energy line break
- Y_r = Loads due the impact from a postulated high energy line break
- Y_m = Missile impact load, or related internal moments and forces, due to a high energy line break

3.8.4.3.1 Dead Loads (D)

Dead loads in the RXB consist of the self-weight of the structure such as the walls, roof, and slabs, and other large permanent loads. This includes the weight of the

pool water, the NPMs, the bioshields, and the RBC. In addition, equipment weights for large components are estimated and included as concentrated point loads (or if several pieces of equipment are located closely together, an equivalent uniform load is applied over the respective area). Approximate weights of significant components are discussed below.

Dead loads in the CRB consist of the self-weight of the structure such as the walls, roof, slabs, steel beams, and columns. Other dead loads considered are the Main Control Room, Technical Services Center, and Control Room Habitability System, Normal Control Room HVAC System, and other safety and nonsafety control and instrumentation systems within the CRB. In addition, weights for large equipment and components were estimated and included as concentrated point loads (or if several pieces of equipment are located closely together, an equivalent uniform load is applied over the respective area).

3.8.4.3.1.1 Concrete Self-Weight

The concrete self-weight is obtained by multiplying the volume of concrete for each structural element in the building by the reinforced concrete density of 154.5 pcf. This normal concrete density of 150 pcf has been increased by 3 percent to account for concrete sections with robust reinforcement. The concrete self-weight for the RXB is approximately 465,420 kips.

The total concrete self-weight of the CRB, is approximately 43,870 kips. The structural steel self-weight is approximately 420 kips. Therefore, the total CRB self-weight is approximately 44,290 kips.

3.8.4.3.1.2 Water Weight

The RXB contains an immense amount of water in the Reactor Pool, Refueling Pool, Spent Fuel Pool and Dry Dock which contribute to a large portion of the total weight of the structure. The water weight in the RXB is approximately 64,700 kips and is calculated based on pool floor surface areas and the pool depth. In reactor bays, the volume occupied by the NPMs is subtracted from the pool volume.

3.8.4.3.1.3 NuScale Power Module Weight

The NPMs are included in the seismic model of the RXB as beam elements. See Section 3.7.2 for a discussion of the RXB seismic model.

The model weight of each NPM is approximately 1,880 kips.

3.8.4.3.1.4 Liner Plate Dead Weight

The liner plate weight is determined by multiplying the surface area of the pool walls and floor by the thickness of the liner and the density of steel. This results in a total liner weight of approximately 2,140 kips. This weight was converted to a density increase for the walls and floor by dividing the weight by the volume of the wall or floor. The weight of the liner increased the density of the

outer walls by 3.03 lbs/ft^3, the inner walls by 7.32 lbs/ft^3 and the floor by 1.33 lbs/ft^3.

3.8.4.3.1.5 Bioshield Weight

The bioshields are included in the model. The total weight of the twelve bioshields is assigned as lumped weight of approximately 2,100 kips on the top of the NPM bay walls.

3.8.4.3.1.6 Reactor Building Crane Weight

The RBC is a bridge crane on a crane rail mounted at elevation 145'-6". The RBC is included as a beam and spring model with a total weight of approximately 2,000 kips.

3.8.4.3.1.7 Fuel Storage Rack Weight

The fuel racks are evaluated fully loaded with fuel elements. This weight is approximately 1,490 kips.

3.8.4.3.1.8 Module Assembly Equipment Weight

The function of the module assembly equipment is to facilitate the delivery of the NPMs to the Reactor Pool. The main components are the Module Import Trolley, the Module Upender, and the Module Inspection Rack.

The Module Import Trolley is a rail mounted low profile trolley located at the west end of the building at EL. 100'-0". The trolley is used for conveying a horizontally-oriented NPM from the loading area into the RXB to the NPM staging area. The Module Import Trolley has a total weight of approximately 360 kips. The Module Upender is located in the dry dock area and moves the Module Import Trolley and the NPM through 90 degree rotation from the horizontal to vertical positions. The Module Upender has a self-weight of approximately 940 kips and the associated Inspection rack has a self-weight of approximately 250 kips.

3.8.4.3.1.9 Stair and Elevator Weight

The stairs and elevator are large components that are considered in the analysis. The weight of each stairwell in the RXB is estimated to be 145 kips. The RXB elevator has an estimated weight of 40 kips. These loads are applied to the top of the foundation at EL. 24' 0".

The CRB elevator weight is estimated at 30 kips and applied at the top of the foundation at El. 50'-0".

3.8.4.3.1.10 Equipment Weights

Table 3.8.4-3 is a summary of the RXB equipment weights per floor. The NPM, bioshields, and RBC are not included in the per floor summary since these loads are applied in the analysis model as described above. The majority of equipment loads are applied as either concentrated nodal loads or uniformly distributed area loads.

Table 3.8.4-4 is a summary of the CRB equipment weights per floor. These loads are applied to the CRB model directly using point loads; or if several pieces of equipment are located in close proximity, an equivalent uniform load is applied over the respective area.

3.8.4.3.1.11 Uniform Equivalent Dead Load

The uniform equivalent dead load for the RXB and CRB is used to account for pieces of equipment less than 1000 lbs in weight not accounted for in the equipment dead loads and for cable trays, piping and ducts. The RXB and CRB floors are designed using a uniform equivalent dead load of 50 psf. The equivalent dead load is 25 psf for the RXB roof and 20 psf for the CRB roof.

3.8.4.3.2 Liquid Loads (F)

The liquid load consists of the water pressure exerted on the walls in the Reactor Pool, Refueling Pool, Spent Fuel Pool and Dry Dock during static and seismic conditions. As noted in Section 3.8.4.3.1.4, the water weight in the RXB is approximately 64,700 kips. This pool water weight is included in the dead load as described above. The CRB does not have liquid loads.

The hydrostatic load considers the water pressure exerted on the structural pool walls in contact with the water. The pressure distribution considers zero pressure at the normal water level of the pool and increasing water pressure with water depth. The hydrostatic pressure varies linearly from the pool surface to the bottom of the pool floor.

These hydrodynamic loads are due to the seismic response from the water in the pools, which exert a water pressure on the structural pool walls in contact with the water. The hydrodynamic load effect is taken into account by distributing the water mass on each affected structural wall in the pool. The entire pool water mass is considered to participate in the hydrodynamic response for the two horizontal and vertical directions. i.e., the water mass in the East-West (X) direction is applied as lumped masses on all wall surface nodes which would resist the fluid motion in the X direction.

Figure 3.8.4-13 shows the water mass regions that contribute to the hydrodynamic response in the longitudinal X-direction. Similarly,
Figure 3.8.4-14 shows the water mass regions corresponding to the hydrodynamic response in the transverse Y-direction. The vertical hydrodynamic effect is simply attained by evenly distributing the entire water mass along the bottom of the pool floor.

Table 3.8.4-5 provides the hydrodynamic water weight for the various regions of the pools due to the hydrodynamic loading in the longitudinal and transverse directions depicted in Figure 3.8.4-13 and Figure 3.8.4-14.

The dynamic finite element analysis uses these nodal masses along with the calculated nodal seismic acceleration to produce the dynamic impulsive pressures on the walls.

The RXB is analyzed with an ANSYS finite element model to determine the combined hydrodynamic pressure inside the RXB from a Fluid-Structure Interaction (FSI) analysis. The additional forces are applied as an equivalent hydrostatic pressure loading in the SAP2000 model using the hydrodynamic pressures and accelerations obtained from the ANSYS FSI analysis. This pressure is scaled for the overall calculation of the demand.

The ANSYS model was also used to determine slosh height. Pool wall accelerations along the top of the pool were obtained from the SASSI2010 analysis and the ANSYS FSI analysis and used to determine sloshing height. These analyses indicate a maximum sloshing height of approximately 2 feet.

3.8.4.3.3 Earth Pressure (H)

The embedded exterior walls of the buildings are subjected to lateral soil pressure loads induced by three types of loads as described below:

- Static Soil Pressure - induced by the weight of soil, hydrostatic pressure and a surcharge load at grade level.
- Dynamic Soil Pressure - induced due to an earthquake event, developed from the SASSI2010 analyses of the standalone RXB and CRB models.
- Structure-Soil-Structure-Interaction Dynamic Soil Pressure - soil pressure determined from the triple building SASSI2010 analysis using the RXB, CRB, and RWB.

For the static soil pressure, the lateral soil pressure is calculated assuming that the soil is completely confined and cannot move. The soil is also considered to be submerged for the total embedment depth because the water table is close to grade level. Therefore, the total horizontal pressure from the submerged soil is calculated as the sum of the hydrostatic pressure and the lateral soil pressure considering the buoyant effect. Because the water provides a buoyant effect, the effective pressure is calculated using the difference between the soil density and water density. For the RXB, the embedment depth used in the mathematical model is 85'.

Maximum Hydrostatic Pressure

γ_ω = 62.4 pcf Unit weight of water, H = 85 ft Embedment depth, u = γ_ω H = 5304 psf

Effective Lateral Pressure

γ_{sat} = 130 pcf Unit weight of saturated soil, $\gamma_b = \gamma_{sat} - \gamma_\omega$ = 67.6 pcf Buoyant unit weight

H = 85 ft Embedment Depth, K_o = 0.5 Coefficient of pressure at rest, $p_{he} = K_o\gamma_b$ H = 2873 psf

Surcharge Loads

p_q= 250 psf Surcharge Load, $p_{hq} = K_o\, p_q$ = 125 psf

Total Maximum Lateral Soil Pressure

The total maximum lateral soil pressure at a depth H is the sum of the hydrostatic pressure, the effective lateral pressure, and the surcharge lateral pressures calculated above.

$p_h = u + p_{he} + p_{hq}$ = 8302 psf

Figure 3.8.4-27 shows a diagram of the total lateral static soil pressure distribution. Seismic soil pressure is computed from the SASSI2010 Soil-Structure Interaction analysis. The normal stresses in the backfill soil solid elements, adjacent to the embedded portion of the RXB exterior walls, represent the soil pressure. For example, for the RXB, the following table provides the summary of total soil pressures on the four walls and total overturning moments induced by the soil pressures.

Wall ID	Total Soil Pressure on Walls (kips)	Total Overturning Moment (Kip-ft)
North wall	570,991	8,911,955
South wall	425,678	7,925,347
West wall	188,731	2,614,131
East wall	178,541	3,096,417

COL Items 2.5-1, 3.7-3, 3.7-5, 3.7-6, and 3.8-2 specify the site-specific geology and soil-structure interaction analysis requirements of the NuScale Power Plants.

3.8.4.3.4 Live Loads (L)

Live loads are a non-permanent weight based upon the maximum loads expected by the use and occupancy of the structure. RXB live loads include floor area loads, lay down loads, fuel transfer casks and equipment handling loads, and similar items.

The RXB uses a base live load of 100 psf, and a live load of 250 psf for the Nuclear Fuel Storage & Refueling Areas and for the portions of the EL. 50'-0" floor supporting the walkways at EL. 62'-0" and a live load of 200 psf for the portions of the EL. 75'-0" floor supporting walkways at EL 86'-0". The floor live loads are not

applied on areas occupied by equipment, whose weight is specifically included as a uniform equipment load or a significant concentrated equipment load.

Floor beams, girders and slabs in the RXB are designed to withstand a 5000 lb concentrated load in locations that maximize moment and shear. Any location where permanent equipment is installed is not designed for this concentrated load. The concentrated loads will not be combined with load combinations that include seismic loads.

The CRB uses a base live load of 100 psf. The offices at EL. 76'-6" and EL. 100'-0" have a 50 psf live load. The floor live load is not applied on areas occupied by equipment, that weight is specifically included as a dead load.

3.8.4.3.5 Roof Live Loads (L_r)

A load of 50 psf is used for the roof live load of both structures.

3.8.4.3.6 Pipe and Equipment Reactions (R_o)

Pipe reactions during normal operation or shutdown conditions are based on the most critical transient or steady state condition.

The CRB does not have any high energy piping. R_o is not a load for the CRB.

3.8.4.3.7 Accident Pipe and Equipment Reactions (R_a)

Pipe and equipment reactions under thermal conditions are generated by the postulated pipe break, including (R_o). This includes their dead load, live load, thermal load, seismic load, thrust load, and transient unbalanced internal pressure loads under abnormal or extreme environmental conditions.

The CRB does not have any high energy or high temperature piping. R_a is not a load for the CRB.

3.8.4.3.8 Operating Thermal Loads (T_o)

Thermal loads are caused by a temperature variation through the concrete wall between the interior temperature and the external environmental temperature. In addition, in the RXB, a thermal gradient could occur in the five foot thick walls surrounding the reactor pool. Section 1.3 of ACI 349.1R (Reference 3.8.4-7) states that thermal gradients should be considered in the design of reinforcement for normal conditions to control concrete cracking. However, a thermal gradient less than approximately 100° F need not be analyzed because such gradients will not cause significant stress in the reinforcement or strength deterioration.

As shown in Table 2.0-1, the external temperature design parameters for the NuScale standard structures are zero percent exceedance dry bulb values of -40°F

and +115°F. The external soil temperature is assumed to be 21°F in the winter and 40°F in the summer.

The RXB has a design internal air temperature range of 70°F to 130°F, and a design pool temperature range of 40°F to 120°F. These temperatures are used to determine the stresses and displacements.

The CRB has a maximum temperature differential of 110°F, based on an external temperature of -40°F and an internal temperature of 70°F. This gradient has been determined not to affect the design stresses in the building. T_0 is not a load for the CRB.

3.8.4.3.9 Accident Thermal Loads (T_a)

The maximum post accident temperature in the RXB is assumed to be 212°F. This temperature is used in conjunction with the external temperature to determine the stresses and displacements.

The CRB does not have any high energy or high temperature piping. T_a is not a load for the CRB.

3.8.4.3.10 Rain Load (R)

The flat portion of the roof of the RXB does not have a parapet or any means to retain water. The CRB roof is sloped and the parapet has scuppers to disperse rainwater. An additional drainage pipe limits the average water depth on the CRB roof to a maximum of 4 inches. Therefore a rain load is assumed bounded by the snow load and extreme snow load.

3.8.4.3.11 Snow Loads (S)

As shown in Table 2.0-1, a roof snow load of 50 psf is assumed for normal load combinations. Equation 3.8-1 (taken from Equation 7-1 of Reference 3.8.4-8) is used to convert from ground-level snow loads to roof snow loads. An exposure factor of 1.0 is used. A thermal factor of 1.0 is used. An importance factor of 1.2 is used for buildings listed as Seismic Category I in Table 3.2-1 and an importance factor of 1.0 is used for the other buildings.

$$p_f = 0.7 C_e C_t I p_g \qquad \text{Equation 3.8-1}$$

where,

p_f is the roof snow load,

C_e is the exposure factor,

C_t is the thermal factor,

I is the Importance Factor, and

p_g is the ground snow load.

3.8.4.3.12 Extreme Snow Loads (S_e)

A wet roof snow load of 75 psf is assumed for extreme environmental load combinations. Extreme ground-level snow loads are converted to extreme roof snow loads using Equation 3.8-1 in the same manner described in Section 3.8.4.3.11.

3.8.4.3.13 Wind Loads (W)

The design wind load pressure on the RXB is 80 psf. This load is 76 psf for the CRB. Wind loads are developed as described in Section 3.3 based on the site parameters in Table 2.0-1.

3.8.4.3.14 Tornado Wind Loads (W_t) and Hurricane Wind Loads (W_h)

These loads are also developed as described in Section 3.3 based on the site parameters in Table 2.0-1. The RXB combined tornado wind and differential air pressure load is 250 psf and the hurricane wind load pressure is 260 psf. Therefore 260 psf is used as the design extreme wind load pressure for the RXB.

The CRB combined tornado wind and differential air pressure load is 225 psf, while the hurricane wind load pressure is 220 psf. For the CRB the extreme wind load pressure is 225 psf.

3.8.4.3.15 OBE Seismic Loads (E_o)

The operating basis earthquake (OBE) is defined as 1/3 of the safe shutdown earthquake (SSE). Earthquake loads from the operating basis earthquake (E_o) are not evaluated.

3.8.4.3.16 SSE Seismic Loads (E_{ss})

The SSE for the site independent evaluation of the RXB and CRB is the CSDRS and the CSDRS-HF from Table 2.0-1. SSE Seismic Loads (E_{ss}) are derived from evaluation of the structures using ground motion accelerations from the CSDRS and the CSDRS-HF as described in Section 3.7.

Seismic dynamic analyses of the buildings considered 100 percent of the dead load and, 25 percent of the floor live load during normal operation and 75 percent of the roof snow load as the accelerated mass.

3.8.4.3.17 Crane Load (C_{cr})

This load comes from the RBC. The RBC is a bridge crane located at EL. 145'-6" and provide lifting and handling for the NPMs. The RBC is described in more detail in Section 9.1 and Section 3.7.3. The RBC has a total weight of approximately 1,000 tons and a lifting capacity of 850 tons.

The crane live loads are used for the design of the runways beams, connections and crane supports. These crane live loads are due to the moving crane and include the maximum wheel load, vertical impact, lateral impact and longitudinal impact loads.

The maximum wheel load for the RBC is produced by the weight of the bridge, plus the sum of the maximum lift capacity and the weight of the trolley positioned on its runway at the location where the resulting load effect is maximum. The hook and trolley are assumed to align with the crane wheel location. Therefore, the trolley and lift load are assumed to act 100% on the ends. The bridge weight is distributed 50% to each end. There are 16 crane wheels at each end of the crane.

There are no large cranes in the CRB. C_{cr} is not a load for the CRB.

3.8.4.3.18 Accident Pressure Loads (P_a)

Accident pressure loads, within a compartment or the entire building are due to the differential pressure generated by a postulated pipe rupture, including the dynamic effects due to pressure time-history is considered in the design. In the RXB an accident pressure of 1.0psi has been evaluated in the pool area to account for the energy release of a high energy line break.

There are no accident pressure loads in the CRB. P_a is not a load for the CRB.

3.8.4.3.19 Jet Impingement Load (Y_j)

This is a localized load on the structure due to the steam/water jet from a high energy line break and is evaluated per COL Item 3.6-2 and COL Item 3.6-3.

There are no high energy lines in the CRB. Y_j is not a load for the CRB.

3.8.4.3.20 Pipe Break Reaction Loads (Y_r)

This is a localized load on the structure generated by the pipe hanger that is due to a high energy line break and is evaluated per COL Item 3.6-2 and COL Item 3.6-3.

There are no high energy lines in the CRB. Y_r is not a load for the CRB.

3.8.4.3.21 Missile Impact Loads (Y_m)

This is a localized load on the structure due to the whipping high energy line or a missile from a high energy line break. Internal missile loads, if they occur, will be evaluated on an individual basis as a localized load per COL Item 3.6-2 and 3.6-3.

There are no high energy lines in the CRB. Y_m is not a load for the CRB.

3.8.4.3.22 Other Loads

3.8.4.3.22.1 Buoyant Force (B)

The buoyant force is the upward pressure exerted on the bottom of the foundation during a saturated condition. It is the equivalent weight of the water that would otherwise occupy the below grade volume of the structure. The buoyant force is equal to the volume of the building below grade multiplied by the density of water. See Section 3.8.5.3 for use of buoyant force with the RXB and the CRB structures.

3.8.4.3.22.2 Construction Loads

Construction loads are loads from events and activities during construction. These loads will be developed in accordance with Standard SEI/ASCE 37-02, "Design Loads on Structures During Construction." Construction loads are not included when determining seismic loads.

3.8.4.3.22.3 Operation with Less than 12 NuScale Power Modules

The NuScale design allows for operation with less than twelve NPMs. The building analysis was performed with all twelve NPMs in place. However, a study was performed as described in Section 3.7.2.9.1 to evaluate the dynamic effects of an earthquake when operating with less than twelve NPMs. That study concluded that the dynamic effects on the building with less than twelve modules installed would be similar to the dynamic effects when all twelve modules are in place.

No static analysis of operation with a reduced population of NPMs has been performed. Each NPM weights approximately 1,800 kips and displaces approximately 11,200 ft^3 of water. The mass of the displaced water is approximately 700 kips. Therefore the overall weight of the building decreases by about 1100 kips for each NPM not present. This decrease in weight is small compared to the overall weight of the building, which is approximately 600,000 kips (concrete + water + equipment).

3.8.4.4 Design and Analysis Procedures

Fixed-base SAP2000 finite element models are used to determine the structural response due to non-seismic loads. The SAP2000 results (element forces and moments) from the various non-seismic loads are used in conjunction with the results of the

seismic analysis described in Section 3.7.2 to perform the design assessments for the Seismic Category I RXB and CRB.

Load combinations are defined in the analysis models according to Table 3.8.4-1 and Table 3.8.4-2. The acceptance criteria are discussed in Section 3.8.4.5, and Appendix 3B provides the results for selected sections within the RXB and CRB.

In the SAP2000 model, the global coordinate axes are as follows:

- X axis - east-west (Positive X direction pointing east)
- Y axis - north-south (Positive Y direction pointing north)
- Z axis - vertical (Positive Z direction pointing upward)

The origin of the global coordinate system of the finite element models is located at the intersection of Grid Lines RX-C and RX-1 as shown in Figure 3.7.2-3 and Figure 3.7.2-4.

The global origin of the CRB is the same origin as the RXB, and the axis are the same.

3.8.4.4.1 Reactor Building Analysis

SAP2000 Model of the Reactor Building

Two SAP2000 analysis models with fixed base boundary conditions were created to consider the conditions of cracked and uncracked concrete. The level of cracking considered for the cracked SAP2000 analysis model was based on guidance from ASCE 43-05 Section 3.4.1 and Table 3-1. Section 3.7.1.2.2 and Table 3.7.1-7 specify the level of cracking used in these models.

The basis associated with the assumed level of cracking is that this approach accounts for fully enveloped conditions. Envelope demand forces and moments from the uncracked and cracked condition are used regardless of the demand moments and the shear reach of their cracking limits.

The purpose of these models is to envelope the extracted demand forces and moments from the cracked and uncracked models from the static analysis. These maximum demand forces and moments are then used in the design. Figure 3.8.4-15 through Figure 3.8.4-20 provides different views of the RXB SAP2000 finite element model. Figure 3.8.4-4 tabulates the total number of joints and elements developed in both the uncracked and cracked SAP2000 analysis models.

The RXB finite element models are developed to represent the primary structural members including walls, beams, columns, pilasters, floors, and roofs. Walls, floor slabs, and roofs are represented by shell or plate elements placed in the middle or near the neutral planes of walls and floor slabs. The beams, columns, and pilasters are modeled by frame (beam) elements. The basemat foundation is modeled by solid elements and shell elements. All shell and frame elements are modeled at their centerlines (neutral planes). The pilasters are modeled using frame elements

with appropriate bending stiffness modifiers such that the model gives similar lateral response as the case where pilasters are modeled using solid elements. A similar approach was used for modeling the concrete T-beams in the floor slabs.

The 10 ft. thick basemat foundation is modeled by two layers of solid elements to assign the proper height of NPM support locations and pool water height. The RXB outer walls, pool walls, and all the walls connected to the foundation are modeled as shell elements and start at the bottom of the foundation level.

Solid elements are added to the exterior of the RXB embedded walls to model the backfill soil with Soil Type 11 properties. The backfill width is modeled as 25 feet.

The penetrations due to major equipment and components in the walls or slabs were accounted for in the model by removing the appropriate shell elements to make openings.

The equipment weights are incorporated into the analysis models by applying uniform area element loads or concentrated nodal loads closest to the actual location of the equipment. The RBC is incorporated into the analysis model per the information established in Section 3.8.4.3.1. The twelve NPMs are added to the analysis model by converting the ANSYS beam element model to a SAP2000 beam element model.

SAP2000 Analysis

All applicable loads are converted to lumped joint masses for use in dynamic analyses. This is accomplished in SAP2000 by using the Mass Source function. In the RXB, mass comes from concrete self-weight, lumped joint masses (RBC, NPMs, and hydrodynamic mass), equipment joint nodal and uniform loads, uniform floor live loads, and roof snow loads. The specified load cases used in computing dynamic mass are defined by specifying the multiplier for each load case considered. In this model, all long term loads were assigned a multiplier of 1.0, live loads a multiplier of 0.25, and snow loads a multiplier of 0.75. Live load mass participation requirements for dynamic analyses are described in Section 3.8.4.3.4. Table 3.8.4-7 lists the additional masses included from various load cases and its corresponding multipliers, which are considered as one of the mass sources for the RXB SAP2000 models for 1-g and dynamic analyses performed. The purpose of the 1-g analysis is to verify the SAP2000 model has been converted accurately to the SASSI2010 model. In addition to comparing structural frequencies of the two models, 1-g analysis (i.e., total weight) is performed in the three global directions, and the total model weight is obtained at the fixed base of the model in the loading direction. As shown in Table 3.8.4-13 and Table 3.8.4-14, total weights of the two models are nearly identical. Thus, it is concluded that the SAP2000 model of the RXB with backfill has been accurately converted to the SASSI2010 model.

Lumped joint masses for use in dynamic analyses also apply to time history analyses performed to assess fluid-structure interaction (FSI) and sloshing of the pool water in the RXB. Table 3.8.4-11 provides the type of dynamic analysis, computer code name, and purpose of these analyses.

The crane weight is included by providing an RBC model in the RXB SAP2000 and SASSI2010 models with its associated mass properties. In the ANSYS models, the RBC self-weight and its lift load are applied as nodal masses along the crane rail locations.

Only load patterns EQ-125, EQ-100, EQ-75, EQ-50, EQ-24, L-LIVE, and S-SNOW, identified in Table 3.8.4-7, apply to the ANSYS models.

Load cases are developed in (or converted to) SAP2000 to address the different design loads discussed in Section 3.8.4.3. These cases are individually evaluated or combined to address the load combinations identified in Table 3.8.4-1 and Table 3.8.4-2 for the RXB.

3.8.4.4.2 Control Building Analysis

SAP2000 Model of the Control Building

Two analysis models with fixed base boundary conditions were created to consider the cracked and uncracked concrete conditions. The level of cracking considered for the cracked SAP2000 analysis model was based on guidance from ASCE 43-05 Section 3.4.1 and Table 3-1. Section 3.7.1.2.2 and Table 3.7.1-7 specify the level of cracking used in these models.

The basis associated with the assumed level of cracking is that this approach accounts for fully enveloped conditions. Envelope demand forces and moments from the uncracked and cracked condition are used regardless the demand moments and shear reach their cracking limits.

The purpose of these models is to envelope the extracted demand forces and moments from the cracked and uncracked models from the static analysis. These maximum demand forces and moments are then used in the design. The two CRB SAP2000 analysis models are identical in geometry and applied loads. Figure 3.8.4-21 through Figure 3.8.4-26 show the CRB SAP2000 model in various isometric and perspective views. Table 3.8.4-8 tabulates the total number of joints and elements developed in both the uncracked and cracked SAP2000 analysis models.

The CRB finite element models are developed to represent the primary structural members including walls, beams, columns, pilasters, floors and roofs. Walls, floors, metal decking and wind siding elements are represented by shell elements and the beams, columns, braces and pilasters are modeled by frame (beam) elements. The basemat foundation is modeled by solid elements and shell elements. The excavated soil is modeled by solid elements only. All shell and frame elements are modeled at their centerlines (neutral planes). All structural steel connections have fixed boundary condition. Penetrations in the walls or slabs are approximated in the SAP2000 model.

The bottom of the foundation basemat of the CRB SAP2000 model has a link element at each node. One end of each link element in the CRB SAP2000 model is connected to the CRB basemat and the other end to a fixed node.

Solid elements are added to the exterior of the CRB embedded walls to model the backfill soil with Soil Type 11 properties (see Section 3.7.1.3). The assumed uniform backfill width is 25 feet.

SAP2000 Analysis

All applicable loads are converted to lumped joint masses for use in 1-g and dynamic analyses. This is accomplished in SAP2000 by using the Mass Source function. In the CRB models, mass comes from concrete and steel self-weight, equipment joint nodal and uniform loads, uniform floor live loads, roof snow loads, and applied nodal masses. The specified load cases used in computing dynamic mass are defined by specifying the multiplier for each load case considered. In this model, all long term loads were assigned a multiplier of 1.0, live loads a multiplier of 0.25, and snow loads a multiplier of 0.75. Live load mass participation requirements for dynamic analyses are given in Section 3.8.4.3.4. Table 3.8.4-9 lists the additional masses to be included from various load cases and its corresponding multipliers, which are considered as one of the mass sources for the CRB SAP2000 models for 1-g and dynamic analyses performed.

Load cases are developed in (or converted to) SAP2000 to address the different design loads discussed in Section 3.8.4.3. These cases are individually evaluated or combined to address the load combinations identified in Table 3.8.4-1 and Table 3.8.4-2 for the CRB.

3.8.4.5 Structural Acceptance Criteria

The load cases for the RXB and CRB are provided in Table 3.8.4-1 and Table 3.8.4-2. These tables identify the design code applied for each load combination.

Code requirements are outlined in Table 3.8.4-12 which indicates the design codes for each Seismic Category based on the type of structure or loading.

Limits for allowable stresses, strains, deformations and other design criteria for the reinforced concrete structures are in accordance with ACI 349/349R and its appendices as modified by the exceptions specified in RG 1.142. Structural acceptance criteria for the steel components are in accordance with AISC N690 (Reference 3.8.4-6). Load combination 10 from Table 3.8.4-1 has been determined to be the controlling load combination. As such, this load combination was used to assess the adequacy of the structures. The use of AISC N690 (Reference 3.8.4-6) was to obtain loads from allowable strength design load combinations for use in the analysis of safety related, seismic category I steel structures. Load combination comparisons are performed on a case by case basis between AISC N690-1994 including Supplement 2 (2004) and AISC N690-2012 for verification that AISC N690-2012 provides the governing case.

Appendix 3B, Reactor Building and Control Building Design Approach and Critical Section Details, provides results for selected sections of both the RXB and CRB.

Section 3.8.5.5 identifies acceptance criteria applicable to additional basemat load combinations.

3.8.4.6 Materials, Quality Control and Special Construction Techniques

3.8.4.6.1 Materials

The principal construction materials for structures are concrete, reinforcing steel, structural steel, stainless steel, bolts, anchor bolts and weld electrodes. Table 3.8.4-10 provides the specifics of the materials considered for the structural design.

3.8.4.6.1.1 Concrete

Structural concrete used in the Seismic Category I RXB and CRB conforms to ACI 349, as supplemented by RG 1.142, and ACI 301. The majority of the structural concrete has a minimum compressive strength (f'c) of 5000 psi. The exception is the external walls of the RXB which require a higher compressive strength of 7000 psi.

Specific concrete mix will be developed based upon site conditions. Concrete mixes are designed in accordance with ACI 211.1, using materials qualified and accepted for this work. The mix will be based on field testing of trial mixtures with actual materials used. However, the concrete constituents conform to the following codes:

Cement

Cement conforms to the requirements of ASTM C150.

Aggregates

Aggregates conform to the requirements of ASTM C33.

ASTM Standards C1260 and C1293 are used in testing aggregates for potential alkali-silica reactivity. Low-alkali cement is used in concrete with aggregates that are potentially reactive.

Admixtures

Air-entraining admixtures, if used, conform to the requirements of ASTM C260. Chemical admixtures, if used, conform to the requirements of ASTM C494. Fly ash and pozzolan admixtures, if used, conform to the requirements of ASTM C618.

Water

Water and ice for mixing is clean, with a total solids content of not more than 2000 ppm.

Construction

Construction, including placement, inspection, and testing is performed in accordance with the following codes and standards:

- ACI 301 Specifications for Structural Concrete for Buildings.
- ACI 304R Recommended Practice for Measuring, Mixing, Transporting, and Placing Concrete.
- ACI 305.1 Specification for Hot-Weather Concreting.
- ACI 306.1 Specification for Cold-Weather Concreting.
- ACI 347 Recommended Practice for Concrete Formwork.
- ACI SP-2 Manual of Concrete Inspection.
- ASTM C94 Specification for Ready-Mixed Concrete.

3.8.4.6.1.2 Reinforcing Steel

Reinforcing steel for all major structures is deformed billet steel bars conforming to ASTM designation A615 grade 60 or ASTM A706 grade 60. The placement of concrete reinforcement is in accordance with ACI -349.

Reinforcing development length and splice length is calculated by formulas specified in ACI 349.

Welded wire fabric for concrete reinforcement conforms to ASTM A185 (plain wire) or A497 (deformed wire).

The standard plant design does not use coated reinforcing steel.

3.8.4.6.1.3 Connections

Steel Bolts and Studs

Bolts of type ASTM A307 with lock washers may be used for stairs, ladders, purlins and girts only. All other bolted connections use high-strength bolts of ASTM A490 or A325 material.

Steel studs meet the requirements of ASTM A108 and Structural Welding Code-Steel AWS D1.1/D1.1M.

Anchor Bolts

Anchor bolts are of type ASTM F1554, 36 ksi or 55 ksi yield strength material. Where higher strengths are required ASTM F1554, 105 ksi yield strength material are used.

If post-installed anchors are used for supports, the flexibility of base plates is accounted for, in determining the anchor bolt loads. Post-installed anchors are also qualified for seismic loading if required.

Welds

Welding electrodes shall be E70XX or unless otherwise noted on drawings or within specification for ASTM A36 steel and E308L-16 or equivalent for ASTM A240, type 304- L stainless steel.

3.8.4.6.1.4 Other

Grating

Grating is welded and galvanized steel, "Metal Bar Type", conforming to the specification contained in ANSI/NAAMM MBG 531-00 and ANSI/NAAMM MBG 532-00. Grating is stainless steel.

Masonry Walls

There are no safety-related reinforced masonry walls in Seismic Category I structures.

Steel-Concrete Modules

The NuScale Power Plant primary safety-related structure design does not use steel-concrete modules.

3.8.4.6.2 Quality Control

Chapter 17 details the quality assurance program.

3.8.4.6.3 Special Construction Techniques

Modular construction, where wall or slab elements (or the rebar reinforcement) is pre-fabricated and then incorporated into the building, will be used when possible. This process is expected to leave sacrificial (non-structural) steel within the buildings. Typically this will be reinforcing beams underneath slabs. The uniform distributed dead load applied in the structural and seismic analyses encompasses the weight of this steel.

3.8.4.7 Testing and Inservice Inspection Requirements

There is no testing or in-service surveillance beyond the quality control tests performed during construction, which is in accordance with ACI 349, and AISC N690 (Reference 3.8.4-6).

COL Item 3.8-1: A COL applicant that references the NuScale Power Plant design certification will describe the site-specific program for monitoring and maintenance of the Seismic Category I structures in accordance with the requirements of 10 CFR 50.65 as

discussed in Regulatory Guide 1.160. Monitoring is to include below grade walls, groundwater chemistry if needed, base settlements and differential displacements.

3.8.4.8 Evaluation of Design for Site Specific Acceptability

The RXB and CRB are designed to remain operable and to transmit forces, moments, and accelerations so that contained safety-related SSC remain operable during and following an earthquake with a spectra equal to the CSDRS or the CSDRS-HF. This is accomplished by confirming the buildings meet code acceptance criteria if situated on a soft soil site, a hard soil/soft rock site, a rock site, and a hard rock site. However, each actual site will have unique soil conditions and a site-specific SSE. The entire analysis described in Section 3.8.4 does not need to be re-performed if it can be shown that non-seismic loads are less than those produced by the site parameters provided in Table 2.0-1 and that the forces experienced within the building from the site-specific earthquake are less than those produced from the CSDRS and CSDRS-HF.

COL Item 3.8-2: A COL applicant that references the NuScale Power Plant design certification will confirm that the site independent Reactor Building and Control Building are acceptable for use at the designated site.

The comparison of the non-seismic parameters is performed as described in COL Item 2.0-1 in Section 2.0. A direct comparison of seismic inputs cannot be made. Therefore the results of the site specific seismic analysis prepared in response to COL Item 3.7-5 and COL Item 3.7-6 in Section 3.7.2.16 are compared as described below.

The site specific foundation input response spectra (FIRS) are compared to the CSDRS and CSDRS-HF (which were used as the FIRS for the site-independent analysis). This demonstrates that the site specific seismic input is bounded by the input used for design.

In-structure response spectra at 5 percent damping are used for comparison within the buildings. The design ISRS may be used as a surrogate for the forces and moments. If the site independent ISRS are larger than the site specific ISRS the forces and moments will also be bounded for the design. The ISRS comparisons are done specifically at the reactor pool floor and the NPM lug restraints to confirm that the forces and accelerations that will be experienced by NPMs are acceptable. In addition, the ISRS at the RBC wheels is checked. The RBC is the only other large risk-significant SSC. As a general check of the buildings, the ISRS are compared at grade and at the roof of the RXB; and at the main control room, grade level and the top of the Seismic Category I portion of the CRB.This will be accomplished by confirming the following site specific characteristics/results are bounded by the DCD design parameters/results:

<u>RXB</u>

- FIRS — Compare to Figure 3.7.1-1 through Figure 3.7.1-4
- ISRS at the reactor pool floor — Compare to Figure 3.7.2-108
- ISRS at the NPM lug restraints — Compare to Figure 3.7.2-116
- ISRS at the RBC wheels — Compare to Figure 3.7.2-114

- ISRS at grade — Compare to Figure 3.7.2-111
- ISRS at the roof — Compare to Figure 3.7.2-113

CRB

- FIRS — Compare to Figure 3.7.1-1 through Figure 3.7.1-4
- ISRS at the main control room — Compare to Figure 3.7.2-119
- ISRS at grade — Compare to Figure 3.7.2-120
- ISRS at Elevation 120'-0" — Compare to Figure 3.7.2-121

3.8.4.9 References

3.8.4-1 SAP2000 Advanced Version 17.1.1, 2015, Computers and Structures, Inc., Walnut Creek, California.

3.8.4-2 SASSI2010 Version 1.0, May 2012, Berkeley, California.

3.8.4-3 ANSYS Computer Program, Release 16.0, January 2015. ANSYS Incorporated, Canonsburg, Pennsylvania.

3.8.4-4 TR-0816-49833, "Fuel Storage Rack Analysis," NuScale, December 2016

3.8.4-5 ACI 349-06, "Code Requirements for Nuclear Safety-Related Concrete Structures and Commentary", American Concrete Institute, 2006

3.8.4-6 ANSI/AISC N690-12, "Specification for Steel Safety-Related Steel Structures for Nuclear Facilities", American Institute of Steel Construction, 2012.

3.8.4-7 ACI 349.1R, "Reinforced Concrete Design for Thermal Effects on Nuclear Power Plant Structures, American Concrete Institute, 2007.

3.8.4-8 American Society of Civil Engineers/Structural Engineering Institute, "Minimum Design Loads for Buildings and Other Structures," ASCE/SEI 7-05, Reston, VA, 2005.

Table 3.8.4-1: Concrete Design Load Combinations

Load Combinations[1]	Design Loads																				ACI 349-06 Section (Equation)
	D	F	H	L	L_r	R_o	R_a	T_o	T_a	R	S	S_e	W	W_t/W_h	E_o	E_{ss}	C_{cr}	P_a	Y_j[2]	Y_m[2]	Y_r[2]	
	1	2	3	4	5	6	7	8	9	10	11	12	13	14	15	16	17	18	19	20	21	
1	1.4	1.4				1.4		1														9.2.1 (9-1)
2	1.2	1.2	1.6	1.6	0.5	1.2		1.2									1.4					9.2.1 (9-2)
3	1.2	1.2	1.6	1.6		1.2		1.2			0.5						1.4					
4	1.2	1.2	1.6	1.6		1.2		1.2		0.5							1.4					
5	1.2	1.2	0.8	0.8	1.6	1.2											1.4					9.2.1 (9-3)
6	1.2	1.2	0.8	0.8		1.2					1.6						1.4					
7	1.2	1.2	0.8	0.8		1.2				1.6							1.4					
8	1.2	1.2	1.6	1.6		1.2									1.6							9.2.1 (9-4)
9	1.2	1.2	1.6	1.6		1.2							1.6									9.2.1 (9-5)
10	1	1	1	0.8		1		1								1	1					9.2.1 (9-6)
11	1	1	1	0.8		1		1						1								9.2.1 (9-7)
12	1	1	1	0.8			1		1								1	1.2				9.2.1 (9-8)
13	1	1	1	0.8			1		1							1		1	1	1	1	9.2.1 (9-9)
14	1	1	1	0.8		1		1				1										-

Notes:

1. The load combinations are also evaluated with 0.9D to assess the adverse effects of reduced dead load.

2. Design loads Y_j, Y_m, and Y_r, from load combination 13 will be re-evaluated per COL Item 3.6-2 and COL Item 3.6.3 for localized effects.

Table 3.8.4-2: Steel Design Load Combinations

Load Combinations[1]	Design Loads																				ANSI/AISC N690-12 Section (Equation)
	D	F	H	L	L_r	R_o	R_a	T_o	T_a	R	S	S_e	W^2	$W_t/W_h{}^2$	E_o	E_{ss}	C_{cr}	P_a	$Y_j{}^3$	$Y_m{}^3$	$Y_r{}^3$	
	1	2	3	4	5	6	7	8	9	10	11	12	12	13	14	15	16	17	18	19	20	
1	1	1	1	1		1		1									1					NB2.6a (NB2-10)
2	1	1	1	1	1	1		1									1					
3	1	1	1	1		1		1			1						1					NB2.6a (NB2-11)
4	1	1	1	1		1		1		1							1					
5	1	1	0.75	0.75	0.75			1									1					NB2.6a (NB2-12)
6	1	1	0.75	0.75				1			0.75						1					
7	1	1	0.75	0.75				1		0.75							1					
8	1	1	0.75	0.75	0.75	1		1					1				1					NB2.6b (NB2-13)
9	1	1	0.75	0.75		1		1			0.75		1				1					
10	1	1	0.75	0.75		1		1		0.75			1				1					
11	1	1	0.75	0.75	0.75	1		1							1		1					NB2.6b (NB2-14)
12	1	1	0.75	0.75		1		1			0.75				1		1					
13	1	1	0.75	0.75		1		1		0.75					1		1					
14	1	1	1	1		1		1								1	1					NB2.6c (NB2-15)
15	1	1	1	1		1		1						1								NB2.6c (NB2-16)
16	1	1	1	1			1		1								1	1				NB2.6c (NB2-17)
17	1	1	1	1			1		1							0.7		1	1	1	1	NB2.6c (NB2-18)
18	1	1	1	1		1		1				1										-

Notes:

1. The load combinations are also evaluated with 0.6D to assess the adverse effects of reduced dead load.
2. The factors for wind loading are taken as 1 instead of 0.6 because the load was designed based on ASCE 7-05 rather than ASCE 7-10.
3. Design loads Y_j, Y_m, and Y_r, from load combination 17 will be re-evaluated per COL Item 3.6-2 and COL Item 3.6-3 for localized effects.

Table 3.8.4-3: Summary of Reactor Building Equipment

Elevation	Total (kip)
EL. 24′-0″	2,457
EL. 50′-0″	726
EL. 75′-0″	1,502
EL. 100′-0″	2,603
EL. 126′-0″[1]	1,554
Total	**8,842**

Notes:
1. Equipment at Elevation 145′-6″ is included at Elevation 126′-0″.

Table 3.8.4-4: Summary of Control Building Equipment

Elevation	Total (kip)
EL. 50'-0"	742
EL. 63'-3"	11.8
EL. 76'-6"	4
EL. 100'-0"	3.9
EL. 120'-0"	55.8
EL. 137'-6"	30
EL. 140'-0"	6.8
Total	**854.4**

Table 3.8.4-5: Hydrodynamic Weight

Hydrodynamic Load Direction	Region	Description	Water Weight (kips)
Longitudinal X-Direction (East-West)	1	Reactor Pool (North NPM Bays)	6,400
	2	Reactor Pool (South NPM Bays)	6,400
	3	Reactor Pool Middle + Refueling Pool (Middle Area)	27,300
	4	Refueling Pool (North Area)	4,000
	5	Refueling Pool (South Area)	4,500
	6	Dry Dock	8,500
	7	Spent Fuel Pool	7,700
Total			**64,700**
Transverse Y-Direction (North-South)	1	Reactor Pool	31,800
	2	Refueling Pool (East Area)	8,200
	3	Refueling Pool (West Area 1)	4,000
	4	Refueling Pool (West Area 2)	4,500
	5	Dry Dock	8,500
	6	Spent Fuel Pool	7,700
Total			**64,700**

Table 3.8.4-6: Reactor Building SAP2000 Joints and Elements

Items	Quantity
Number of Joints	30,762
Number of Joint with Restraints	2,342
Number of Joint with Mass	3,465
Number of Frame Elements	6,453
Number of Shell Elements	18,818
Number of Solid Elements	12,075
Number of Link/Support Elements	1,114

Table 3.8.4-7: Reactor Building SAP2000 Mass Sources

Mass From	Load Pattern	Multiplier	Remarks
All	EQ-125	1	100% of all equipment weight on floor slab at elevation 125′-0″
All	EQ-100	1	100% of all equipment weight on floor slab at elevation 100′-0″
All	EQ-75	1	100% of all equipment weight on floor slab at elevation 75′-0″
All	EQ-50	1	100% of all equipment weight on floor slab at elevation 50′-0″
All	EQ-24	1	100% of all equipment weight on foundation at elevation 24′-0″
All	L-LIVE	0.25	25% of all floor live load
All	S-SNOW	0.75	75% of roof snow load
All	EQ-86	1	100% of all equipment weight on foundation at elevation 86′-0″
All	EDL	1	100% of all equivalent dead load
All	EDL-P3	1	100% of all additional Phase 3 equipment weight
All	EDL-ROOF	1	100% of all equivalent dead load at roof
All	STAIRWELL	1	100% of all stair dead load
All	ELEVATOR	1	100% of all elevator dead load
All	PIPELOAD-EL125	1	100% of all pipe loads

Table 3.8.4-8: Control Building SAP2000 Joints and Elements.

Items	Quantity
Number of Joints	8,872
Number of Joint with Restraints	864
Number of Frame Elements	1,393
Number of Shell Elements	4,069
Number of Solid Elements	3,966
Number of Link/Support Elements	457

Table 3.8.4-9: Control Building SAP2000 Mass Sources

Mass From	Load Pattern	Multiplier	Remarks
All	EQ-140-CRB	1.00	100% of all equipment weight on roof at elevation 140′-0″
All	EQ-120-CRB	1.00	100% of all equipment weight on floor slab at elevation 120′-0″
All	EQ-50-CRB	1.00	100% of all equipment weight on floor slab at elevation 50′-0″
All	EDL	1.00	Equivalent Dead Load of 50 psf for all floor slabs
All	L-Live	0.25	25% of all floor live load
All	S-SNOW	0.75	75% of roof snow load
All	MetalDeck	1.00	100% of superimposed roof dead load at elevation 140′-0″

Table 3.8.4-10: Material Properties

Item	Value
Concrete Compressive Strength	f'_c = 5,000 psi typical f'_c = 7,000 psi for exterior walls of the RXB above grade
Concrete Poisson's Ratio	v_c= 0.17
Concrete Modulus of Elasticity	E_c= 4,031 ksi
Concrete Shear Modulus	G_c= 1,722 ksi
Concrete Density	ρ_c= 150 pcf
Concrete Coefficient of Thermal Expansion	α_c= 5.5 E-06
Reinforcing Steel Yield Strength	F_y = 60 ksi
Reinforcing Steel Modulus of Elasticity	E_s = 29,000 ksi

Table 3.8.4-11: Additional Dynamic Analyses

Dynamic Analysis Type	Computer Code Name	Purpose
Time history analysis to assess FSI	ANSYS, Release 15.0	The purpose of this analysis is to provide a method to account for the correct hydrodynamic pressures on the pool walls in the RXB analysis models. This is done by performing an FSI analysis, which involves performing time history analyses on the RXB in ANSYS, modeling the pool water with fluid elements. These same time history analyses are performed on the RXB in SASSI2010 modeling the pool water as lumped masses on the pool walls. Hydrodynamic pressures are computed from the ANSYS and SASSI2010 results and the maximum pressure difference between ANSYS and SASSI2010 is found. This pressure difference is accounted for in SAP2000 by amplifying the gravity load.
Time history analysis to assess RXB pool water sloshing	ANSYS, Release 16.0	The purpose of this analysis is to determine the pool water sloshing height. This is done by performing an FSI analysis, which involves performing time history analyses on the RXB in ANSYS, modeling the pool water with fluid elements. The maximum sloshing height is determined in ANSYS.

Table 3.8.4-12: Seismic Categories and Design Codes

Structure/Loading	Seismic Category I	Seismic Category II*	Seismic Category III
Concrete structures	ACI 349	ACI 349	ACI 318
Steel structures	AISC N690	AISC N690	AISC 360
Cold rolled members	AISI	AISI	AISI
Minimum design loads	ASCE 7	ASCE 7	ASCE 7
Seismic analysis/design	ASCE 4	ASCE 4	IBC

*Seismic Category II SSC that are not part of a structure's primary vertical or horizontal load resisting system may be designed to the codes and standards of Seismic Category III SSC (ACI 318 and AISC 360). However, interaction of Non-Seismic Category I Structures with Seismic Category I SSC shall be addressed as required by DSRS 3.7.2.

Table 3.8.4-13: Total Weight in Kips, SAP2000 Model

Load Case	Global FX	Global FY	Global FZ
1GX	868,025	0	0
1GY	0	871,940	0
1GZ	0	0	859,078

Table 3.8.4-14: Total Weight in Kips, SASSI2010 Model

Load Case	Global FX	Global FY	Global FZ
1GX	868,025	0	0
1GY	0	871,940	0
1GZ	0	0	859,077

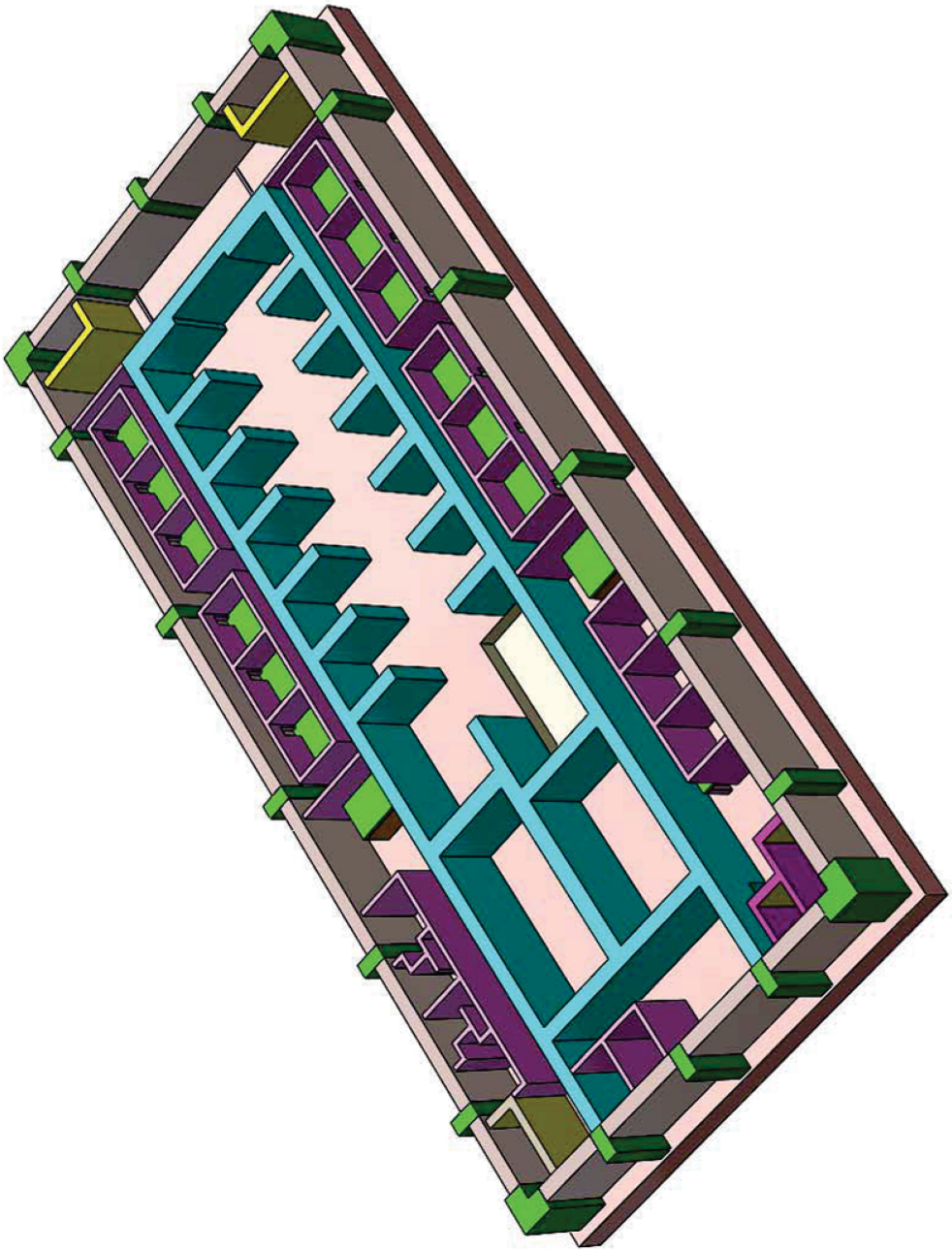

Figure 3.8.4-1: Reactor Building Concrete Structural Sections at First Floor (EL. 24'-0")

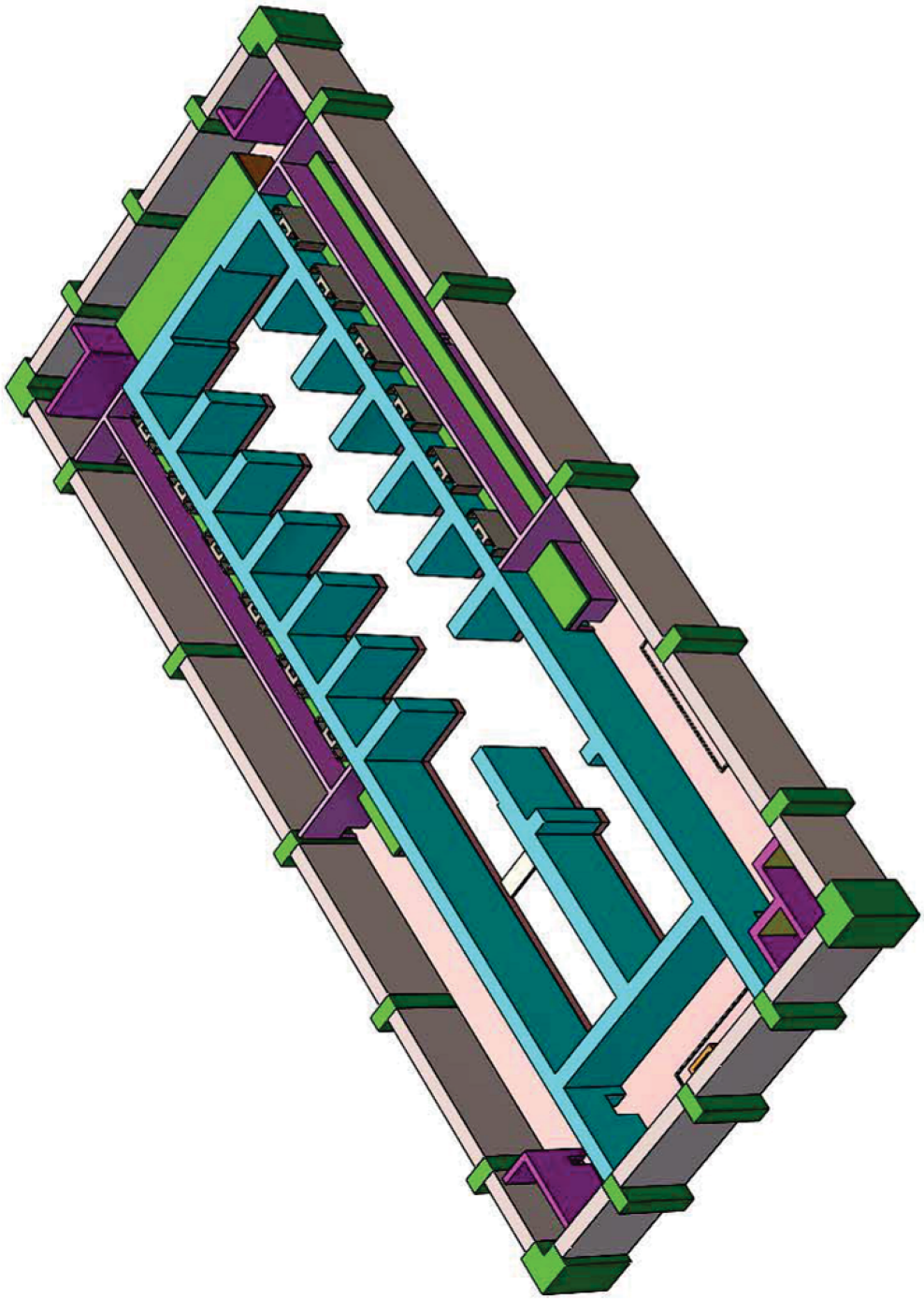

Figure 3.8.4-2: Reactor Building Concrete Structural Sections at Second Floor (EL. 50'-0")

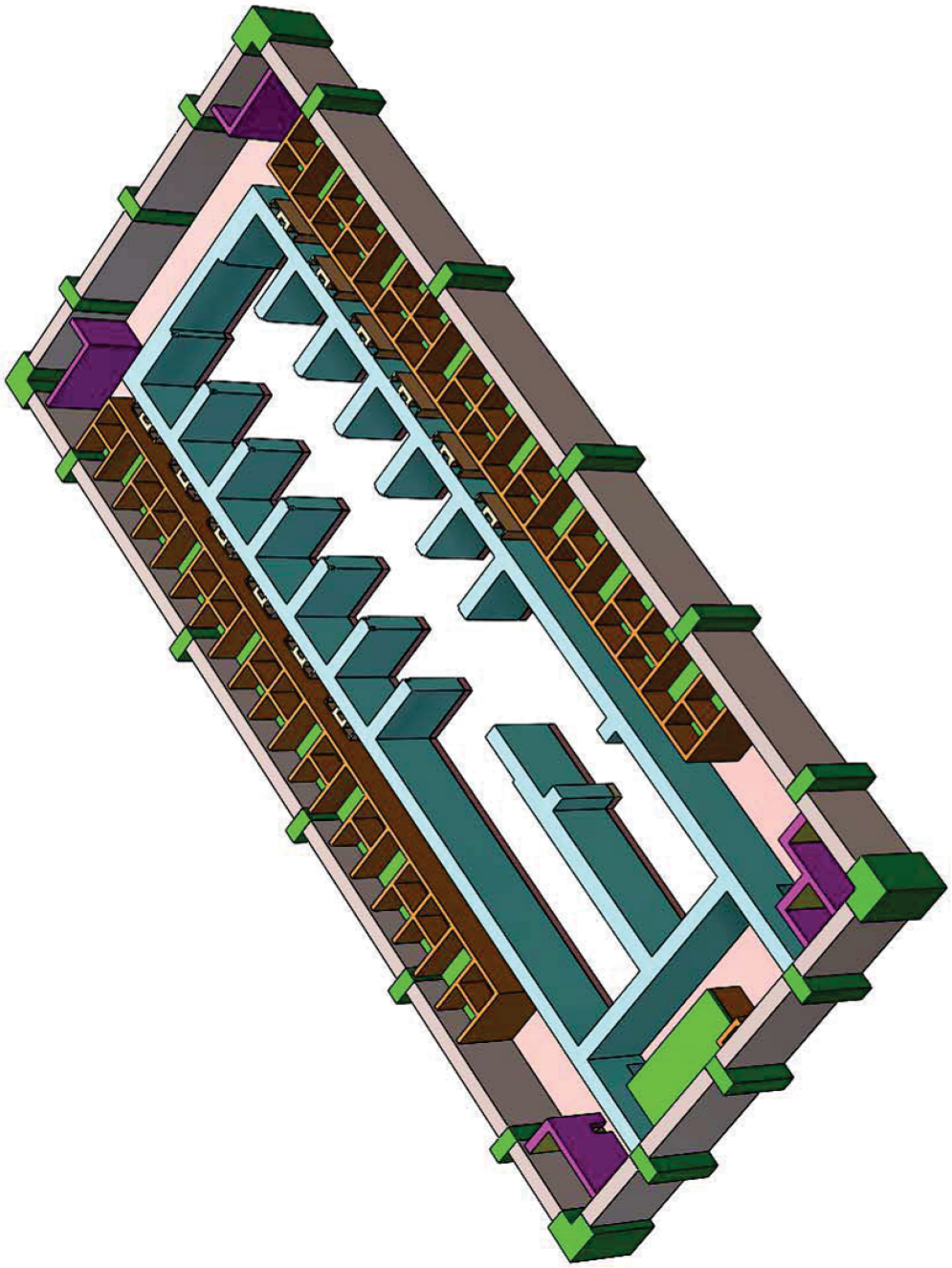

Figure 3.8.4-3: Reactor Building Concrete Structural Sections at Third Floor (EL. 75'-0")

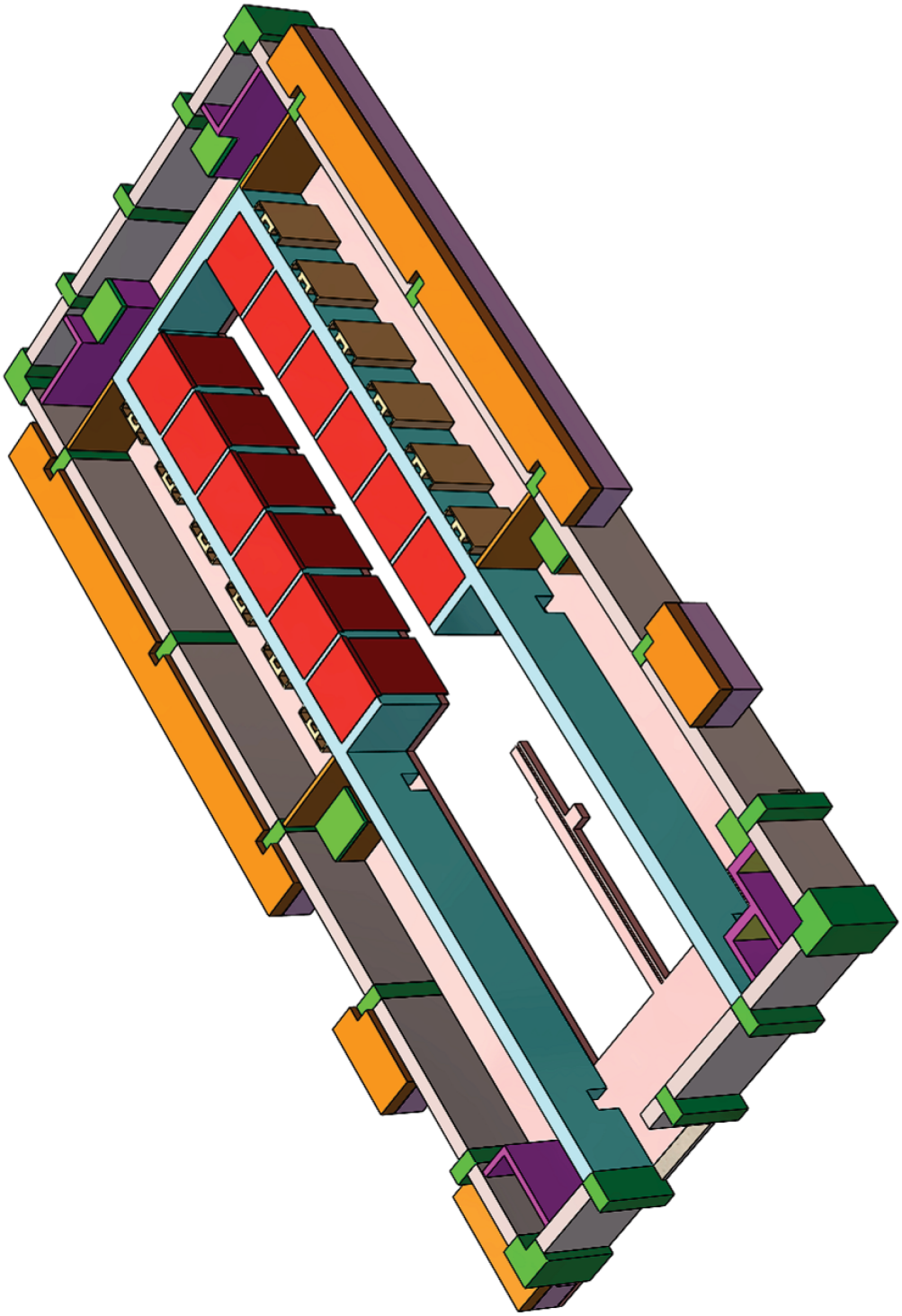

Figure 3.8.4-4: Reactor Building Concrete Structural Sections at Fourth Floor (EL. 100'-0")

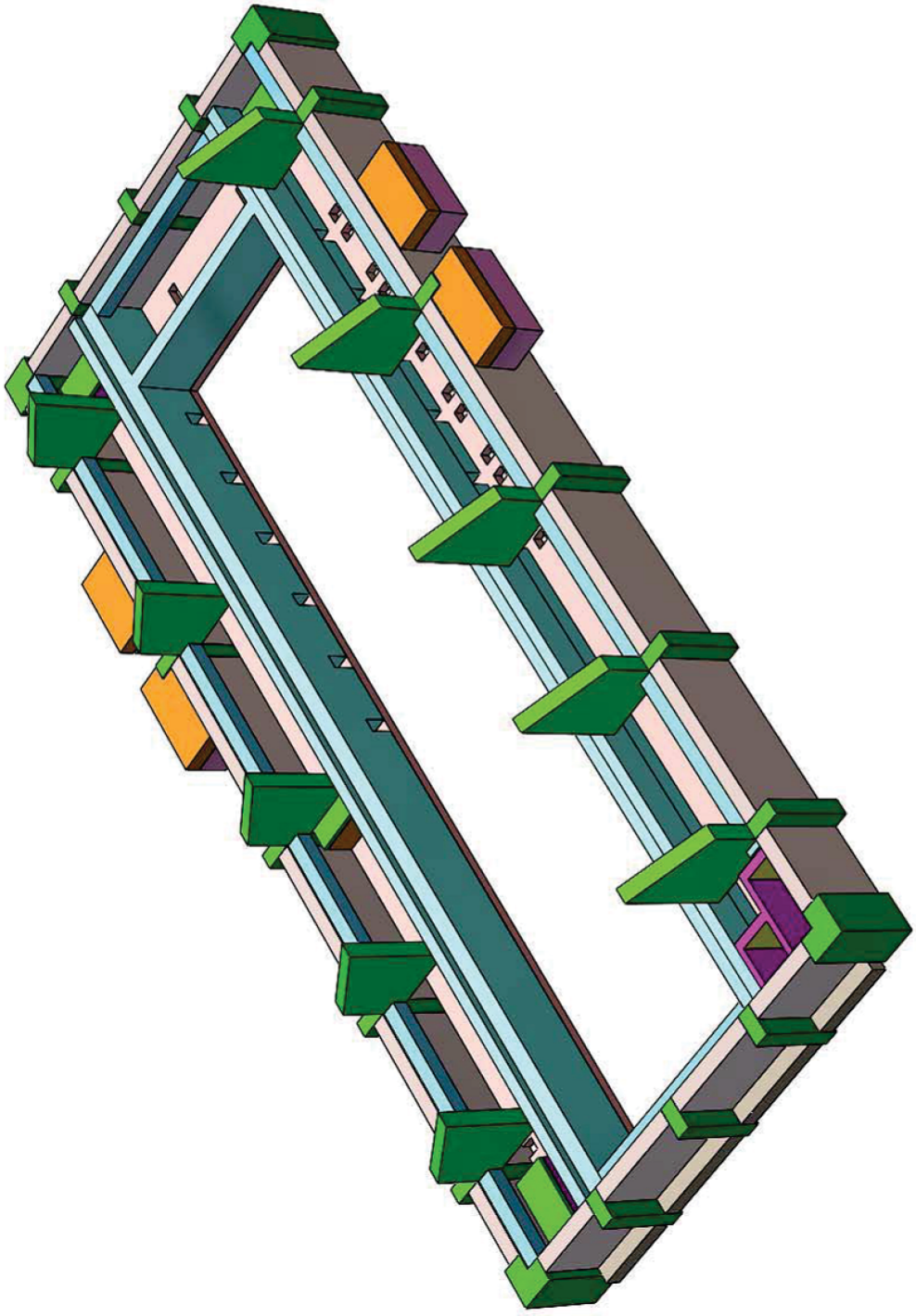

Figure 3.8.4-5: Reactor Building Concrete Structural Sections at Fifth Floor (EL. 126'-0")

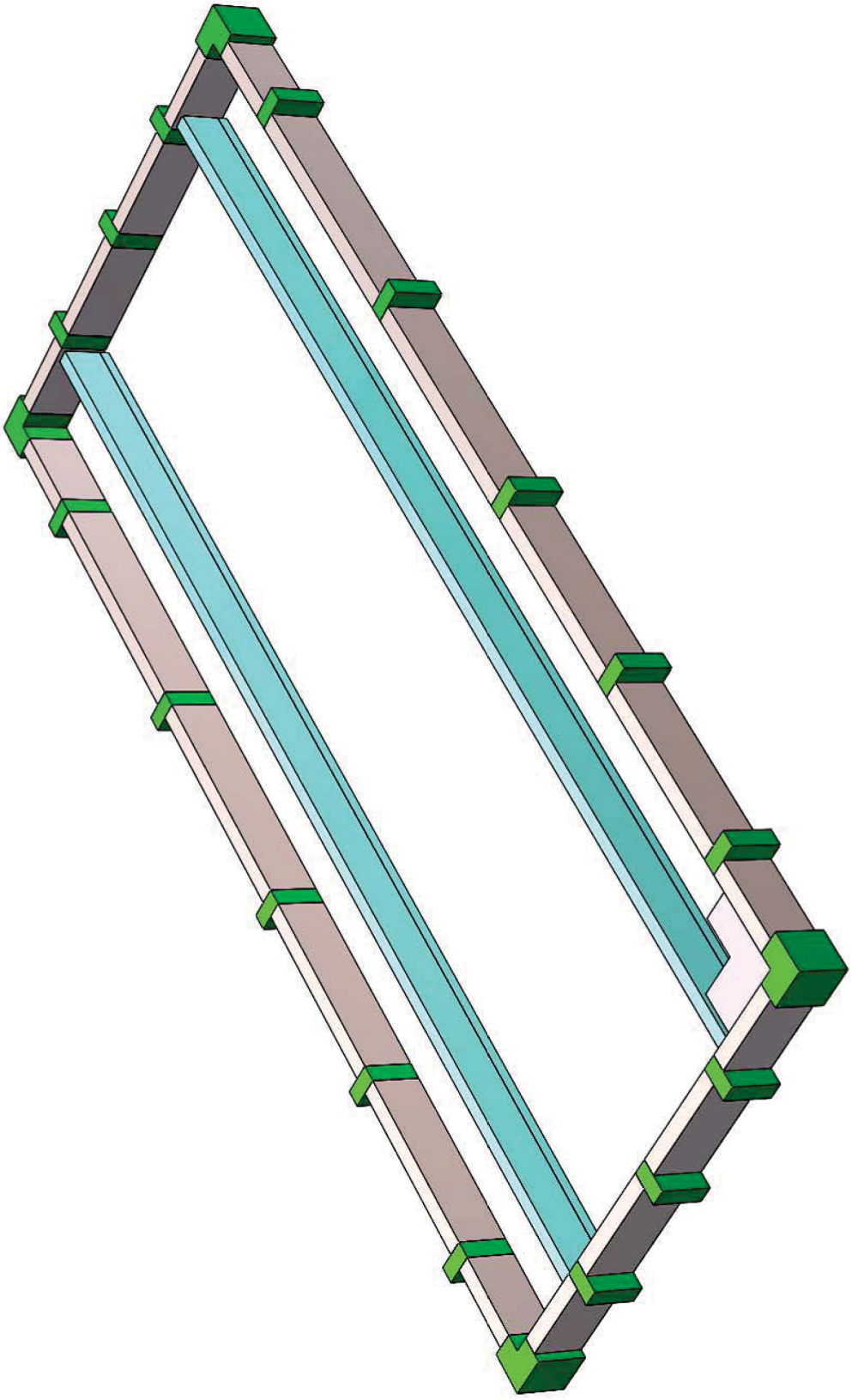

Figure 3.8.4-6: Reactor Building Concrete Structural Sections at RBC (EL. 145'-6")

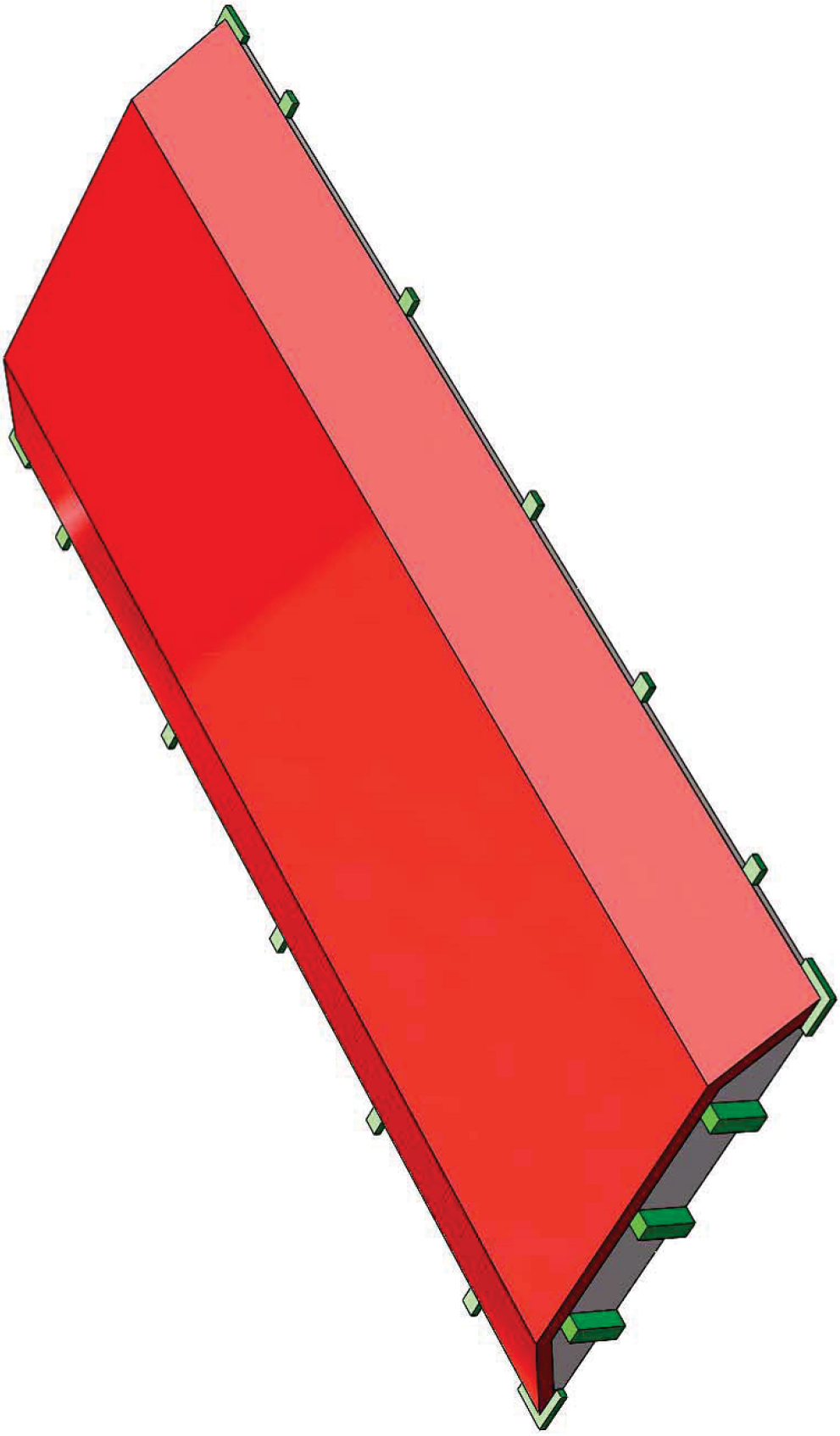

Figure 3.8.4-7: Reactor Building Concrete Structural Sections at Roof (EL. 181'-0")

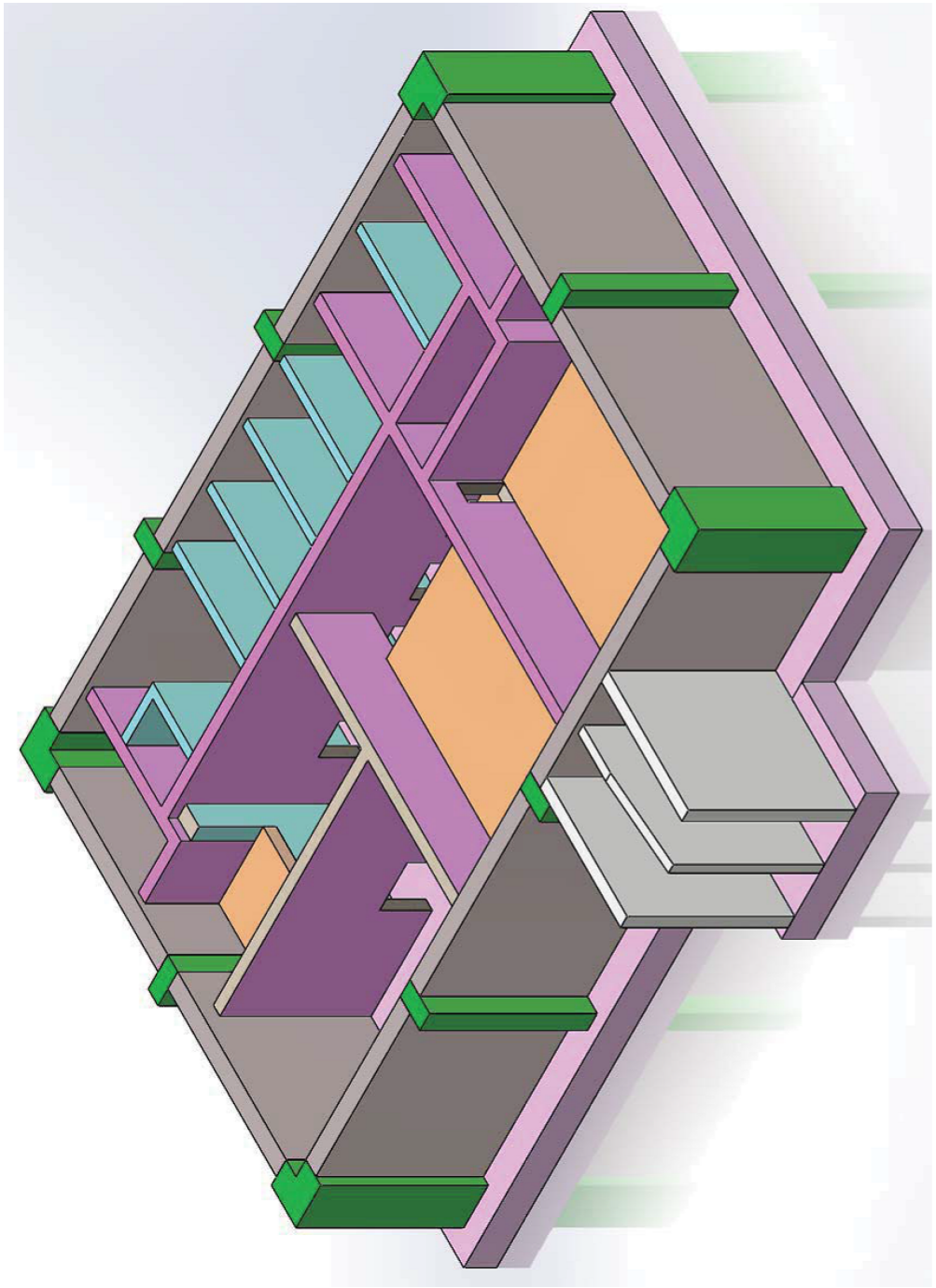

Figure 3.8.4-8: Control Building Concrete Structural Sections at First Floor (EL. 50'-0")

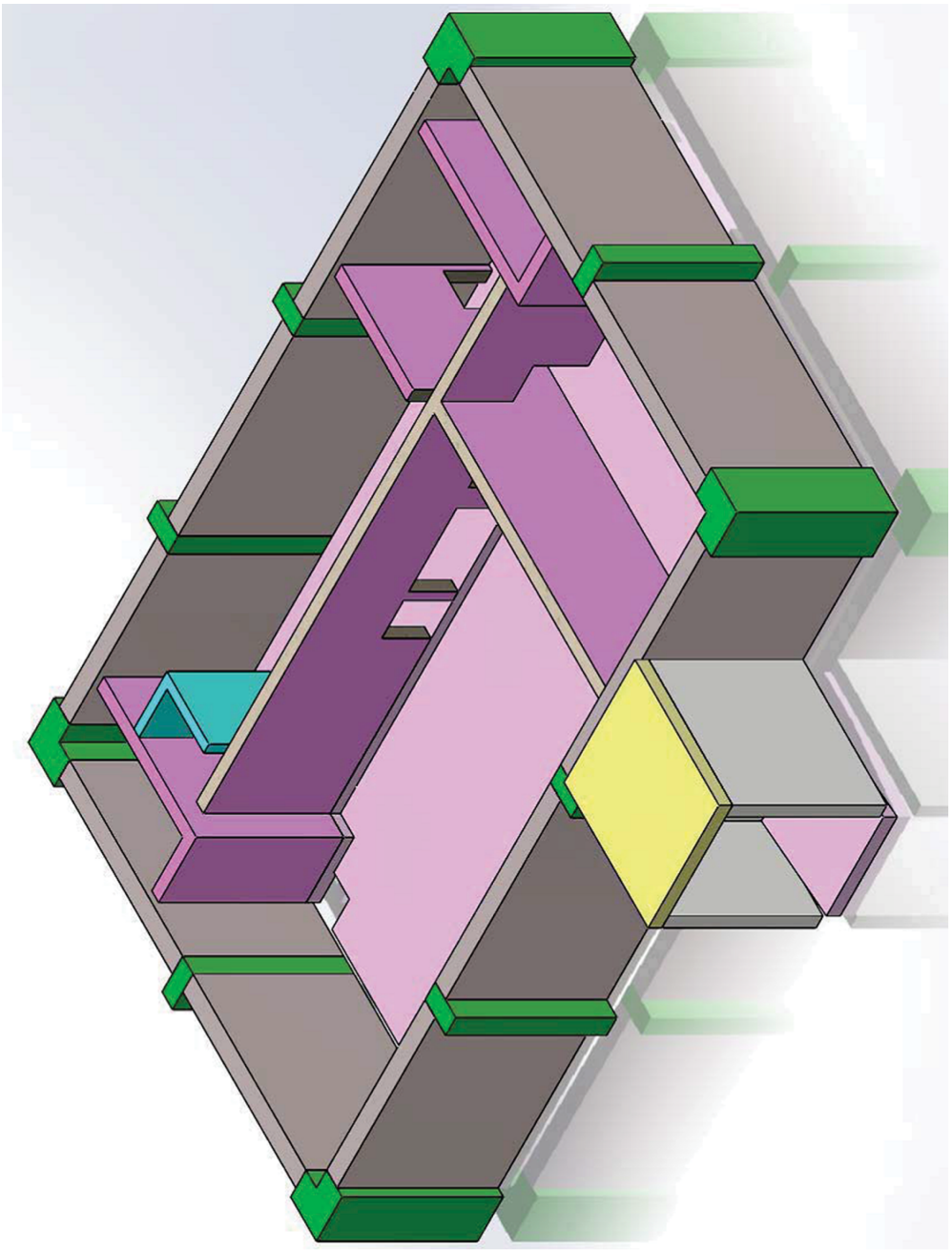

Figure 3.8.4-9: Control Building Concrete Structural Sections at Second Floor (EL. 76'-6")

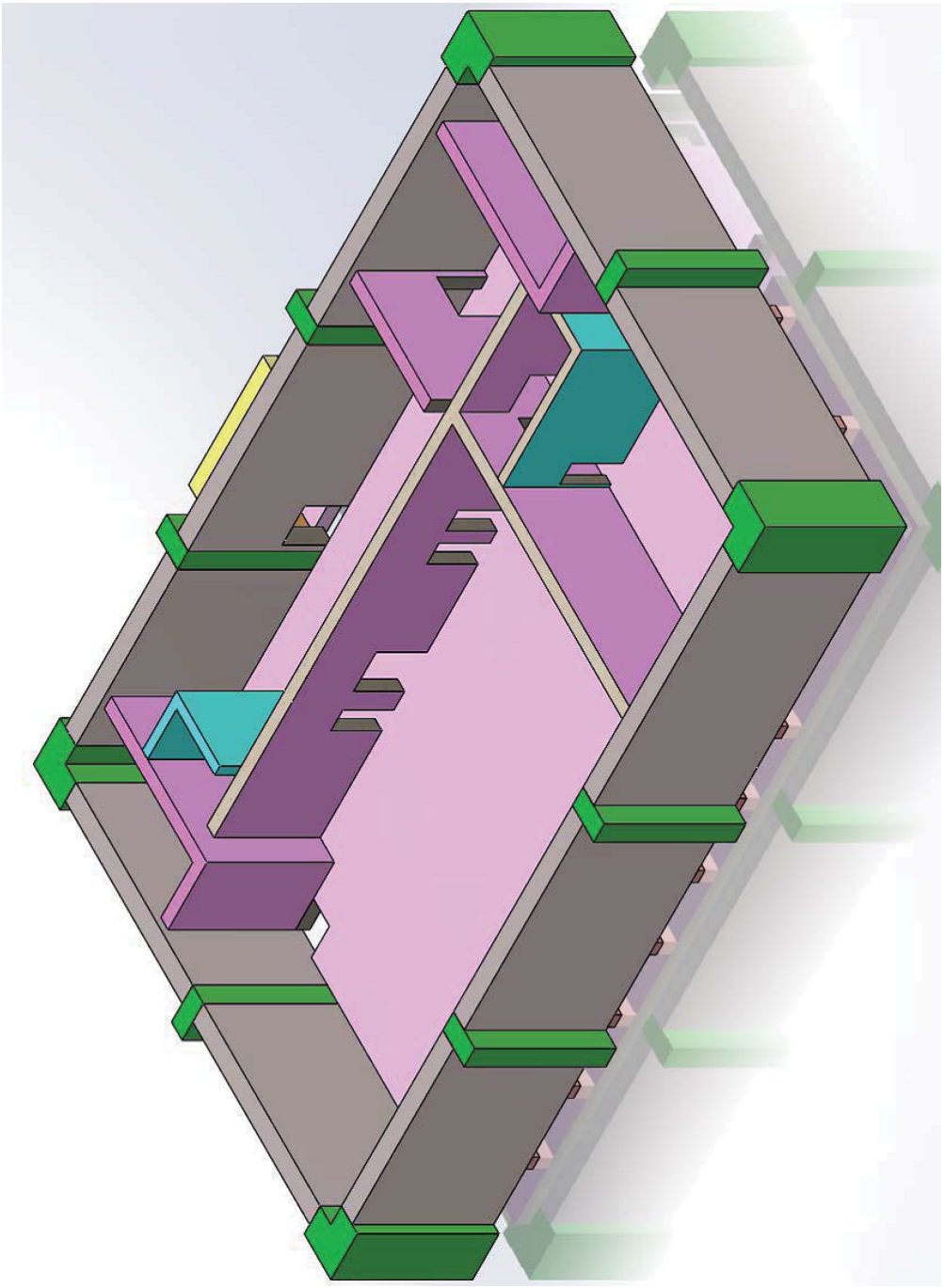

Figure 3.8.4-10: Control Building Concrete Structural Sections at Third Floor (EL. 100'-0")

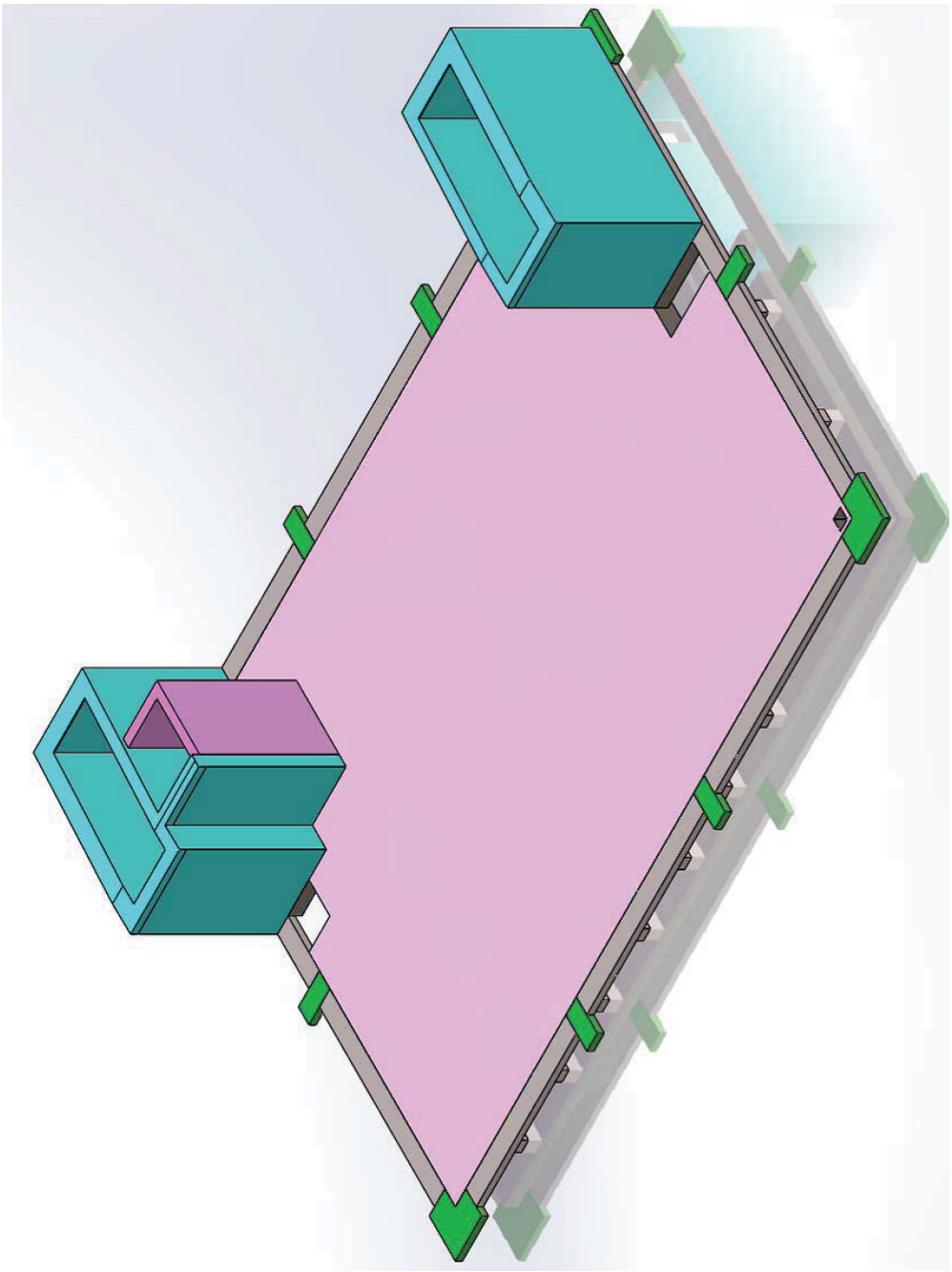

Figure 3.8.4-11: Control Building Concrete Structural Sections at Fourth Floor (EL. 120'-0")

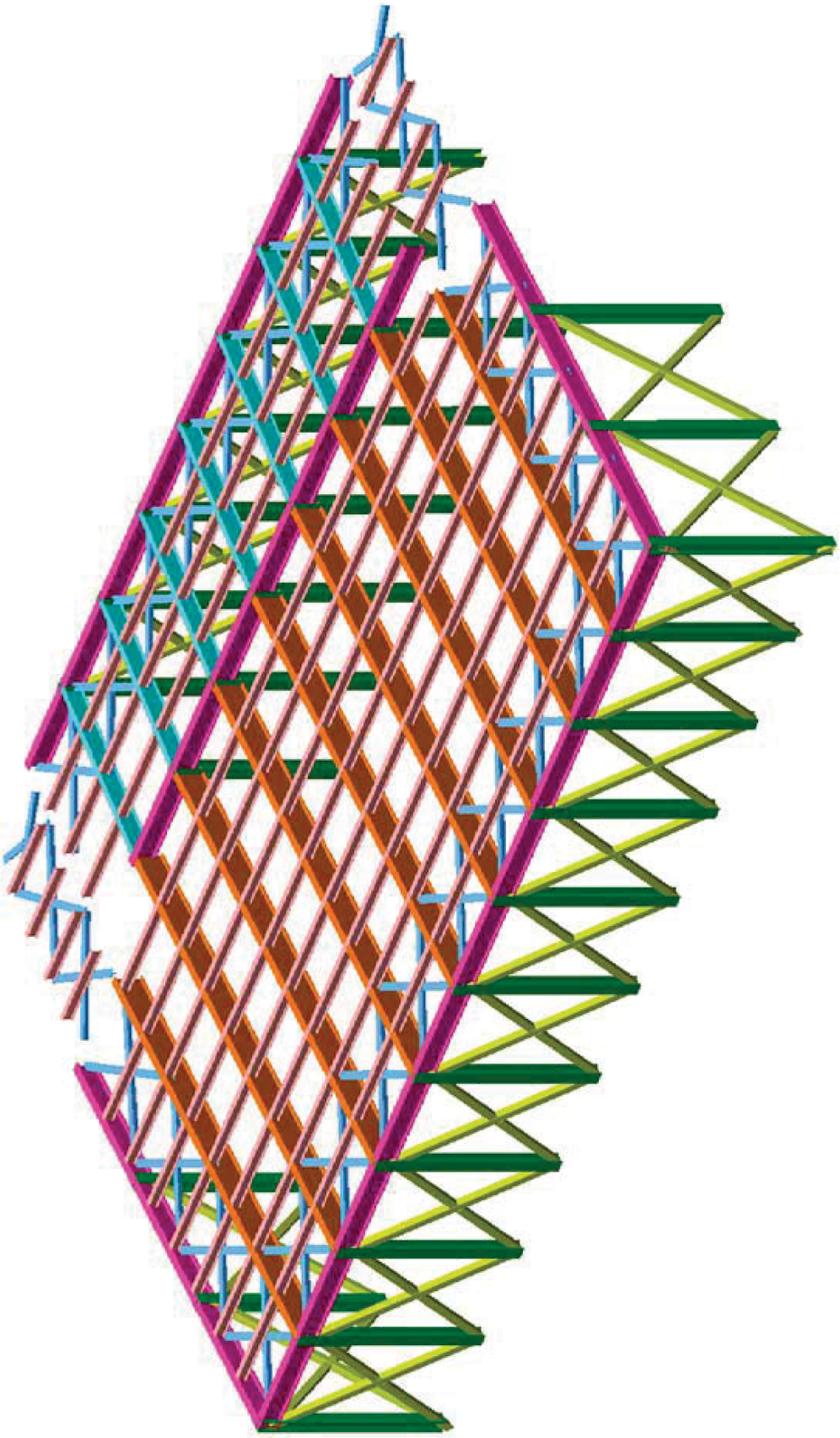

Figure 3.8.4-12: Control Building Steel Framing of Roof to EL. 141' 2"

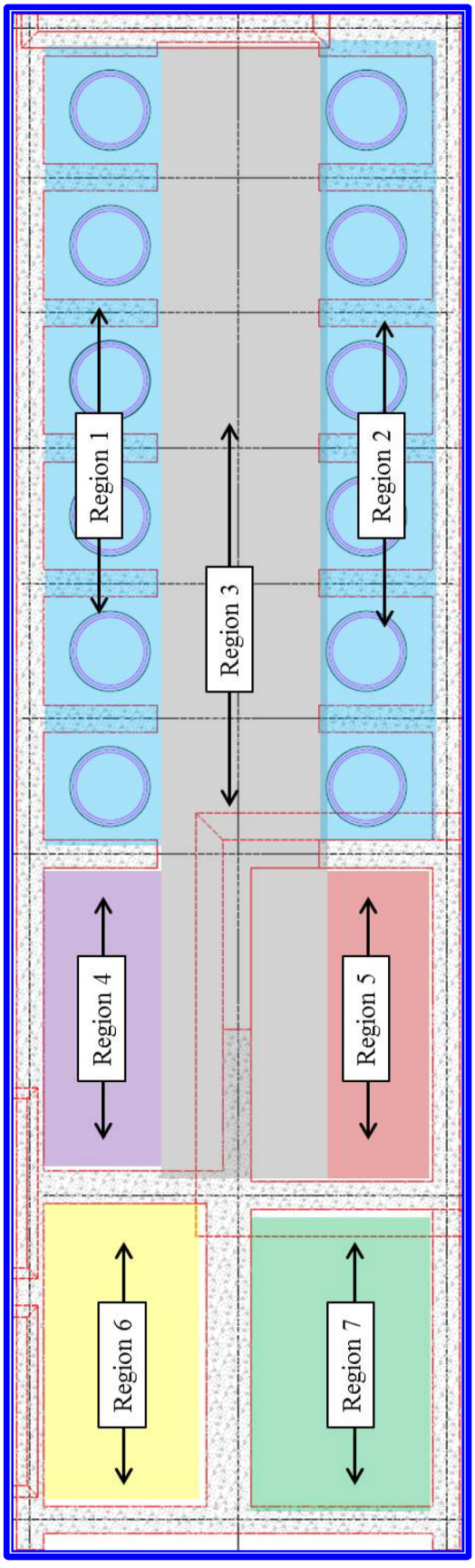

Figure 3.8.4-13: East-West (X) Longitudinal Hydrodynamic Load Regions

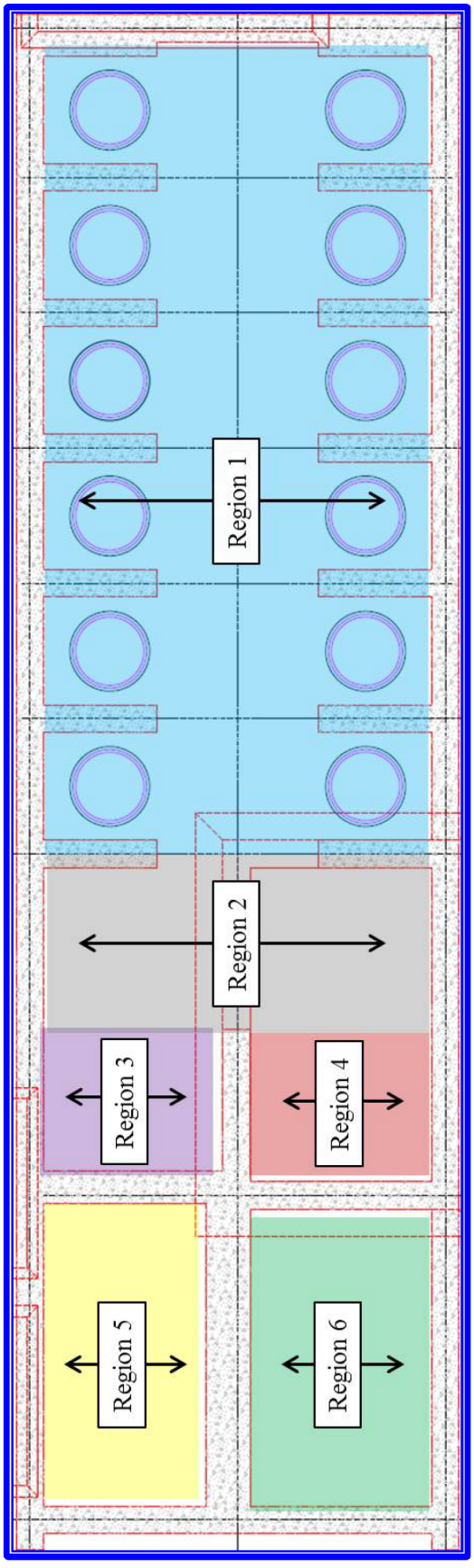

Figure 3.8.4-14: North-South (Y) Transverse Hydrodynamic Load Regions

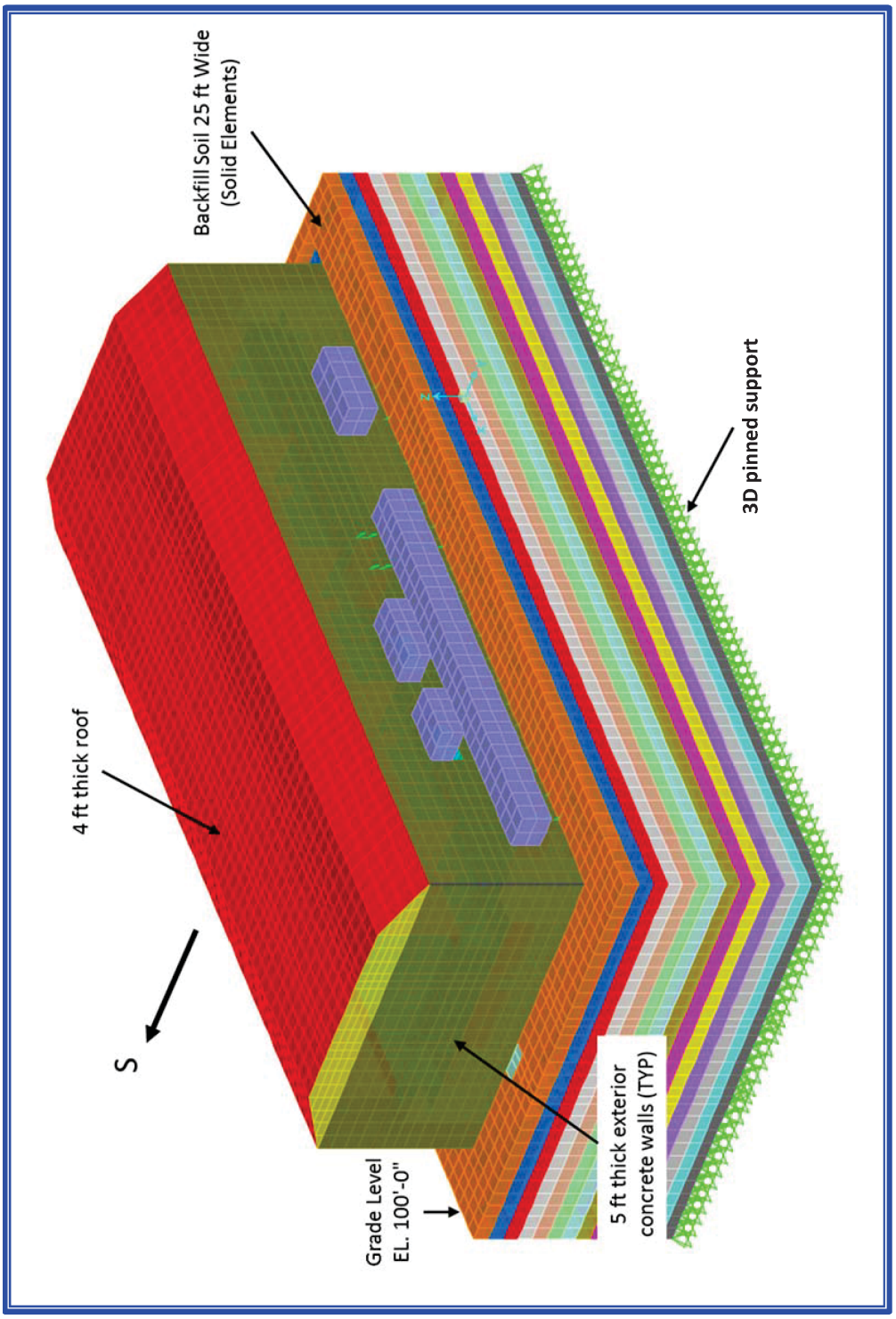

Figure 3.8.4-15: Reactor Building SAP2000 Model (Looking Southwest)

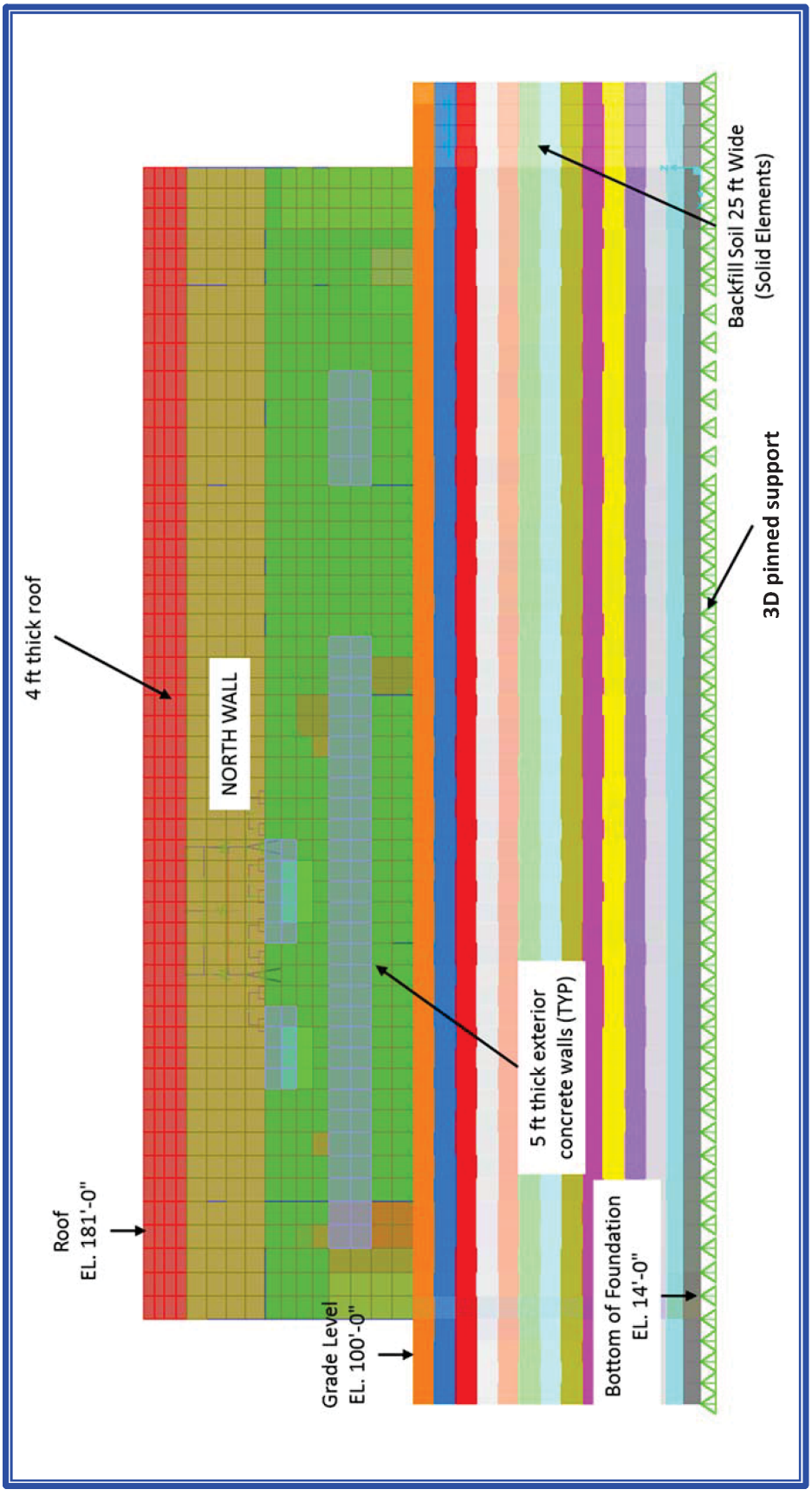

Figure 3.8.4-16: Elevation View of Reactor Building SAP2000 Model Looking South

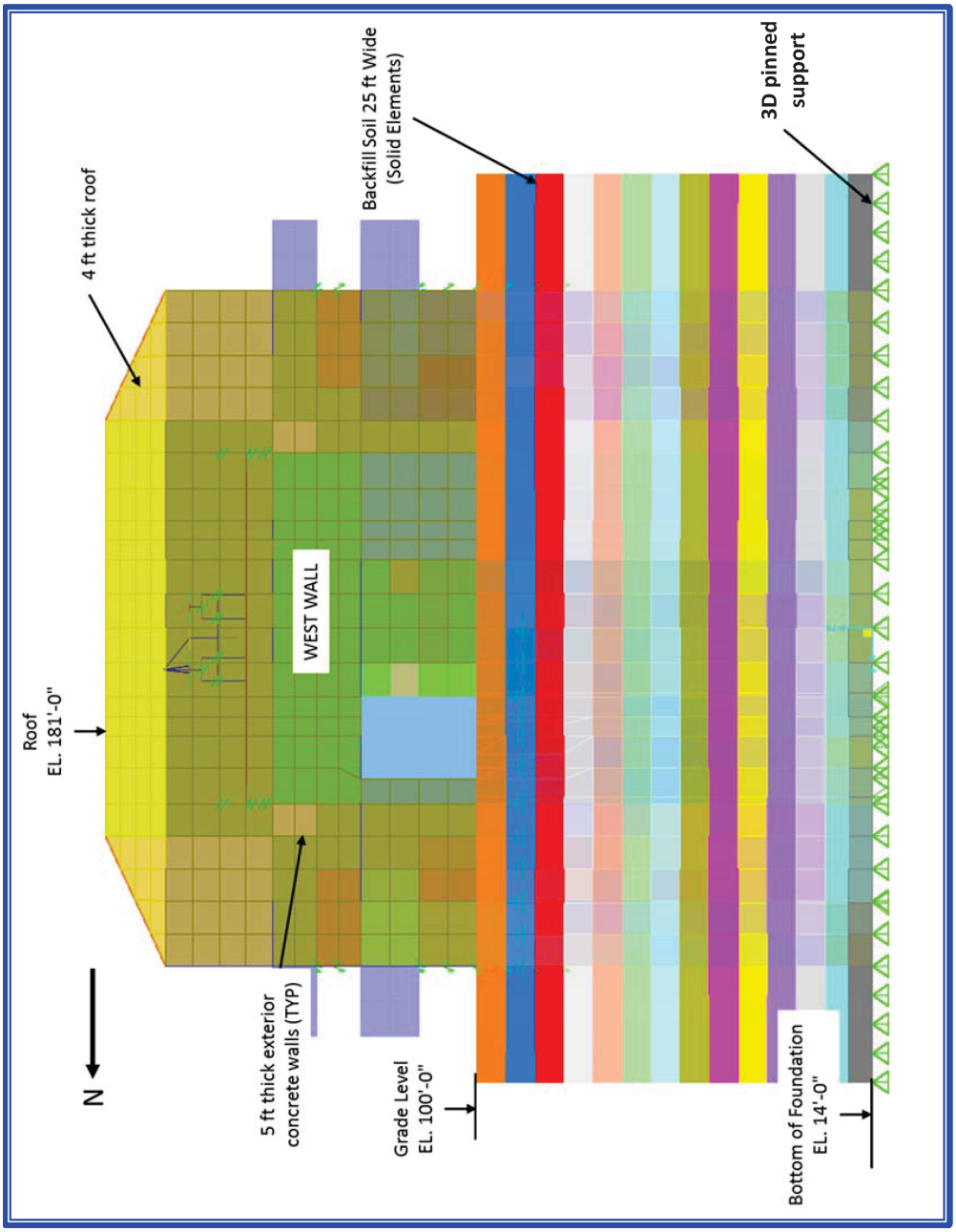

Figure 3.8.4-17: Elevation View of Reactor Building SAP2000 Model Looking East

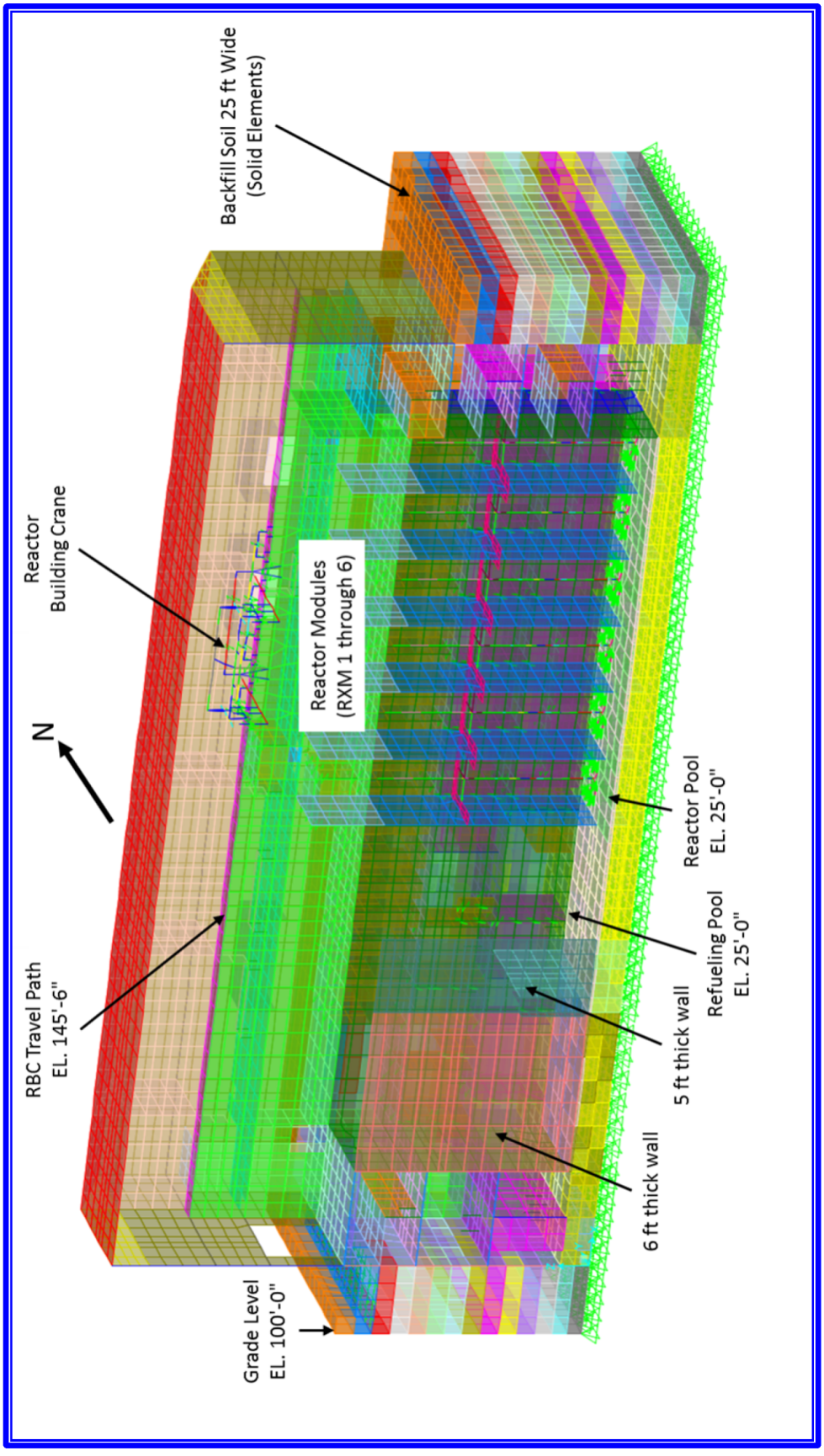

Figure 3.8.4-18: Longitudinal Section View of Reactor Building SAP2000 Model

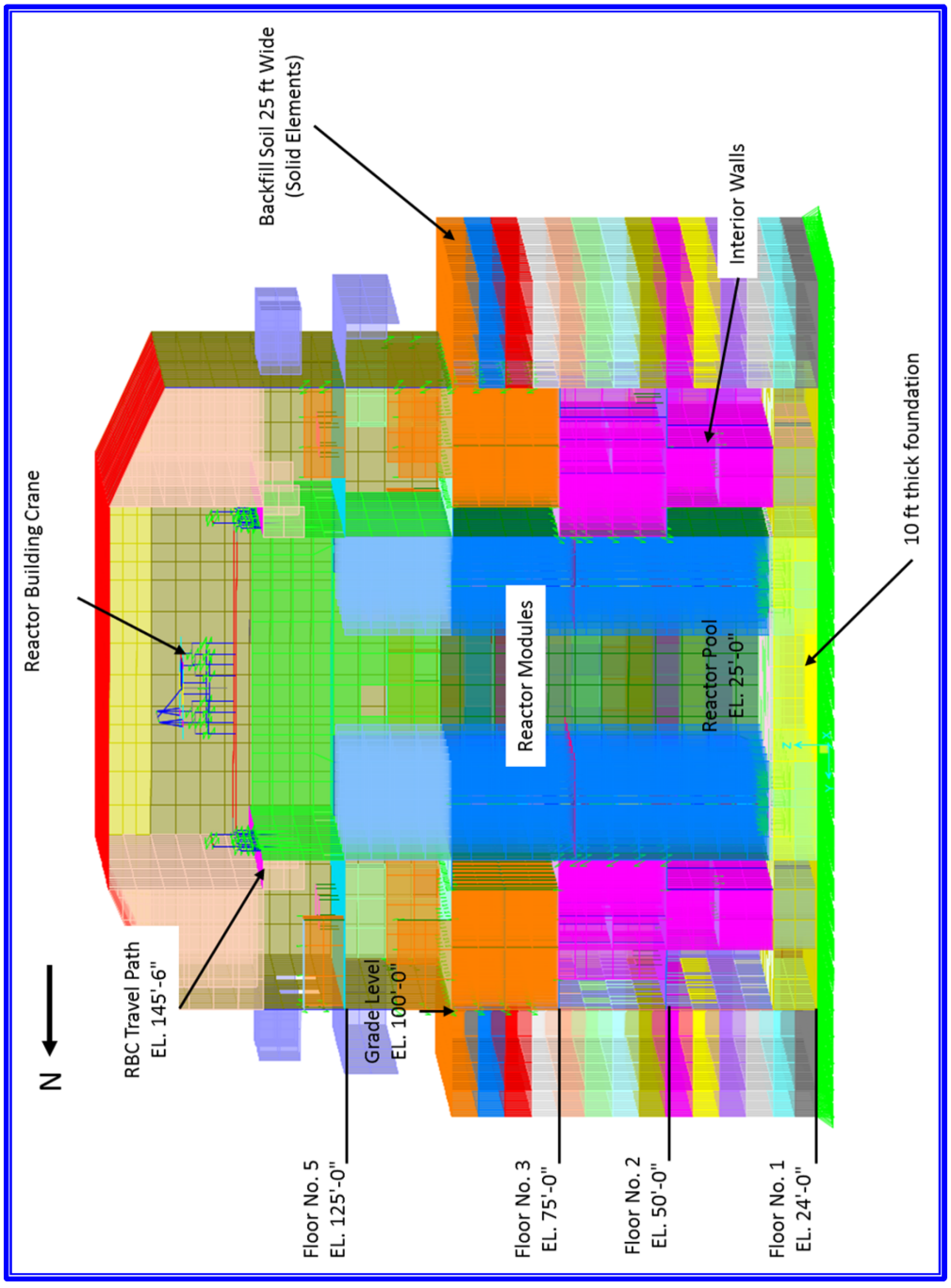

Figure 3.8.4-19: Transverse Section View of Reactor Building SAP2000 Model

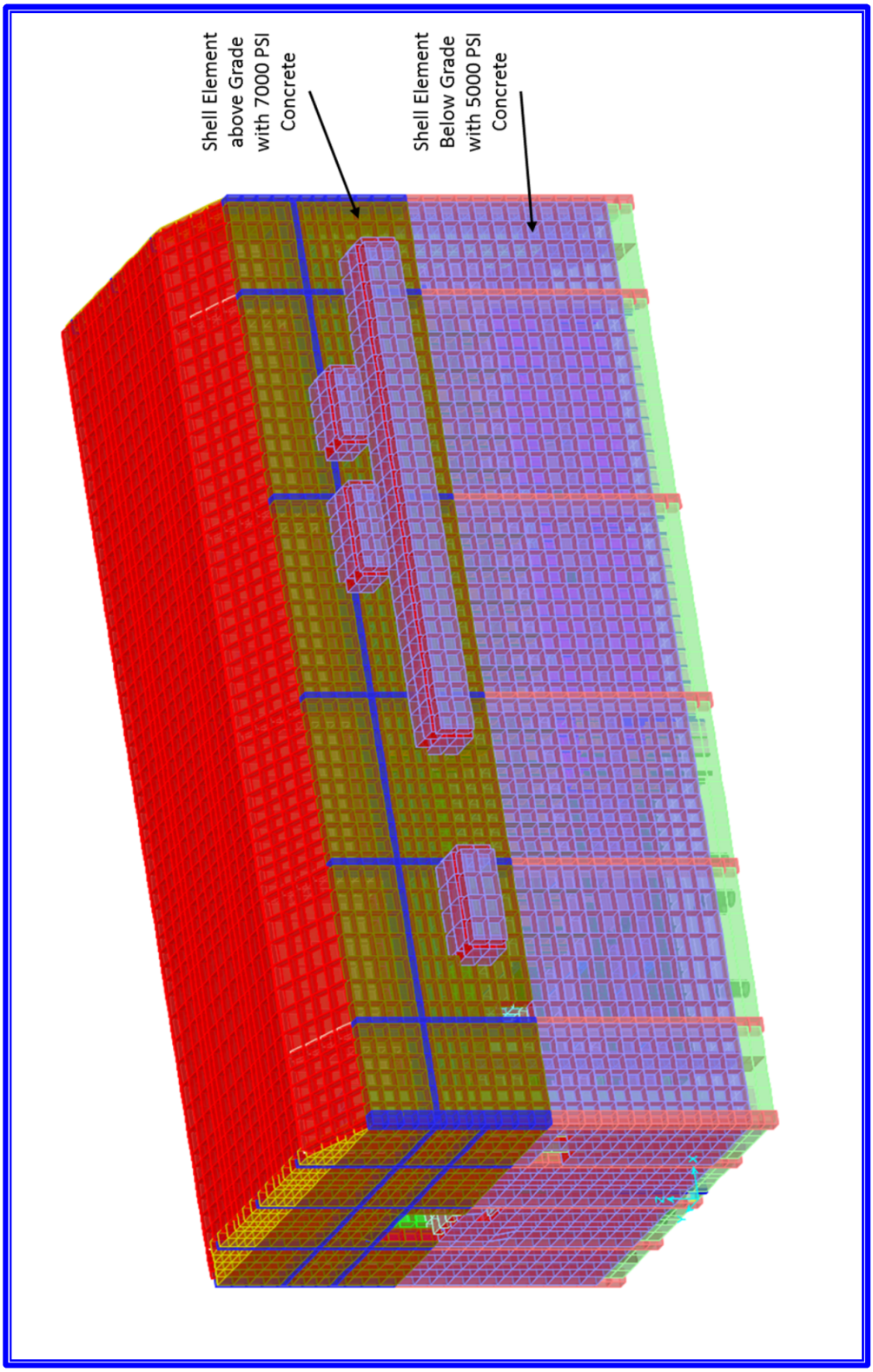

Figure 3.8.4-20: Reactor Building Exterior Walls with 7000 psi and 5000 psi Concrete

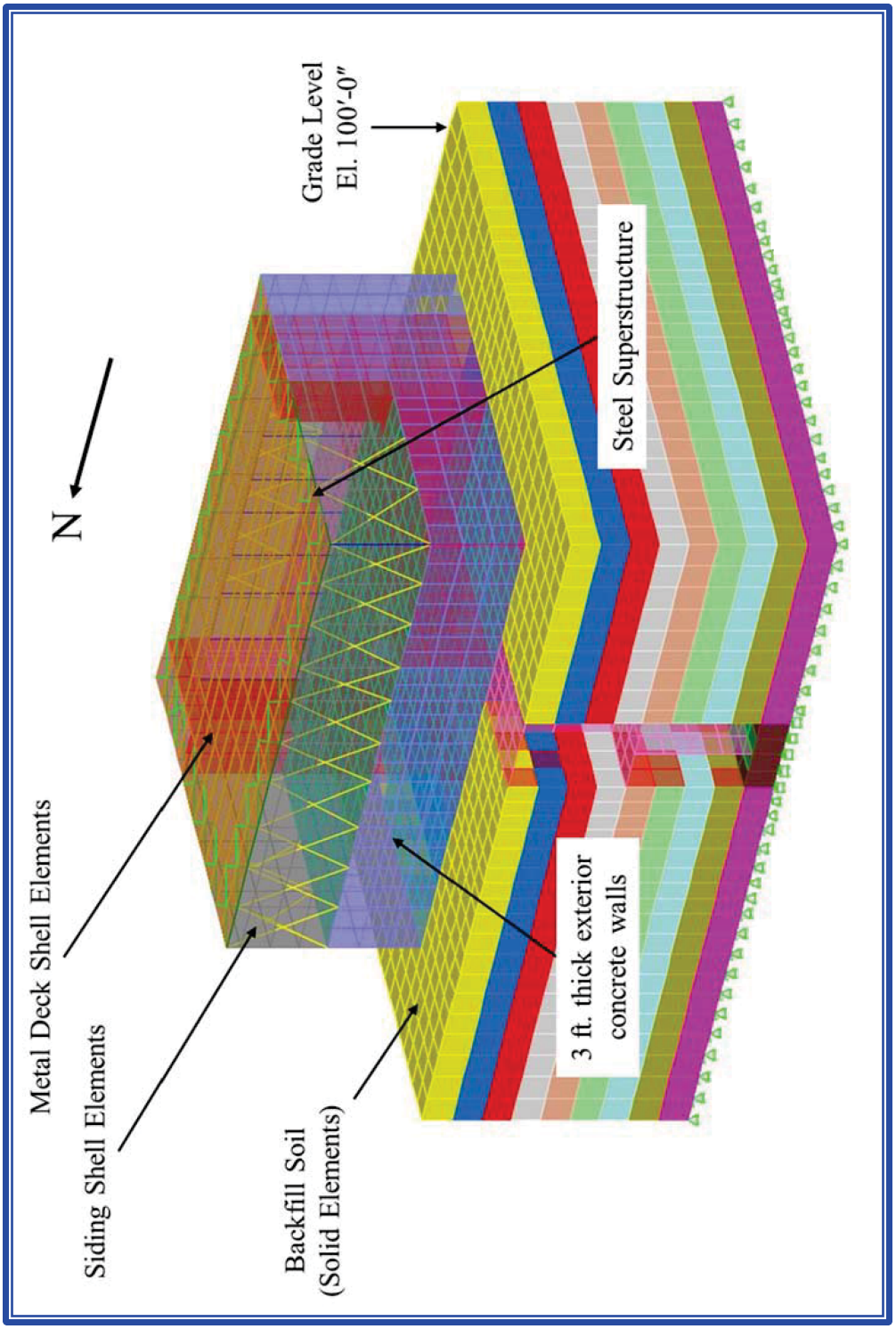

Figure 3.8.4-21: Control Building SAP2000 Model With Soil

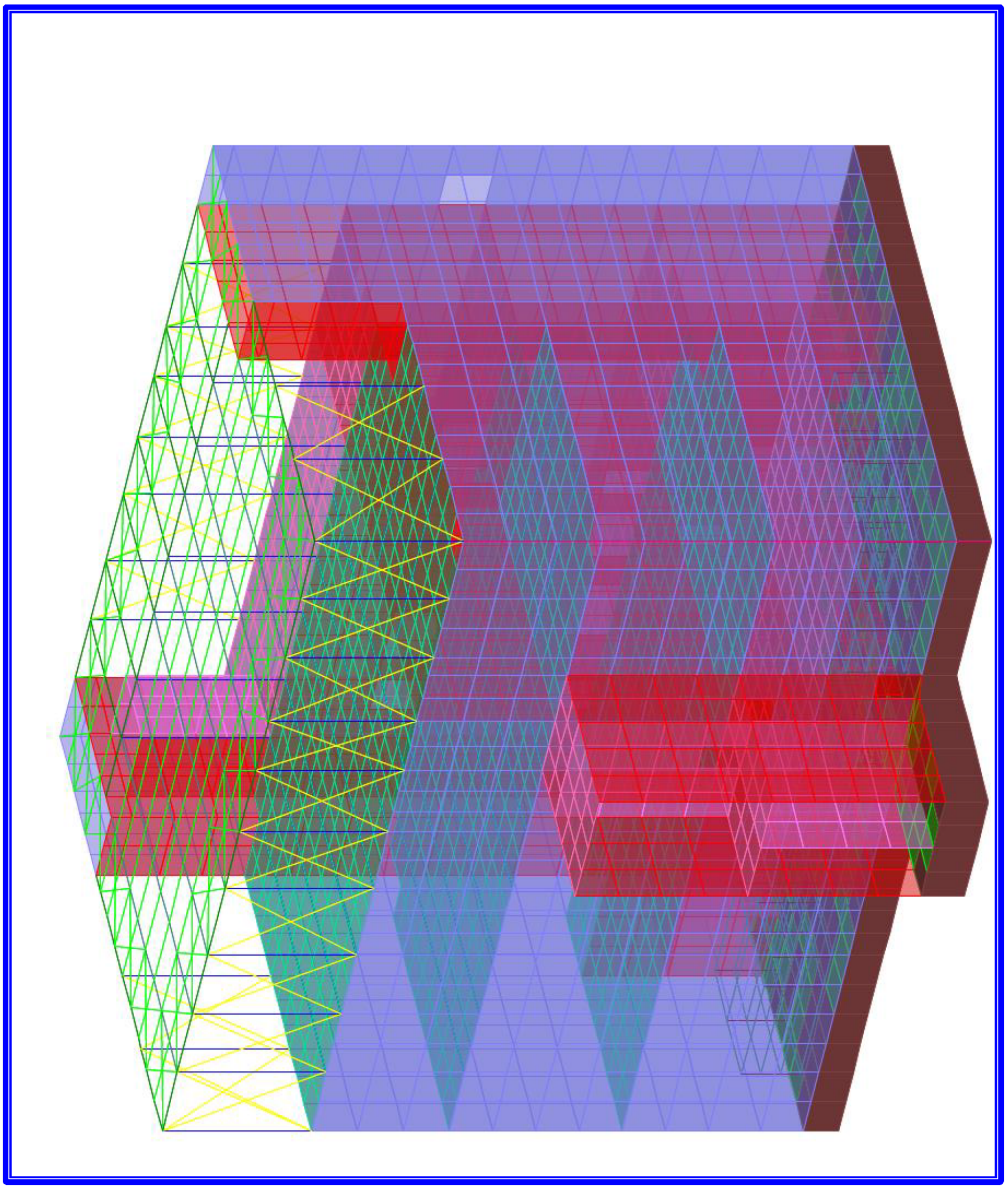

Figure 3.8.4-22: Control Building SAP2000 Model Without Soil

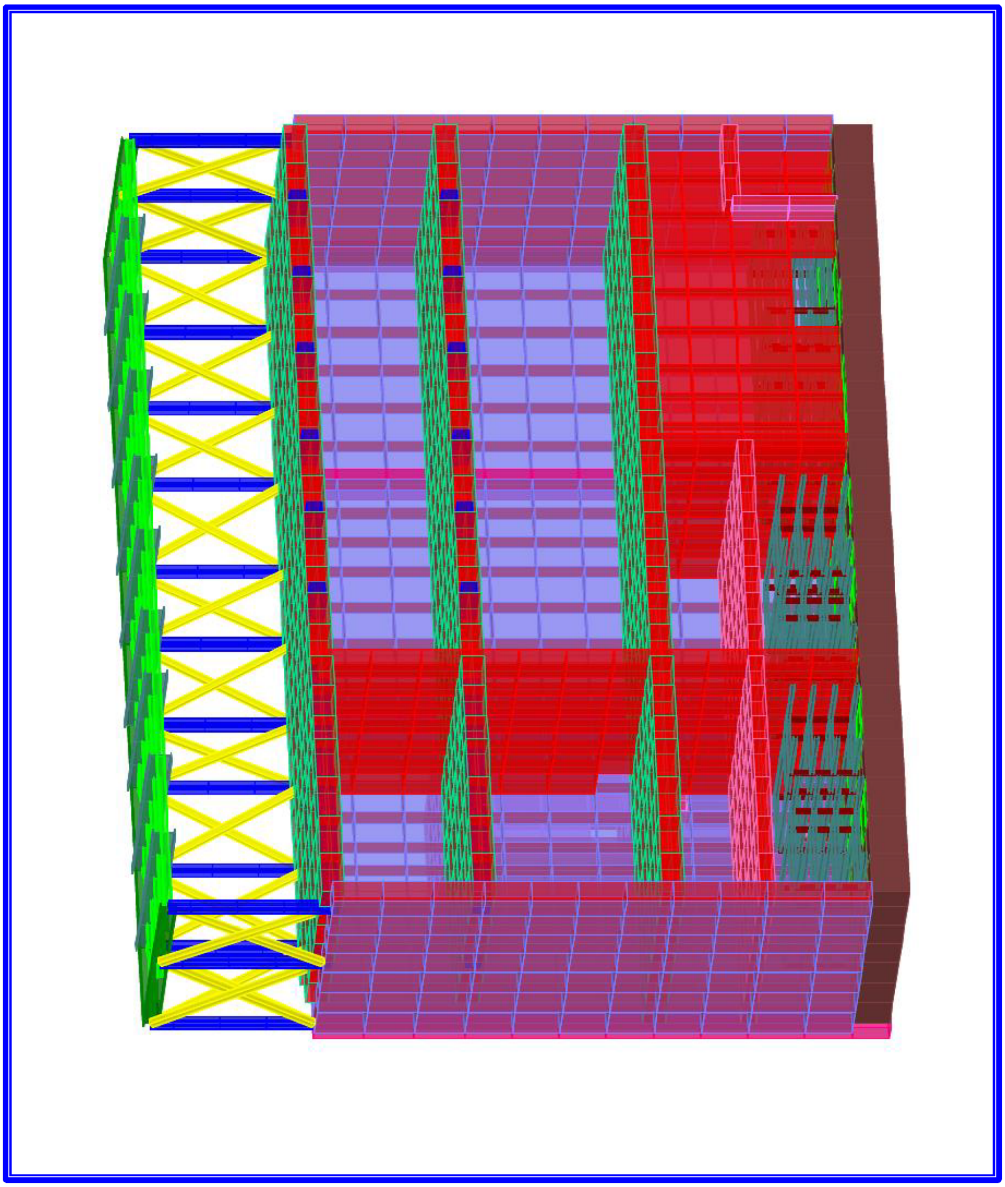

Figure 3.8.4-23: Control Building SAP2000 Model View Looking West

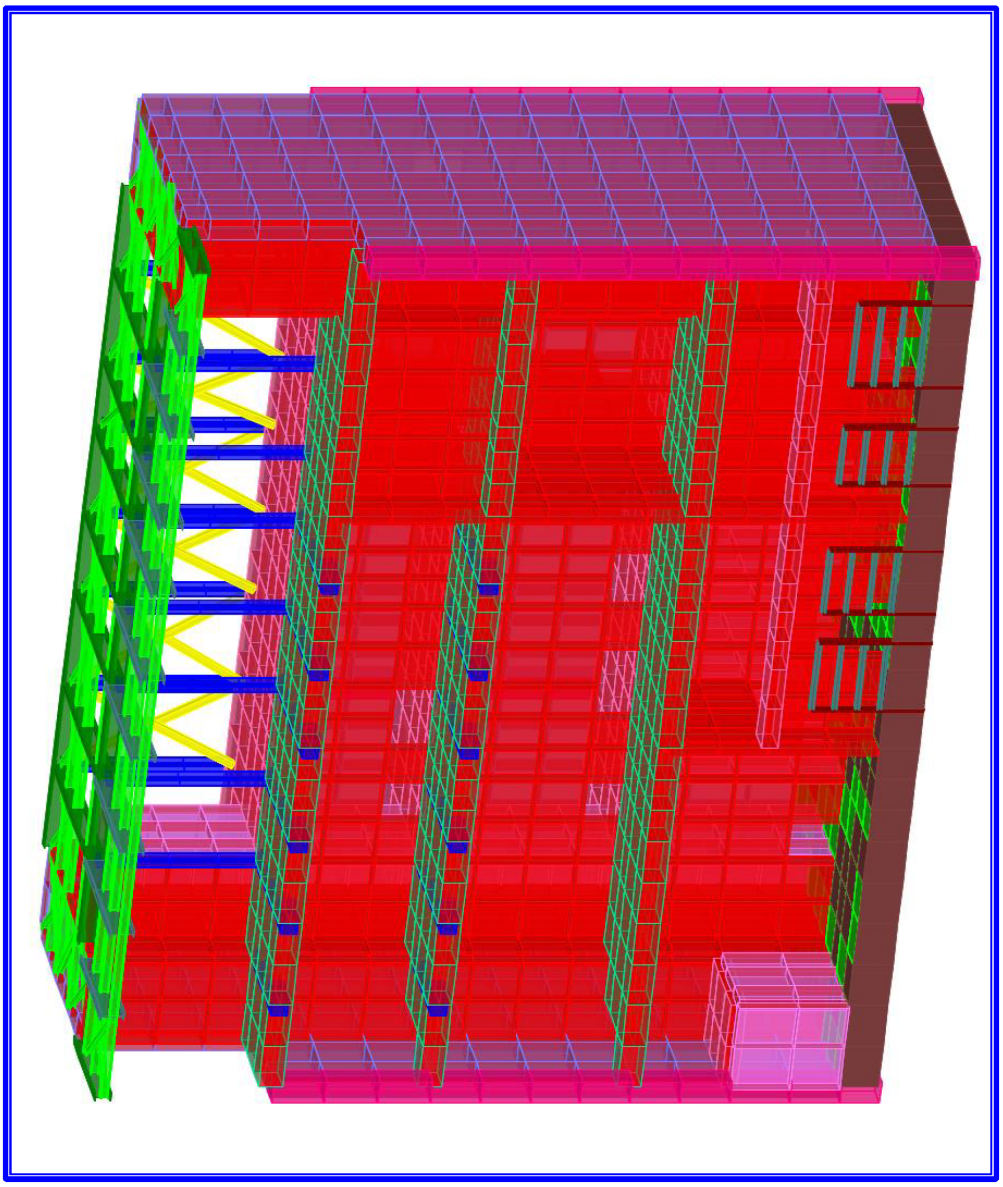

Figure 3.8.4-24: Control Building SAP2000 Model View Looking East

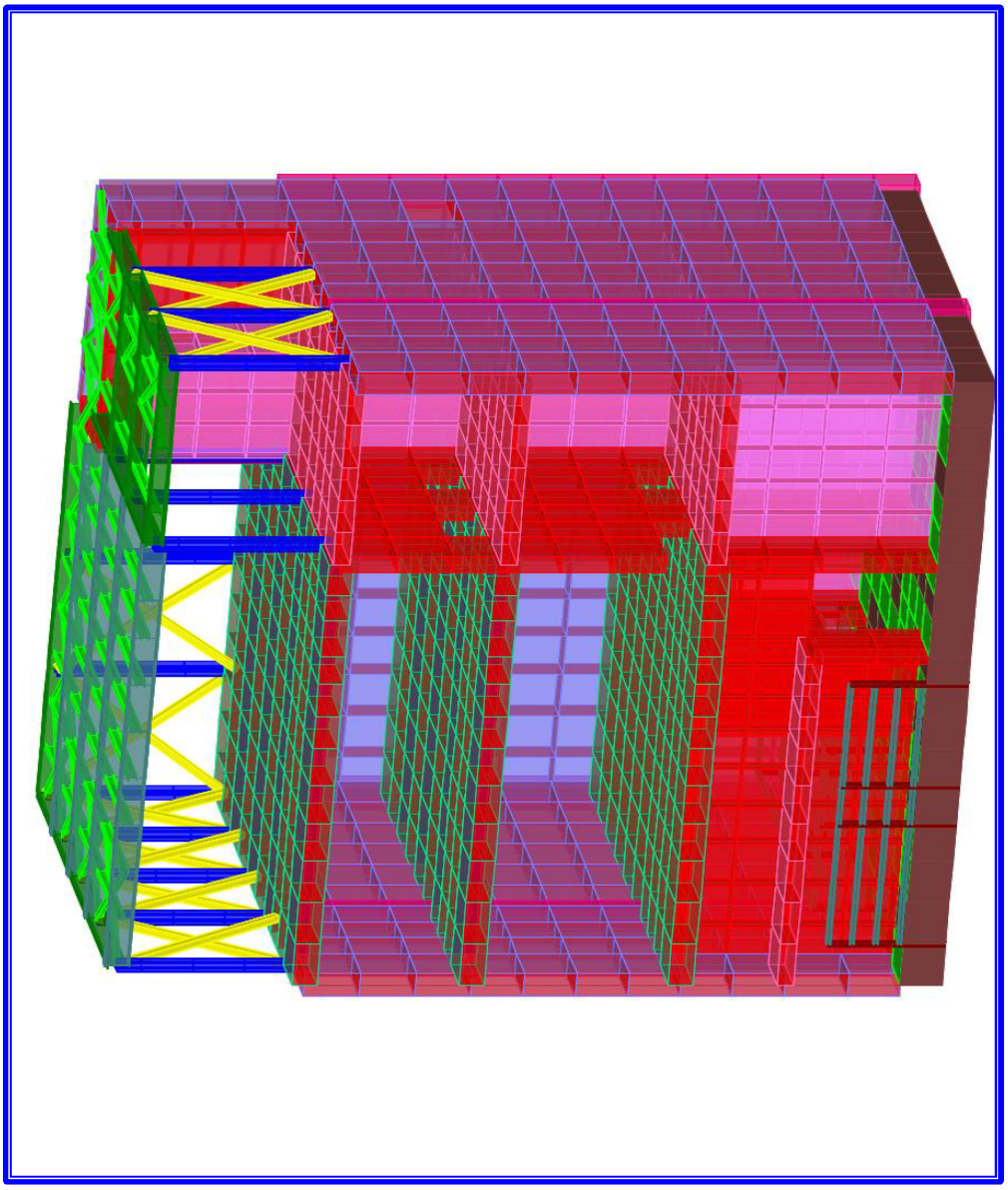

Figure 3.8.4-25: Control Building SAP2000 Model View Looking North

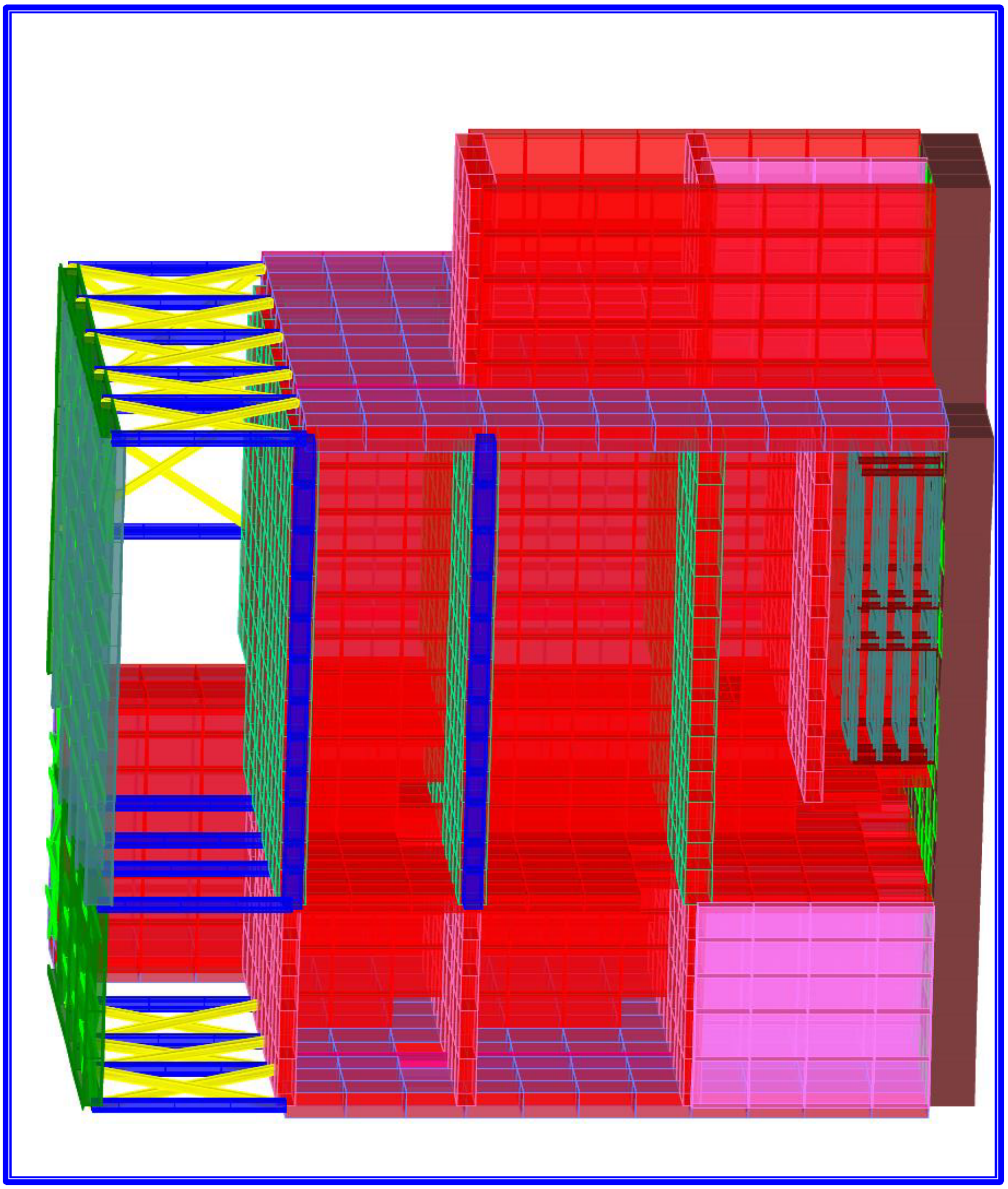

Figure 3.8.4-26: Control Building SAP2000 Model View Looking South

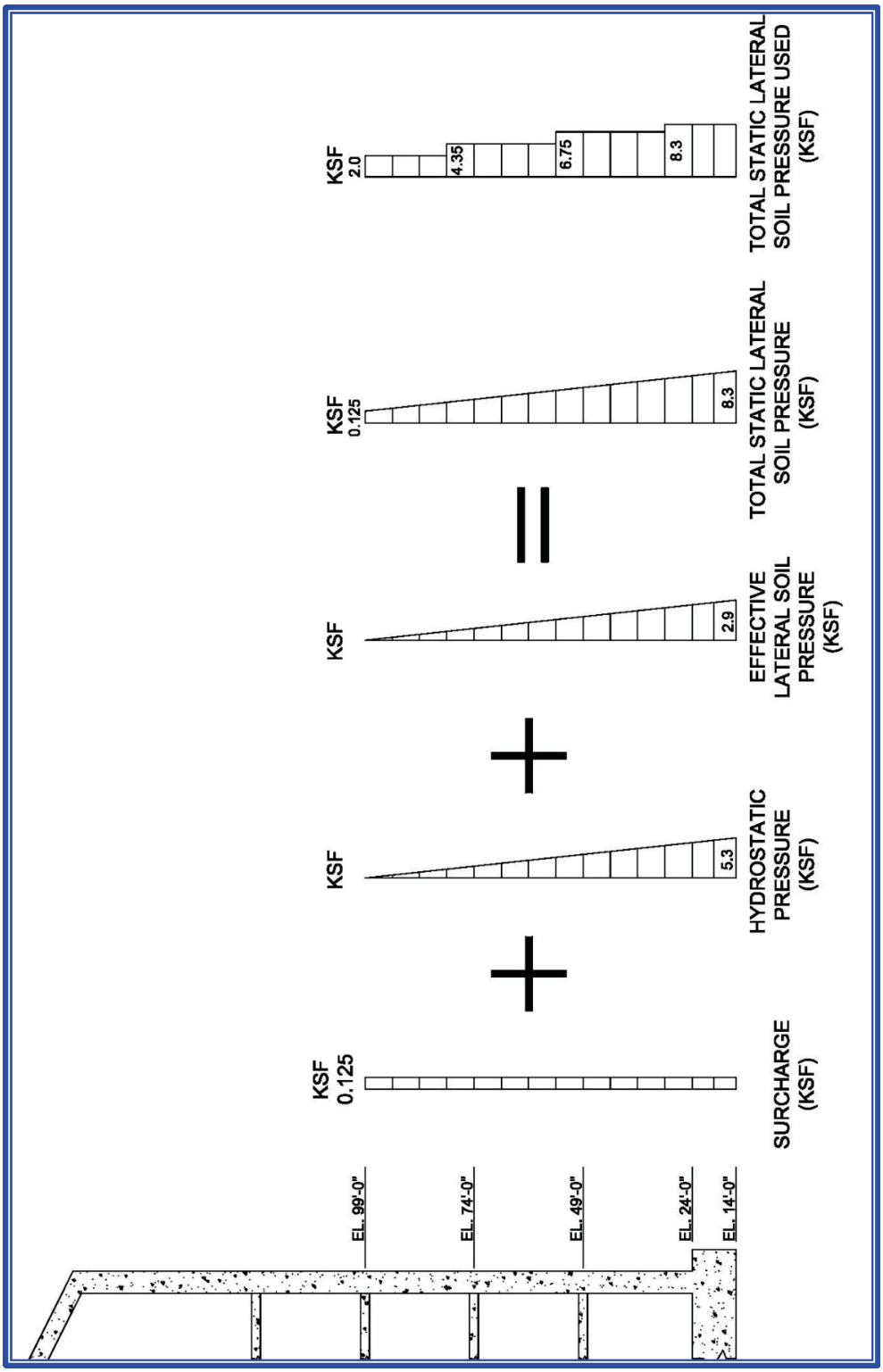

Figure 3.8.4-27: Total Static Lateral Soil Pressure Distribution Reactor Building

3.8.5 Foundations

3.8.5.1 Description of Foundations

The Seismic Category I Buildings are the Reactor Building (RXB) and the Control Building (CRB). These buildings are approximately 30 feet apart, and are connected by a tunnel. The Seismic Category II Radioactive Waste Building (RWB) is approximately 25 feet from the RXB. The RXB, CRB and RWB are described in Sections 1.2 and 3.8.4. The foundations of the RXB and CRB are described below.

Reactor Building Foundation

The RXB basemat foundation is 10 feet thick. The basemat is larger than the building and measures approximately 358 feet by 163 feet. The foundation top of concrete (TOC) elevation is 24'-0". The foundation for the refueling pool area has a top of concrete elevation of approximately 19 feet. Similarly, the elevator has a TOC of approximately 17 feet and sumps have a TOC elevation of approximately 20 feet. For the locations where the top of concrete is less than 24'-0" the foundation depth is increased to maintain the 10 foot minimum thickness.

The basemat reinforcement pattern is 6 layers of #11 bars at 12" centers each way (i.e., north-south and east- west) top and bottom for main reinforcing steel, and 2-legged stirrups of #6 bars at 12" centers each way at the perimeter of the basemat, extending 15 feet from the centerline of the exterior walls. The interior section of the basemat is 4 layers of #11 bars at 12" centers each way top and bottom for main reinforcing steel, and 1-legged stirrups of #6 bars at 12" centers each way.

Control Building Foundation

The CRB basemat foundation is 5 feet thick, with dimensions of approximately 130 feet by 91 feet with TOC at 50'-0".

The reinforcement pattern for the basemat is 3 layers of #11 bars at 12" centers each way top and bottom for main reinforcing steel, and 2-legged stirrups of #6 bars at 12" centers each way. The perimeter of the main slab contains 4 layers of #11 bars at 12" centers each way top and bottom for main reinforcing steel, and 2-legged stirrups of #6 bars at 12" centers each way.

3.8.5.2 Applicable Codes, Standards and Specifications

The codes, standards, and specifications that are used to design and construct the RXB and CRB are identified in Section 3.8.4.2. These codes are applicable to the foundations as well.

3.8.5.3 Loads and Load Combinations

The loads and load combinations used for the design of the RXB and CRB, including the design of the foundations, are discussed in Section 3.8.4.3.

Stability Load Combinations

The load combinations used for the assessment of stability (flotation, uplift, sliding, overturning) are discussed below.

Five load combinations are considered:

A. $D + H + E_{OBE}$

B. $D + H + W$

C. $D + H + E_{SSE}$

D. $D + H + W_t$

E. $D + B$

Load case A is not analyzed. The OBE is defined as one-third of the SSE and analysis is not required. In addition, the wind loads are bounded by the seismic loads as discussed in Section 3.8.4. Therefore load cases B and D are also not analyzed.

The loads are discussed in Section 3.8.4.3, but are summarized below:

D is the dead load. This is equal to 587,147 kips for the RXB (equipment and water weight) and 45,774 kips (includes equipment weight) for the CRB.

B is the buoyant force generated by the water table. This is equivalent to the embedded volume of the building times the weight of water. This load is +279,445 kips for the RXB and 40,500 kips for the CRB.

E_{SSE} is the seismic load generated by the CSDRS or CSDRS-HF.

H is the lateral static soil pressure.

W_t = Loads generated by the design basis tornado that cause tornado wind pressure, tornado-created differential pressures, and tornado generated missiles.

3.8.5.3.1 Lateral Soil Force and Seismic Loads

The RXB and CRB are embedded structures and, therefore, the surrounding soil contributes significantly to the stability of the structures. The surrounding soil imposes lateral soil pressures. The seismic inertia loads cause sliding and overturning forces. These pressures are calculated using the backfill soil which has a density of 130 pcf and an assumed angle of internal friction, f, of 30°. The coefficient of friction (COF) used for the calculation of friction resistance between soil and basemat is 0.58. The friction is defined between concrete and clean gravel, gravel-sand mixture, or coarse sand with a friction angle of 30°. Thus, the COF = tan (30°) = 0.57735, which rounds to 0.58.

The static lateral soil pressure values on walls are established in Section 3.8.4.3. The RXB values are converted to force in accordance with the following example for the static effective soil force on the RXB North (F_{y1}) (or South (F_{y2})) wall:

$$F_{y1} = K_o \times \left[0.250 \times H + \frac{1}{2} \times (0.13 - 0.0624) \times H \times H\right] \times EW \qquad \text{Eq. 3.8-1}$$

$= 46{,}967$ kips

where

K_0	Soil Coefficient of Pressure at rest = 0.5 (Table 3.8.5-1)
H	RXB Embedment = 86' (Table 3.8.5-1)
EW	RXB East-West Length between Exterior Faces of 5' Walls = 346' (Table 3.8.5-1)
0.250 ksf	Surcharge (Table 3.8.5-1)
0.13 kcf	Soil Density
0.0624 kcf	Water Density

Substituting the North-South length of 150.5' between exterior faces, the RXB East and West Walls experience a static effective soil force of 20,429 kips.

The CRB static effective soil forces are calculated similarly, as for the CRB East or West walls:

$$F_{y1} = K_o \times \left[0.250 \times H + \frac{1}{2} \times (0.13 - 0.0624) \times H \times H\right] \times NS \qquad \text{Eq. 3.8-2}$$

$= 6{,}914$ kips

where

K_o	Soil Coefficient of Pressure at rest = 0.5 (Table 3.8.5-9)
H	CRB Embedment = 55' (Table 3.8.5-9)
NS	CRB North-South Length between exterior faces of walls = 119'-8" (Table 3.8.5-9)
0.25 ksf	Surcharge (Table 3.8.5-9)
0.13 kcf	Soil Density

0.0624 kcf Water Density

Substituting the East-West length of 81' between exterior faces, the CRB North and South Walls experience a static effective soil force of 4,698 kips.

The static effective soil forces for the RXB are presented in Table 3.8.5-2. The total static lateral soil pressures for the CRB are presented in Table 3.8.5-10.

Base reactions are obtained based on a step-by-step algebraic summation of the reaction time histories in all the base springs. This is calculated for the 68 combinations from the two different RXB models, two concrete conditions, four soil types, and six different earthquake time histories. These RXB forces are presented in Table 3.8.5-3. The CRB base reactions presented in Table 3.8.5-3 are calculated for two concrete conditions, two soil types, and six different earthquake time histories. The maximum forces for the Triple Building base reactions in each direction all come from different time histories; however they all come from Soil Type 7.

3.8.5.3.2 Frictional Resistance Loads

Frictional resistance loads are considered to stabilize the structure against sliding and overturning loads since the RXB and CRB are deeply embedded structures.

The frictional resistance against sliding consists of two force resultant components, listed below:

1) Total Sliding Frictional Resistance on Foundation Surface from Effective Vertical Load, $D_{effective}$

2) Total Sliding Frictional Resistance on Embedded Wall Surfaces from Static Soil Pressure

Frictional resistance against overturning consists of the total restoring moment due to frictional resistance on embedded wall surfaces from effective static soil pressure. Effective static soil pressure is defined as soil pressure that includes the effect of the water table, i.e., the weight of saturated soil.

3.8.5.3.3 Effective Vertical Load

For stability evaluations, the effective vertical load of the building is an important stabilizing force. There are two components of vertical forces involved in the calculation of the flotation stability:

1) Dead weight of the building

2) Buoyancy Load from the water table at grade, which reduces effective dead weight

Using these forces, the effective vertical load, $D_{effective}$, calculation is described below.

Reactor Building Effective Dead Weight with Water Table Buoyancy

The effective dead weight, or buoyant weight, is calculated using the following equation:

$$D_{effective} = W_{RXB} - R_{buoyancy} \quad \text{Eq. 3.8-3}$$

where,

W_{RXB} = 587,147 kips.

Therefore,

$D_{effective}$ = 587,147 - 279,445 = 307,702 kips

Control Building Effective Dead Weight with Water Table Buoyancy

The effective dead weight, or buoyant weight, is calculated using the following equation:

$D_{effective} = W_{CRB} - R_{buoyancy}$, where

W_{CRB} = 45,774 kips.

Therefore,

$D_{effective}$ = 45774 - 40,500 = 5,274 kips

3.8.5.4 Design and Analysis Procedures

3.8.5.4.1 Foundation Basemat Analysis

Foundation basemats are analyzed and designed for static and seismic loads. Forces and moments in the basemat and pressures below the basemat are evaluated. Where a linear analysis did not provide acceptable results, a nonlinear analysis showed satisfatory conclusions.

3.8.5.4.1.1 Analysis of Reactor Building Basemat

RXB Basemat and Stability Linear Analysis

The design input parameters used to perform the flotation, sliding, and overturning evaluations are listed in Table 3.8.5-1.

3.8.5.4.1.2 RXB Basemat Analysis Model Description

For the RXB basemat model, the two layers of the solid elements modeling the RXB concrete foundation were replaced by a single layer of shell elements. The thickness of the shell elements is the same as the foundation thickness

(i.e., 120") and the centerline of the shell elements is at the bottom of the basemat. The pilasters on the building perimeter and walls within the footprint were connected to the shell elements, thereby acting as inverted supports to the basemat. All the pilaster and wall joints at the top of the foundation (i.e., Z = 120") are restrained for the six degrees of freedom. Elements above the elevation Z = 120" were deleted.

Table 3.8.5-17 shows a summary of the RXB basemat model.

Figure 3.8.5-1 shows the SAP2000 RXB basemat model. The area elements shown in light red tinge are shell elements representing the base slab.

Figure 3.8.5-2 and Figure 3.8.5-3 show the static and seismic base pressure contours on the shell foundation in the RXB basemat model.

Figure 3.8.5-4 and Figure 3.8.5-5 show the main bending moments due to static base pressures in the RXB basemat model.

Figure 3.8.5-6 and Figure 3.8.5-7 show the main bending moments due to seismic base pressures in the RXB basemat model.

For both the seismic and static base pressures, the applied base pressures will directly give the forces and moments for the foundation. The demands obtained thus are acceptable for foundation solid elements that are not connected to any wall or pilaster. However, for foundation solid elements that are connected to walls or pilasters, the demands will be much higher than what is obtained by the application of base pressures. In view of this, for solid elements that are connected to the walls and pilasters, the fixed end forces and moments are added to the affected foundation shell element responses.

The static forces and moments in the basemat are calculated with both the standalone and the combined building SAP2000 models.

The seismic forces, moments and stresses in all structural elements such as walls, pilasters, and basemat were calculated using the standalone and combined SASSI2010 models. The enveloped base pressures were applied to the solid foundation model to evaluate the responses. To be consistent with the SASSI2010 analysis, absolute values of all responses obtained by applying base pressures from SASSI2010 were used together with the fixed end forces and moments from walls and pilasters to arrive at the seismic demands.

As shown in Table 3.8.5-5, the linear analysis for stability gave factors of safety less than 1 for sliding. Therefore a nonlinear analysis was performed for RXB Sliding.

Nonlinear Analysis Approach for RXB Sliding where Linear Analysis is too conservative

Where the RXB linear sliding analyses did not yield acceptable factors of safety results for sliding, detailed nonlinear sliding analyses were performed using

ANSYS. The fixed base boundary conditions for this analysis were compared favorably with the SAP2000 linear analysis boundary conditions, and the model is shown in Figure 3.8.5-8. The nonlinear ANSYS analysis uncoupled the soil domain from the building to permit simulation of sliding under seismic conditions by creating two coincident joint/nodes in the finite element mesh, one belonging to the RXB and one belonging to the backfill soil. The coincident nodes were used to define a nonlinear contact region as shown on Figure 3.8.5-9. A coefficient of friction of 0.5 was used so that the tangential force required for overcoming compressive normal force resistance to allow the building to slide and uplift relative to the soil is equal to half of the normal force between the RXB walls and soil.

The seismic analyses were performed in SASSI for Soil Type 11 backfill. The SASSI results yielded acceleration versus time in the global N-S, E-W, and vertical direction for each node on the external surface of the RXB and the backfill soil. The SSI seismic input acceleration histories in the three orthogonal directions obtained at representative skin node 946 were applied to 5,822 RXB and backfill soil nodes in contact with the in-situ soil. These nodes are shown on Figure 3.8.5-11 and Figure 3.8.5-12. There were a total of three time histories for each soil type considered.

Rather than directly applying the SASSI accelerations to the RXB and backfill soil, coincident nodes were created. Nonlinear node-to-node CONTA178 elements were defined between the coincident nodes as shown in Figure 3.8.5-13 and Figure 3.8.5-14. Figure 3.8.5-15 illustrates the CONTA178 definition wherein forces are transferred between the end node-I and node node-J only when the gap is closed, i.e., transmitting compression but not tension. The elements directly under the RXB basemat have a coefficient of friction of 0.58 defined to resist sliding.

A pressure of 36.92 psi was applied to the bottom of the basemat to account for buoyancy effects as shown on Figure 3.8.5-16. The static surcharge effects from the backfill soil against the RXB outer wall are ignored.

Table 3.8.5-6 shows the number of elements in the ANSYS structural analysis model including joints, frame elements, shell elements, solid elements, and links/supports.

East-west and north-south unidirectional, horizontal time-history analyses were performed for each of the surrounding Soil Types 7, 8, and 11. For all cases, the respective acceleration time-history from the SASSI representative skin node 946 was applied uniformly to all the boundary nodes in the ANSYS model, while the displacements in the other two directions were constrained. Thus, for each soil type, the cases performed were acceleration time history in the east-west direction, with the displacements in the vertical and north-south directions fixed and acceleration time history in the north-south direction, with the displacements in the vertical and east-west directions fixed.

Figure 3.8.5-17 through Figure 3.8.5-19 show the input acceleration time histories for each of the Soil Type 7 cases.

Figure 3.8.5-20 through Figure 3.8.5-22 show the input acceleration time histories for each of the Soil Type 8 cases.

Figure 3.8.5-23 through Figure 3.8.5-25 show the input acceleration time histories for each of the Soil Type 11 cases.

3.8.5.4.1.3 Analysis of Control Building Basemat

The static load results are obtained from the SAP2000 model of the CRB. Both the stand-alone and the combined CRB SAP2000 models are used to obtain the static forces and moments in the basemat, using the most critical static load combination for the calculation of structural responses.

The seismic forces, moments, and stresses in the structural elements, such as walls, beam elements, and basemat, are calculated using the stand-alone and combined SASSI2010 models. The enveloped seismic pressures contours on the CRB basemat are shown in Figure 3.8.5-3a. The enveloped seismic pressures are obtained as a result of the four-step, post-processing method described in Section 3.7.2.4.1. These maximum pressures are loaded into an SAP2000 model of the CRB basemat from where the seismic forces and moments for the basemat design are obtained. Absolute values of the responses obtained by applying base pressures from SASSI2010 are used to arrive at the total seismic demands.

Control Building Basemat and Stability Linear Analysis

Acceptance criteria for flotation/ uplift, sliding, and overturning is based on a factor of safety (FOS) determined from the ratio of the driving force to the resisting force. These analyses are performed statically using the maximum forces from the combinations of soil profiles, time histories, and cracked/ uncracked conditions discussed in Section 3.7. The FOS performed for the CRB yielded unacceptable results (less than 1.1 FOS) for uplift stability; therefore, the uplift, sliding and overturning of the CRB is determined by a nonlinear sliding and uplift analysis.

3.8.5.4.1.4 Control Building Basemat Nonlinear Analysis Model Description

For the nonlinear analysis, the ANSYS CRB model with fixed-base boundary sliding and uplift conditions was changed to:

1) Provide independence of the building and soil domain by establishing coincident joints/nodes for the building and soil in the finite element mesh.

2) Define a nonlinear frictional contact region with the coincident nodes as shown in Figure 3.8.5-26. A coefficient of friction of 0.5 (between the CRB walls and soil) was used so that the tangential force required to overcome the resistance from any compressive normal force is equal to half the normal force, allowing the building to slide and uplift relative to the soil.

3) Obtain, at a typical skin node near the CRB basemat, the seismic input acceleration time histories in the three orthogonal directions for the Soil Type 11 backfill in combination with the surrounding Soil Type 7 and Soil Type 11. Three time histories for each soil type were considered by uniformly applying the time histories from the typical skin node to the CRB and backfill soil nodes, as shown in Figure 3.8.5-27, which are in contact with the in-situ soil. The SASSI time histories for the Capitola input case were selected since that case produced the largest horizontal base reactions, as shown in Table 3.8.5-3. The three time histories are shown in

   - Acceleration time history for each of the Soil Type 11 cases (Figure 3.8.5-28 through Figure 3.8.5-30)
   - Acceleration time history for each of the Soil Type 7 cases. (Figure 3.8.5-31 through Figure 3.8.5-33)

4) Create coincident nodes and define nonlinear node-to-node CONTA178 elements as shown on Figure 3.8.5-34 and Figure 3.8.5-35 to accurately model the contact gap between CRB and soil. The typical definition of CONTA178 elements is shown in Figure 3.8.5-15, where forces are transferred between node-I and node-J only when the gap is closed. The elements directly under the CRB foundation have a coefficient of friction of 0.55 defined to resist sliding, i.e., transmitting compression but not tension. The elements on the sides of the CRB have a coefficient of friction of 0.50 defined to resist sliding.

5) Account for buoyancy effects by applying a pressure of 29.399 psi to the bottom of the basemat, as shown in Figure 3.8.5-36. The buoyancy pressure was determined as follows:

   Total area = basemat area + tunnel area = 78' × 116.667' + 25' × 18.667'

   = 9,100 ft^2 + 466.67 ft^2 = 9,566.67 ft^2

   Buoyancy pressure = 40,500,000 lbs / (9,566.67×144) in^2 = 29.399 psi

6) Include Poisson's ratio effect in the static soil pressure profile due to the deadweight of the backfill soil on the CRB walls as a conservative measure. The pressure profile is shown in Figure 3.8.5-37. The Poisson's ratio effect produces a complex pressure distribution depending on the local flexibility of the walls (Figure 3.8.5-38 and Figure 3.8.5-39).

The model summary showing quantity of elements in the ANSYS structural analysis model including joints, frame elements, shell elements, and solid elements is shown in Table 3.8.5-11. A comparison of the SAP2000, SASSI2010, and ANSYS models also is shown in Table 3.8.5-11.

The coordinate system for the nonlinear analysis is represented by the CRB SAP2000 model as shown in Figure 3.8.5-40. The X axis points to the East, the Y axis point to the North, and the Z axis points vertically upward. The X-

coordinate of the west side of the CRB tunnel is 350'-0" (4,200") in the global X-direction (East-West) from the origin of the global SAP2000 coordinate system.

3.8.5.5 Evaluation Criteria for Stability Analysis

3.8.5.5.1 Flotation and Uplift Stability Analysis Approach

Flotation is calculated for static conditions and uplift is calculated with the earthquake present.

The factor of safety is calculated as follows, with load combination E for flotation and load combination C for uplift:

$$FOS = \frac{F_{resisting}}{F_{driving}} \quad \text{Eq. 3.8-4}$$

$$FOS_{flotation} = \frac{D}{B} \quad \text{Eq. 3.8-5}$$

$$FOS_{uplift} = \frac{D + F}{B + Rz} \quad \text{Eq. 3.8-6}$$

Where

$F_{resisting}$ is the resistance of the buried portion of the structure. This includes two components:

D= the weight of the building

F = Vertical friction due to static soil pressure

The driving forces for uplift are from groundwater and seismic motion. This includes two components:

B = the buoyant force from groundwater or floodwater at grade.

Rz = Upward inertia = Seismic vertical base reaction (when soil moves downward in the direction of gravity).

3.8.5.5.2 Sliding Stability Analysis Approach

The sliding stability evaluation is done with load combination C as described in Section 3.8.5.3.

The stability evaluation is determined by comparing the total resisting sliding forces and the total driving sliding forces. A sliding evaluation is performed for both directions separately; one for east-west movement (Global X-direction) and one for North-South movement (Global Y-direction).

The RXB and CRB are deeply embedded structures, therefore, the frictional resistance provided by the interaction of soil and structure on the exterior walls and basemats is considered.

The sliding driving force is the inertia force due to seismic. By neglecting insignificant damping forces, the total inertia force equals the sum of all reaction forces on walls and basemat. The inertia force is thus calculated by adding seismic reactions.

Friction Resistance to N-S Sliding

Two force components result in frictional resistance against North-South sliding:

- Friction resistance between foundation and soil.
- Frictional resistance on East and West walls from effective static soil pressure. See Section 3.8.5.3.2 for the definition of effective static soil pressure.

Friction Resistance to E-W Sliding

Two force components result in frictional resistance against East-West sliding:

- Friction resistance between foundation and soil
- Frictional resistance on North and South walls from effective static soil pressure. See Section 3.8.5.3.2 for the definition of effective static soil pressure.

Friction between Basemat and Soil due to Effective (or Buoyant) Dead Weight

For sliding stability evaluation, the effective dead weight, or buoyant weight, of the RXB is an important stabilizing force.

The RXB buoyant dead weight is calculated in Section 3.8.5.3.3 as:

$D_{effective}$ = 307,702 kips

The RXB friction resistance R_sliding between basemat and soil against N-S or E-W sliding is calculated by multiplying the buoyant weight and the friction coefficient as follows:

$R_{sliding} = D_{effective} \times \mu$ (Eq 3.8-6) = 307,702 × 0.58 = 178,467 kips

Similarly, the CRB buoyant dead weight, calculated in Section 3.8.5.3.3, is 5,274, kips. The frictional resistance $R_{sliding}$ between the basemat and soil against N-S or E-W sliding is:

$R_{sliding} = D_{effective} \times \mu$ = 5,274 x 0.58 = 3,059 kips

3.8.5.5.3 Overturning Stability Analysis Approach

The overturning stability evaluation is done with load combination C as described in Section 3.8.5.3. The factor of safety for overturning is calculated as follows:

$$FOS_{overturning} = \frac{M_{restoring}}{M_{overturning}} \quad \text{Eq. 3.8-7}$$

The overturning evaluation is determined by comparing the total resisting overturning moment and the total driving overturning moments. An overturning evaluation is performed for both directions separately; one for the North-South movement (moment about Global X-direction) and one for the East-West movement (moment about Global Y-direction).

The RXB is a deeply embedded structure, therefore, the frictional resisting moments provided by the interaction between soil and structure on the exterior walls and basemat are considered. The restoring moment due to the effective vertical load is also included in the evaluation.

Three components result in resistance to overturning:

- Friction on Parallel Walls
- Friction on Perpendicular Walls
- Effective Dead Weight

The North-South overturning pivot for the RXB is the north edge of the foundation. The East-West overturning pivot is the west wall edge of the foundation.

RXB Resistance to North-South Overturning

The resisting moment resulting from friction on the East and West walls is:

$$M_1 = (F_{EAST} + F_{WEST}) \times r_{cg} \quad \text{Eq. 3.8-8}$$

where

F_{EAST} = total friction force on the East wall

F_{WEST} = total friction force on the West wall

r_{cg} = Moment arm = perpendicular distance from pivot point (edge of North wall) to line of friction force = (150.5'/2) + 6' = 81.25' (Table 3.8.5-7)

The resisting moment resulting from friction on the South wall is:

$$M_2 = (F_{SOUTH}) \times L_{NS} \quad \text{Eq. 3.8-9}$$

where

F_{SOUTH} = total friction on the south wall

L_{NS} = moment arm = North-South width of the foundation = 156.5'

The resisting moment resulting from buoyant dead weight is:

$$M_3 = (D_{effective}) \times L_{NS1} \quad \text{Eq. 3.8-10}$$

where

$D_{effective}$ = 307,702 (Section 3.8.5.3.3)

L_{NS1} = moment arm = half width of North-South width of foundation = 81.25'

M_3 = 307,702 x 81.25 = 25,000,824 kip-ft

The resultant frictional resistance to North-South overturning is:

$M_{NS} = M_1 + M_2 + M_3$

RXB Resistance to East-West Overturning

The resisting moment resulting from friction on the North and South walls is:

$$M_4 = (F_{NORTH} + F_{SOUTH}) \times r_{cg} \quad \text{Eq. 3.8-11}$$

where

F_{NORTH} = total friction on the North wall

F_{SOUTH} = total friction on the South wall

r_{cg} = moments arm = perpendicular distance from pivot (edge of West Wall) to line of friction force = (346'/2) + 6' =179'

The resistant moment resulting from friction on the East wall:

$$M_5 = (F_{EAST}) \times L_{EW} \quad \text{Eq. 3.8-12}$$

where

F_{EAST} = Total friction on the East wall

L_{EW} = moment arm = East-West width of the foundation = 352'

The resisting moment resulting from buoyant dead weight is:

$$M_6 = (D_{effective}) \times L_{EW} \quad \text{Eq. 3.8-13}$$

where

$D_{effective}$ = 307,702 kips (Section 3.8.5.3.3)

L_{EW} = moment arm = half of East-West width of foundation = 179'

M_6 = 307,702 X 179 = 55,078,739 kip-ft

The resultant resistance to East-West overturning is:

$$M_{EW} = M_4 + M_5 + M_6$$

3.8.5.5.4 Bearing Pressure Approach

Average Bearing Pressure

Average static bearing pressure is calculated by dividing the building weight by the building footprint. Seismic average bearing pressure is calculated by the algebraic summation of reaction time histories in the rigid springs below the basemat. The springs connect the basemat with the free-field soil. The algebraic summation yields three time histories of total basemat reactions in the three global directions due to each seismic input. From the time histories, the maximum reactions can be obtained. The vertical reaction divided by the total area of the basemat yields the average bearing pressure.

Localized Bearing Pressure

Localized bearing pressure under each building's basemat is calculated using the forces in the rigid springs, which connect the RXB and the CRB basemats to the excavated free-field soil (or to a fixed support for the static case). The vertical force in a spring is divided by the tributary area of the spring to obtain the localized nodal soil pressure. For the seismic case, reactions are obtained as a result of the four-step post-processing method described in Section 3.7.2.4.1.

3.8.5.5.5 Settlement Approach

A large-scale SAP2000 finite element model is used to determine the effect of foundation differential movements. To maximize the effect of the differential movements and to have flexibility in the construction sequence, the soil is modeled using the softest soil profile, i.e. Soil Type 11. In addition, the soil stiffnesses are further reduced by 50 percent to amplify the effect of differential movements or settlements. The size of the soil included in the model is so large that the static displacements induced by the static loads of the structures become negligible on the edges of the freefield soil model. The model is analyzed for both the cracked and uncracked concrete conditions.

The size of the freefield soil block in the model is 2005.5' long, 768.5' wide, and 360' deep. Figure 3.8.5-41 shows the overall size of the freefield soil block with the three embedded buildings.

As discussed in Section 3.8.4, Load combination 10 using Equation 9-6 of ACI 349 governs

$U = D + F + H + 0.8L + C_{cr} + T_o + R_o + E_{sse}$

For the dynamic analyses, the dead weight of the building was increased to account for the effect of live and snow loads.

3.8.5.6 Results Compared with Structural Acceptance Criteria

3.8.5.6.1 RXB Stability

Factors of safety (FOS) were determined for 16 cases for the RXB. The cases include enveloping seismic loads from two RXB models (a standalone RXB model and an integrated RWB+RXB+CRB triple building model), two concrete conditions (cracked and uncracked with 7 percent damping) and four soil profiles (Soil Types 7, 8, 9, and 11) and are shown in Table 3.8.5-5. The results in this table indicate that the linear analysis for RXB sliding stability did not yield a FOS of greater than 1.

The minimum acceptable factor of safety for flotation, uplift, sliding and overturning is 1.1. This was not achieved for RXB sliding. Table 3.8.5-5 summarizes the factors of safety for the RXB.

A nonlinear analysis was performed for the RXB to show sliding was insignificant.

Bearing pressure is used to establish a design parameter for bearing capacity for site selection. The bearing capacity of the soil should provide a factor of safety of 3.0 for the static bearing pressure and a factor of safety of 2.0 for dynamic bearing pressure. The maximum allowable tilt settlement for the Reactor Building is 1" total or ½" per 50 feet in any direction at any point in the structure. The maximum allowable total settlement at any foundation node is four inches.

3.8.5.6.1.1 RXB Uplift

As shown in Section 3.8.5.5.1,

$$FOS = \frac{F_{resisting}}{F_{driving}} \qquad FOS_{flotation} = \frac{D}{B} \qquad FOS_{uplift} = \frac{D + F}{B + Rz}$$

The FOS for flotation is shown in Table 3.8.5-5 for each of the 16 cases considered, including cracked and uncracked conditions, Soil Types 7, 8, 9 and 11, and for RXB model and the triple building model. For each of the cases, an acceptable FOS for overturning was met.

3.8.5.6.1.1.1 Dynamic RXB Uplift Ratio

The effect of foundation uplift has been evaluated for the RXB. The linear SSI analysis methods are acceptable if the ground contact ratio is equal to or greater than 80 percent. The ground contact ratio can be calculated from the linear SSI analysis using the minimum basemat area that remains in compression with the soil. The seismic total vertical base reactions are calculated by the time step-by-time step algebraic summation of all nodal vertical reactions of the nodes of the RXB basemat. The maximum seismic vertical reactions for the cracked and uncracked concrete conditions for the two models are summarized in Table 3.8.5-4. The base vertical reaction results for the uncracked condition are similar to those for the cracked concrete condition.

As shown in Table 3.8.5-4, the seismic reactions are much less than the total dead weight reaction over the rectangle basemat area of 471,487 kips. Thus, the net reactions are always in compression.

The typical total basemat vertical reaction time histories are shown in Figure 3.8.5-42 through Figure 3.8.5-47. Figure 3.8.5-42 and Figure 3.8.5-43 show the reactions for comparison between the cracked and uncracked concrete conditions. Each of the CSDRS- and CSDRS-HF-compatible seismic inputs contain three acceleration components, X (EW), Y (NS), and Z (vertical).

Figure 3.8.5-44 through Figure 3.8.5-47 are for the cracked concrete condition for the CSDRS Capitola input and CSDRS-HF Lucerne input. As can be seen in these figures, the total reactions are always in compression. The cracked and uncracked total reactions can be compared using Figure 3.8.5-42 for the cracked reaction and Figure 3.8.5-43 for the uncracked reaction due to Capitola input for Soil Type 7. The differences in total reactions are small because the differences between the cracked and uncracked seismic reactions and between standalone RXB and triple building models are small as shown in Table 3.8.5-4.

Based on the examination of the total vertical reaction force underneath the basemat, all net vertical reactions are in compression. Thus, the basemat is 100 percent in contact.

3.8.5.6.1.2 Reactor Building Sliding

As shown in Section 3.8.5.5.1,

$$FOS_{sliding} = \frac{R_{resisting}}{R_{driving}} \qquad \text{Eq. 3.8-14}$$

Linear evaluations have shown that an acceptable FOS for sliding is not met, as shown on Table 3.8.5-5. Therefore, a nonlinear sliding analysis has been performed to show that sliding is insignificant.

Nonlinear Analysis

Figure 3.8.5-52 shows the designations used (A through D) for the locations on the RXB basemat where lateral displacements (sliding) were assessed between two end nodes of CONTA178 elements.

Figure 3.8.5-53 through Figure 3.8.5-60 show the E-W and N-S sliding displacements for Soil Type 7 for the four foundation locations (A, B, C, and D).

Figure 3.8.5-61 through Figure 3.8.5-68 show the E-W and N-S sliding displacements for Soil Type 11 for the four foundation locations (A, B, C, and D).

Figure 3.8.5-69 through Figure 3.8.5-76 show the E-W and N-S sliding displacements for Soil Type 8 for the four foundation locations (A, B, C, and D).

A detailed summary of the sliding displacement results are provided in Table 3.8.5-12. The results indicate that the deeply embedded RXB experiences less than 1/8" of sliding horizontal displacement. The magnitude of the displacements presented is insignificant.

3.8.5.6.1.3 RXB Overturning

As shown in Section 3.8.5.5.3,

$$FOS_{overturning} = \frac{M_{restoring}}{M_{overturning}}$$

The FOS for overturning is shown in Table 3.8.5-5 for each of the 16 cases considered, including cracked and uncracked conditions, Soil Types 7, 8, 9, and 11, and for RXB model and the triple building model. For each of the cases, an acceptable FOS for overturning was met.

3.8.5.6.2 CRB Stability

The minimum acceptable factor of safety for flotation, uplift, sliding, and overturning is 1.1. This was not achieved for the CRB uplift.

Linear analyses were overly conservative and showed unsatisfactory results for the CRB Stability Analyses, so nonlinear evaluation was used. The uplift, sliding, and overturning stability analysis of the Control Building is performed using a nonlinear sliding and uplift analysis. A nonlinear sliding, overturning, and uplift analysis was performed for the CRB to show that sliding, overturning, and uplift are insignificant.

Figure 3.8.5-48 shows the designations used (A through I) for the locations on the CRB basemat where the relative vertical displacements (uplift) and lateral displacements (sliding) were assessed between the two end nodes of the CONTA178 elements.

Bearing pressure is used to establish a design parameter for bearing capacity for site selection. The bearing capacity of the soil should provide a factor of safety of 3.0 for the static bearing pressure and a factor of safety of 2.0 for dynamic bearing pressure. The maximum allowable tilt settlement for the Control Building is 1" total or 1/2" per 50 feet in any direction at any point in the structure. The maximum allowable total settlement at any foundation node is 4 inches.

3.8.5.6.2.1 CRB Uplift

The key results are:

The relative displacements between the nodes at the basemat of the CRB are considered as actual uplift between CRB and surrounding soil. (Negative displacement values are considered as penetrations; a negligible amount of penetration is expected for penalty stiffness based contact algorithms.)

The elements transfer loads only when the contact is made. Therefore, the reactions drop to zero when there is a contact gap or uplift. This can be clearly seen from the force versus uplift comparison at location A in Figure 3.8.5-49 and Figure 3.8.5-50. The CRB is in an uplifted state at this corner location A for an infinitesimal duration of time just before the 10 seconds mark, resulting in zero reaction forces. The maximum uplift at location A is less than 1/64". The magnitude of this displacement is insignificant. Thus, the potential for uplift is insignificant.

3.8.5.6.2.1.1 Dynamic CRB Uplift Ratio

The effect of the foundation uplift has been evaluated for the CRB. The linear SSI analysis methods are acceptable if the ground contact ratio is equal to or greater than 80%. The ground contact ratio can be calculated from the linear SSI analysis using the minimum basemat area that remains in compression with the soil. The seismic total vertical base reactions are calculated by the time step-by-time step algebraic summation of all nodal vertical reactions of the nodes of the CRB basemat. The maximum seismic vertical reactions for the cracked and uncracked concrete conditions are summarized in Table 3.8.5-15. The base vertical reaction results for the uncracked condition are similar to those for the cracked concrete condition.

As shown in Table 3.8.5-15, the seismic reactions are much less than the total dead weight reaction over the rectangle basemat area of 45,680 kips (based on SAP2000 calculations). Thus, the net reactions are always in compression.

The typical total basemat vertical reaction time histories are shown in Figure 3.8.5-77 through Figure 3.8.5-82. The first two show the reactions for comparison between the cracked and uncracked concrete conditions. Others are all for the cracked concrete condition for the CSDRS Capitola input and CSDRS-HF Lucerne input. As can be seen in these figures, the total reactions are always in compression. Each of the CSDRS- and

CSDRS-HF-compatible seismic inputs contain three acceleration components, X (EW), Y (NS), and Z (vertical).

The cracked and uncracked total reactions can be compared using Figure 3.8.5-77 for the cracked reaction and Figure 3.8.5-78 uncracked reaction due to Capitola input for Soil Type 7. The differences in total reactions are small because the differences between the cracked and uncracked seismic reactions are small as shown in Table 3.8.5-15.

Based on the examination of the total vertical reaction force underneath the basemat, all net vertical reactions are in compression. Thus, the basemat is 100 percent in contact.

3.8.5.6.2.2 Control Building Sliding

Figure 3.8.5-51 shows the relative sliding between the nodes at location A. In contrast to penetration compatibility, sliding can exhibit both positive and negative values equally since the nodes could move away from each other, towards one side or the other. Maximum sliding at A is approximately 0.006".

A summary of the results is provided in Table 3.8.5-13. The magnitudes of these displacements are insignificant. Thus, the potential for sliding is insignificant.

3.8.5.6.2.3 Control Building Overturning

The results provided in Table 3.8.5-13 show that the deeply embedded Control Building experiences less than 1/10" of sliding displacement and less than 1/64" of total vertical uplift displacement. The magnitudes of these displacements are insignificant. Thus, the potential for overturning is insignificant.

3.8.5.6.3 Average Bearing Pressure

As stated in Section 3.8.5.5.4, the average static bearing pressure is the dead load of the building divided by the footprint.

The weight of the RXB is 587,147 kips and the calculated footprint is 58,175 ft^2. This results in an average pressure of 10.1 ksf. This results in a factor of safety of 6.9 to the minimum soil bearing capacity of 75 ksf specified in Table 2.0-1. The weight of the CRB (based on static vertical gravity reaction (1GZ) and soil weight) is 75,779 kips with a base area of 11,800 ft^2. This results in a static bearing pressure of 6.42 ksf. This value for the CRB static bearing pressure provides a factor of safety of 10.9 to the minimum soil bearing capacity of 75 ksf in Table 2.0-1.

The average dynamic bearing pressure is obtained as described in Section 3.8.5.5.4, with the vertical reaction for the entire basemat computed at each time step. The RXB foundation average dynamic pressure is 4.6 ksf. The CRB average foundation dynamic pressure is 2.3 ksf.

3.8.5.6.4 Settlement

Displacement values are provided for selected nodes in the foundation in Table 3.8.5-8. The location of these nodes is shown in Figure 3.8.5-10. As can be seen from the values in Table 3.8.5-8, total settlement at any foundation node, tilt settlement, and differential settlement are minimal. The maximum allowable differential settlement between the RXB and CRB, and between the RXB and RWB is 0.5 inch.

The RXB settles approximately 1¾ inch on the west end and approximately 2 inches on the east end. The tilt settlement of 0.25" is less than 1" as cited in Section 3.8.5.6.1. There is negligible tilt north to south. The east end of the building contains the pool and the NPMs.

The CRB settles approximately 1¾ inch on the west end and approximately 1 inch on the east end. The tilt settlement of 0.75" is less than the 1" limit cited in Section 3.8.5.6.2. North to south tilt is negligible. The CRB tilts toward the RXB. Differential settlement between the two buildings is on the order of ¼ inch.

The Seismic Category II Radioactive Waste Building settles approximately ½ inch on the west end and approximately 1½ inch on the east end. The RWB tilts toward the RXB. The RWB tilts approximately 1/5 inch in the north-south direction. Differential settlement between the RWB and the RXB is also on the order of ¼ inch.

3.8.5.6.5 Thermal Loads

During normal operation, a linear temperature gradient across the RXB foundation may develop.

An explicit analysis considering these loads has not been performed, as thermal loads are a minor consideration. Thermal loads are, by nature, self-relieving by means of concrete cracking and moment distribution. This is especially true of the NuScale RXB, as it is not a traditional pre-stressed/post-tensioned, cylindrical containment vessel, but, rather, a rectangular reinforced concrete building with several members framing into the roof, external walls, and basemat.

3.8.5.6.6 Construction Loads

The entire RXB basemat is poured in a very short time. The building is essentially constructed from the bottom up. The main loads (the reactor pool and the NPMs) are not added until the building is complete. Therefore, there are no construction-induced settlement concerns. The CRB basemat is much smaller and will be poured later than the RXB basemat in the construction sequence.

3.8.5.6.7 Basemat Soil Pressures along Basemat Edges (Toe Pressures)

The static deadweight reaction at an edge node is added to the seismic reaction of the node to calculate the total reaction. The bearing pressure is calculated by dividing the total reaction by the tributary area of the node. The edge bearing pressures, or toe pressures, along the edges are averaged to obtain the average toe

pressures of the basemat. The average toe pressures for the RXB and CRB are shown in Table 3.8.5-14 and Table 3.8.5-16, respectively. The values shown in these tables indicate that two times the maximum toe pressure is less than the minimum soil bearing pressure capacity of 75 ksf as specified in Table 2.0-1.

3.8.5.6.8 Leak Detection

Groundwater has the potential to leak through the RXB exterior walls through microscopic concrete cracks. Due to the exterior concrete wall thickness, these leaks will be very slow (<<1 gallon per day (gpd)). This leak rate through the wall is not enough to cause an interior flood in any of the rooms that share an exterior wall. Leaks of this nature will be discovered and dealt with in accordance with plant concrete maintenance specifications. Further reduction of groundwater seepage can be accomplished with a building dewatering system surrounding the RXB.

A leak chase system is provided in the RXB basemat to detect any leakage from the reactor pool.

3.8.5.7 Materials, Quality Control, and Special Construction Techniques

Section 3.8.4.6 describes the materials, quality control, and special construction techniques applicable to the RXB and CRB including the foundations.

3.8.5.8 Testing and Inservice Inspection Requirements

Section 3.8.4.7 identifies the testing and inservice surveillances applicable to the RXB and CRB including the foundations.

Table 3.8.5-1: RXB Stability Evaluation Input Parameters

Data Description	Value
RXB Dead Weight (kips)	**587,147**
RXB East-West Length (ft) (between exterior faces of walls)	**346**
RXB North-South Length (ft) (between exterior faces of walls)	**150.5**
RXB Height (ft)	**167**
RXB Embedment Depth (ft)	**86**
Foundation East-West Length (ft)	**358**
Foundation North-South Length (ft)	**162.5**
Foundation Area (ft^2)	**58,175**
Soil Density, γ_{soil} (pcf)	**130**
Coefficient of Friction between Wall and Soil	**0.5**
Coefficient of Friction between Basemat and Soil	**0.58**
Effective Soil Density, $\gamma_{eff} = \gamma_{soil} - \gamma_{water}$ (pcf)	**67.6**
Angle of Internal Friction	**30°**
Soil Coefficient of Pressure at Rest, K_o	**0.5**
Surcharge (psf)	**250**

Table 3.8.5-2: Reactor Building Static Effective Soil Force

Definition	Symbol	Results	Units
Reactor Building			
Total Effective Soil Force on North Wall	F_{y1}	46,967	Kips
Total Effective Force on South Wall	F_{y2}	46,967	Kips
Total Effective Force on West Wall	F_{x1}	20,429	Kips
Total Effective Force on East Wall	F_{x2}	20,429	Kips
Total Static Wall Force	Ftotal	**134,792**	Kips

Table 3.8.5-3: Seismic Base Reactions

Model	Concrete Case	Soil Type	Seismic Load Case	Global FX (kips)	Global Fy (kips)	Global Fz (kips)
Reactor Building	Cracked 7% Damping	S7 CSDRS	Capitola	326528	177221	222932
			Chi Chi	303442	185109	254142
			El Centro	253932	190969	264163
			Izmit	273116	171747	234397
			Yermo	277421	196458	254684
		S8 CSDRS	Capitola	306274	206799	205032
			Chi Chi	318687	200201	229313
			El Centro	250271	212788	234071
			Izmit	298958	211286	226435
			Yermo	268717	235929	233072
		S11 CSDRS	Capitola	151960	135837	185963
			Chi Chi	188520	126654	182918
			El Centro	143366	166150	191453
			Izmit	146440	168663	199958
			Yermo	171040	135521	199400
		S7 CSDRS- HF	Lucerne	119790	77946	147529
		S9 CSDRS- HF	Lucerne	126622	82652	162443
	Uncracked 7% Damping	S7 CSDRS	Capitola	331587	203856	225014
			Chi Chi	306830	192224	258618
			El Centro	271625	197785	254444
			Izmit	272082	190891	242807
			Yermo	281972	190668	257452
		S8 CSDRS	Capitola	311880	212752	208268
			Chi Chi	320551	215363	234958
			El Centro	263147	219067	230481
			Izmit	296880	212060	228292
			Yermo	281020	234460	238766
		S11 CSDRS	Capitola	152056	138287	186456
			Chi Chi	188000	128106	185511
			El Centro	143524	167620	189535
			Izmit	147560	170244	201724
			Yermo	172026	135712	201374
		S7 CSDRS- HF	Lucerne	114361	82076	156119
		S9 CSDRS- HF	Lucerne	155572	99573	167031
Control Building	Cracked 7% Damping	S7 CSDRS	Capitola	23416	31065	22228
			Chi-Chi	22129	26172	26415
			El Centro	20588	25473	27118
			Izmit	21529	29205	24628
			Yermo	21544	27899	25374
		S9 CSDRS-HF	Lucerne	15018	19859	21209
	Uncracked 7% Damping	S7 CSDRS	Capitola	25705	32251	23455
			Chi Chi	23304	28272	26333
			El Centro	21920	26926	26885
			Ismit	23147	31104	25146
			Yermo	23161	28982	23616
		S9 CSDRD-HF	Lucerne	16523	20795	21017

Table 3.8.5-3: Seismic Base Reactions (Continued)

Model	Concrete Case	Soil Type	Seismic Load Case	Global FX (kips)	Global Fy (kips)	Global Fz (kips)
Triple Building	Cracked 7% Damping	S7 CSDRS	Capitola	343944	244056	231397
			Chi Chi	336167	239971	250624
			El Centro	267968	269922	256483
			Izmit	297510	245331	251341
			Yermo	297715	236510	263351
		S8 CSDRS	Capitola	290751	274276	196053
			Chi Chi	303767	234230	223377
			El Centro	248628	267201	229007
			Izmit	287011	252901	216609
			Yermo	263706	265195	232279
		S11 CSDRS	Capitola	168396	119565	181518
			Chi Chi	199376	117941	179024
			El Centro	149150	165393	186060
			Izmit	152976	161973	193875
			Yermo	173035	120733	195737
		S7 CSDRS- HF	Lucerne	110986	91038	139697
		S9 CSDRS- HF	Lucerne	129899	98212	162049
	Uncracked 7% Damping	S7 CSDRS	Capitola	**345847**	277296	233754
			Chi Chi	340014	239492	255071
			El Centro	284727	**285248**	253962
			Izmit	289695	248614	241686
			Yermo	300881	233505	**267641**
		S8 CSDRS	Capitola	292384	271970	202190
			Chi Chi	305827	241469	226832
			El Centro	259244	267925	221740
			Izmit	284855	249438	219512
			Yermo	273286	261749	236003
		S11 CSDRS	Capitola	170042	122301	180745
			Chi Chi	200463	119167	180987
			El Centro	151215	166685	183803
			Izmit	153733	163189	195697
			Yermo	174920	125096	196915
		S7 CSDRS- HF	Lucerne	105895	95761	134547
		S9 CSDRS- HF	Lucerne	143621	102666	165813
			Maximum:	**345847**	**285248**	**267641**

These loads are the maximums of the total base reaction time histories obtained by the step-by-step combination of the reactions in all springs below the foundation

Table 3.8.5-4: Seismic Vertical RXB Base Reactions and Dead Weight

Soil Type	Seismic Load Case	Standalone Model		Triple Building Model		Dead Weight (kips)
		Cracked Seismic Vertical Reaction (kips)	Uncracked Seismic Vertical Reaction (kips)	Cracked Seismic Vertical Reaction (kips)	Uncracked Seismic Vertical Reaction (kips)	
S7† CSDRS	Capitola	222,932	225,014	231397	233754	471,487
	Chi-Chi	254,142	258,618	250624	255071	471,487
	El Centro	264,163	254,444	256483	253962	471,487
	Izmit	234,397	242,807	251341	241686	471,487
	Yermo	254,684	257,452	263351	267641	471,487
S8 CSDRS	Capitola	205,032	208,268	196053	202190	471,487
	Chi-Chi	229,313	234,958	223377	226832	471,487
	El Centro	234,071	230,481	229007	221740	471,487
	Izmit	226,435	228,292	216609	219512	471,487
	Yermo	233,072	238,766	232279	236003	471,487
S11 CSDRS	Capitola	185,963	186,456	181518	180745	471,487
	Chi-Chi	182,918	185,511	179024	180987	471,487
	El Centro	191,453	189,535	186060	183803	471,487
	Izmit	199,958	201,724	193875	195697	471,487
	Yermo	199,400	201,374	195737	196915	471,487
S7 CSDRS-HF	Lucerne	147,529	156,119	139697	134547	471,487
S9 CSDRS-HF	Lucerne	162,443	167,031	162049	165813	471,487

†S7, S8, S9, S11 designate Soil Types 7, 8, 9, and 11, respectively.

Table 3.8.5-5: Factors of safety - RXB Stability

Cracked Condition				Uncracked Condition			
Stability	**Vertical**	**N-S**	**E-W**	**Stability**	**Vertical**	**N-S**	**E-W**
Case 1: Cracked RXB Model, Soil Type 7				**Case 2: Uncracked RXB Model, Soil Type 7**			
Flotation	2.34	-	-	Flotation	2.34	-	-
Sliding	-	1.06	0.78	Sliding	-	1.00	0.76
Overturning	-	1.52	1.53	Overturning	-	1.51	1.52
Case 3: Cracked Triple Model, Soil Type 7				**Case 4: Uncracked Triple Model, Soil Type 7**			
Flotation	2.34	-	-	Flotation	2.34	-	-
Sliding	-	0.79	0.76	Sliding	-	0.86	0.75
Overturning	-	1.49	1.50	Overturning	-	1.50	1.50
Case 5: Cracked RXB Model, Soil Type 8				**Case 6: Uncracked RXB Model, Soil Type 8**			
Flotation	2.34	-	-	Flotation	2.34	-	-
Sliding	-	1.03	0.82	Sliding	-	1.00	0.80
Overturning	-	1.66	1.66	Overturning	-	1.64	1.65
Case 7: Cracked Triple Model, Soil Type 8				**Case 8: Uncracked Triple Model, Soil Type 8**			
Flotation	2.34	-	-	Flotation	2.34	-	-
Sliding	-	0.85	0.84	Sliding	-	0.85	0.83
Overturning	-	1.71	1.71	Overturning	-	1.69	1.70
Case 9: Cracked RXB Model, Soil Type 11				**Case 10: Uncracked RXB Model, Soil Type 11**			
Flotation	2.34	-	-	Flotation	2.34	-	-
Sliding	-	1.50	1.47	Sliding	-	1.49	1.47
Overturning	-	1.95	1.96	Overturning	-	1.94	1.95
Case 11: Cracked Triple Model, Soil Type 11				**Case 12: Uncracked Triple Model, Soil Type 11**			
Flotation	2.34	-	-	Flotation	2.34	-	-
Sliding	-	1.60	1.40	Sliding	-	1.58	1.38
Overturning	-	2.00	2.00	Overturning	-	2.00	2.00
Case 13: Cracked RXB Model, Soil Type 9				**Case 14: Uncracked RXB Model, Soil Type 9**			
Flotation	2.34	-	-	Flotation	2.34	-	-
Sliding	-	2.66	1.86	Sliding	-	2.21	1.51
Overturning	-	2.31	2.31	Overturning	-	2.24	2.25
Case 15: Cracked Triple Model, Soil Type 9				**Case 16: Uncracked Triple Model, Soil Type 9**			
Flotation	2.34	-	-	Flotation	2.34	-	-
Sliding	-	2.24	1.81	Sliding	-	2.14	1.64
Overturning	-	2.31	2.32	Overturning	-	2.26	2.26

Table 3.8.5-6: RXB ANSYS Model Summary

Items	ANSYS
Number of Joints	40009
Number of Joint with Restraints	5822
Number of Joint with Lumped Mass	7877
Number of Frame Elements	1541
Number of Shell Elements	15851
Number of Solid Elements	15012
Number of Link/Spring Elements	120
Number of Nonlinear Contact Elements	2100
Number of Nonlinear Gap Elements	5822

Table 3.8.5-7: Overturning Forces and Overturning Arms

Overturning Force	Overturning Moment Arm	Arm Length
Overturning Moment about the Y-Axis (E-W)		
Vertical Seismic Reaction	Half of East-West Width of Basemat	179′
Friction Forces on North and South Walls	Perpendicular Distance between Line of Action of Friction Force Centroid and Pivot	179′
Friction Force on East Wall	East-West Width of Basemat	352′
Effective Structural Dead Weight (Buoyant Weight)	Half of East-West Width of Basemat	179′
Overturning Moment about the X-Axis (N-S)		
Vertical Seismic Reaction	Half of North-South Width of Basemat	81.25′
Friction Forces on East and West Walls	Perpendicular Distance between Line of Action of Friction Force Centroid and Pivot	81.25
Friction Force on South Wall	North-South Width of Basemat	156.5′
Effective Structural Dead Weight (Buoyant Weight)	Half of North-South Width of Basemat	81.25′

Table 3.8.5-8: Settlement values for the RXB, CRB and RWB

Building	Node No.	Displacements (inch)								
		Uncracked			Cracked			Coordinates (inch)		
		EW	NS	Vertical	EW	NS	Vertical	X	Y	Z
RWB	41173	-0.101	0.006	-0.598	-0.099	0.006	-0.599	-2460	-825	570
	41206	-0.086	0.025	-0.525	-0.081	0.027	-0.526	-2460	1149	570
	42517	-0.122	0.008	-1.633	-0.121	0.007	-1.635	-300	-825	570
	42552	-0.126	0.030	-1.418	-0.126	0.031	-1.419	-300	1317	570
RXB	129	-0.022	-0.035	-1.749	-0.021	-0.037	-1.750	0	-873	0
	151	-0.023	0.039	-1.750	-0.022	0.040	-1.750	0	873	0
	857	-0.009	-0.008	-1.887	-0.009	-0.009	-1.888	2019.5	-873	0
	879	-0.014	0.026	-1.880	-0.014	0.027	-1.880	2019.5	873	0
	1616	0.017	-0.023	-1.948	0.017	-0.024	-1.949	4092	-873	0
	1638	0.010	0.053	-1.944	0.010	0.055	-1.944	4092	873	0
CRB	31066	0.143	0.008	-1.753	0.139	0.009	-1.754	4470	-705	345
	31089	0.152	0.022	-1.735	0.148	0.022	-1.737	4470	705	345
	31559	0.163	0.007	-1.037	0.159	0.007	-1.037	5406	-705	345
	31582	0.167	0.021	-1.020	0.163	0.021	-1.020	5406	705	345